RESEARCH ON URBAN TRANSIT RELIABILITY USING SMART CARD DATA

SUN LIJUN

NATIONAL UNIVERSITY OF SINGAPORE

2014

RESEARCH ON URBAN TRANSIT RELIABILITY USING SMART CARD DATA

SUN LIJUN

(B. Eng. Tsinghua University)

A THESIS SUBMITTED
FOR THE DEGREE OF DOCTOR OF PHILOSOPHY
DEPARTMENT OF CIVIL AND ENVIRONMENTAL ENGINEERING
NATIONAL UNIVERSITY OF SINGAPORE

2014

NUS
National University
of Singapore

(FCL) FUTURE CITIES LABORATORY 未来城市实验室

(SEC) SINGAPORE-ETH CENTRE 新加坡－ETH研究中心

Declaration

I hereby declare that this thesis is my original work and it has been written by me in its entirety. I have duly acknowledge all the sources of information which have been used in the thesis.

The thesis has also not been submitted for any degree in any university previously.

Sun Lijun

10 October, 2014

Acknowledgements

First of all, I would like to thank National Research Foundation and Singapore-ETH Centre for the research scholarship. After four years of living, studying and research at National University of Singapore, it is time for me to acknowledge the people who have guided, helped and accompanied me. My deepest appreciation goes to the three wise men who appeared to lead me on my Ph.D. journey.

Prof. Lee Der-Horng — my supervisor who provides me with his support whenever needed, who is receptive to my research ideas, who teaches me to believe in my own work, who not only steers me through but also push me further than I thought I could go in academic. I have enjoyed every conversation and meeting with him because of his great sense of humor. I am also grateful to the freedom and encouragement he has given to me on research.

Prof. Kay W. Axhausen — my supervisor at ETH Zürich. I am grateful to him for accepting me to join the wonderful Future Cities Laboratory, providing me both research advice and career guidance, and going through every paper with stimulating discussion and valuable feedback. To me, he was and remains the best role model for a researcher, mentor and teacher.

Dr. Alexander Erath — my 'boss' at Future Cities Laboratory. As the coordinator of the transportation module at FCL, he has given me more research freedom than I have ever expected. I have enjoyed and benefited from fruitful research conversations with him. I am very grateful to his kindness and support on my personal life and career. I feel fortunate and honored for having the pleasure to work with him.

I would like to thank my thesis committee members, Prof. Meng Qiang and Prof. Diao Mi, for their encouragement and insightful discussion. I am indebted to Dr. Jin Jian Gang, who is now a Professor at Shanghai Jiao Tong University. To me he is not only a senior, but also served as an advisor during the most difficult time of my research. I would also like to thank

Prof. Alex (Sandy) Pentland at MIT, for accepting me as a member of 'pentlandians'. I have benefited a lot from the inspiring weekly meetings during my exchange at MIT Media Lab.

I want to thank all my colleagues at FCL, ITVS and SMART for their companionship, support and encouragement: Artem Chakirov, Pieter Fourie, He Nanxi, Li Siyu, Lu Zhaoyang, Dr. Lu Yang, Sergio Ordonez, Qin Han, Tan Rui, Teresa Tan, Michael van Eggermond, Dr. Wu Xian and Zhao Kangjia. You make my Ph.D. life colorful.

I own my deepest gratitude to my parents and my elder sister. Their unconditional love and support made me who I am today. Finally, this thesis is dedicated to my wife, Ye Qing. I know, you are the best thing, that ever happened to me.

Table of Contents

Executive Summary

With the increasing demand and range of urban mobility, public transport systems are playing an increasingly important role in accelerating the transition to sustainable urban development worldwide, providing people with efficient and affordable access to education, employment, markets and other key services with less environmental impact. Considering the growing dependency of urban mobility on public transport systems, providing reliable and efficient transit services becomes one of the greatest challenges to transit authorities and operators. Current practice shows that sufficient data from actual operation is of ultimate importance to understanding operational characteristics and improving service quality. Thanks to the emergence of automated fare collection (AFC) systems, nowadays transit users generate large quantities of data with high spatial-temporal resolution through daily transit use. The wealth of such smart card data provides us with a great opportunity to apply a data-driven approach to study urban transit systems.

This thesis is dedicated to the application of smart card data in understanding service operations and enhancing transit reliability by conducting extensive analyses and constructing realistic models. With a particular focus on real-world problems faced by transit agencies and operators, this thesis follows a sequential approach and can be divided into three parts: (1) *understanding transit service reliability*, (2) *modeling transit service reliability* and (3) *developing methodologies to enhance transit service reliability*. The three parts are arranged around general topics and areas of interest in urban transit research. The research in the first part is intended to develop tools for processing the smart card data and then refine new knowledge and understandings from it. Operational characteristics of bus services and travel time variability of metro systems are studied by extracting passenger transit activities from smart card data. The second part is devoted to more realistic mathematical models to explain the interaction

between passenger behavior and service reliability. Taking advantage of the high temporal resolution of activity transactions, this part addresses the impact of vehicle configuration on passenger boarding/alighting dynamics and investigates passenger flow dynamics in a complex metro network. With the knowledge from understanding and modeling urban transit operations, the third part centers on enhancing service quality and efficiency by using advanced operational strategies, and studies how operations can be made more resilient and reliable to disruptions. In this part, we examine the interaction between passenger demand and transit service supply at different domains and introduce two optimization frameworks on identifying optimal control point for bus services and designing demand-sensitive timetables for metro services.

In summary, the three parts have overlaps and interconnections, contributing new insights and knowledge on using smart card data to understand, model and enhance urban transit reliability. Ultimately, it provides data-driven mindsets and approaches to researchers, decision makers and in particular transit authorities and operators, helping them to better cope with the challenges arising from daily operation.

List of Tables

List of Figures

Chapter 1

Introduction

1.1 Research Background

With the rapid progress in urbanization and civilization globally, understanding the impact of the revolution and the nature behind the phenomena occurring in urban environments is emerging as a promising research direction. In order to better understand urban dynamics including traffic flows, human behaviors, mobility patterns, social dynamics, energy consumption and environmental changes, both researchers and practitioners are now trying to take full advantage of data collected from various sources in urban space, such as cell phone call/text logs, trajectories of people and vehicles from global positioning system (GPS), records from traffic detectors and environment sensors, smart card transactions from public transport systems (Zheng et al., 2014). The emergence of these data provides us the opportunity to enhance both human life and urban environment intelligently, by means of discovering the hidden knowledge behind it, especially for public transport systems.

In Singapore, public transport is playing an increasingly important role in urban transportation. As shown in Table 1.1, the average daily ridership has increased from 4.3 million to 6.1 million during the last 12 years. Public transport shares about 63% of the demand in morning peak hours (Land Transport Authority, 2008). Towards a more people-centric land transport environment, public transport systems must be well integrated from commuter's perspective, providing improved transit services in terms of reliability, comfort and convenience, to reduce passenger waiting time and delay. However, public transport systems are born unstable due to the uncertainty in operation, such as imbalanced demand in peak/off-peak time, traffic congestion, signal controls and other interruptions, resulting in various problems like bus bunching, long waiting times, long journey times, overcrowding and service disruptions. Understanding the factors and results behind such uncertainty is crucial to maintaining and improving service quality.

Table 1.1: Average daily transit trips from 2000 to 2012 (in millions)

Year	Metro	Bus	Total
2000	1.09	3.25	4.34
2001	1.11	3.28	4.39
2002	1.12	3.20	4.32
2003	1.22	2.99	4.21
2004	1.33	2.81	4.14
2005	1.39	2.78	4.17
2006	1.48	2.83	4.31
2007	1.61	2.93	4.54
2008	1.79	3.09	4.88
2009	1.87	3.05	4.92
2010	2.17	3.20	5.37
2011	2.41	3.39	5.80
2012	2.65	3.48	6.13

* Source: Land Transport Authority, Singapore. Data on Ridership is averaged over the period from January to December.

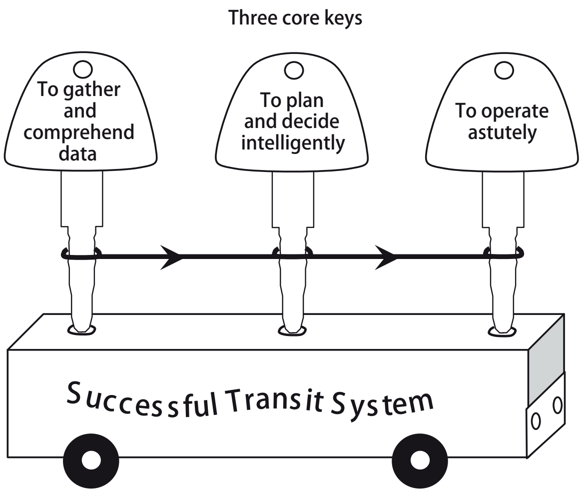

Figure 1.1: The three important keys for a successful transit system (adapted from Ceder 2007)

Current practice of transit operators shows that sufficient data plays an important role in monitoring, operating, and planning (Ceder, 2007). As shown in Figure 1.1, the basis of a successful transit system is to gather and comprehend data. However, data collection is a difficult task in public transport research, as most conventional approaches conduct physical surveys and collect information manually, which is known to be both time consuming and labor intensive. For example, collecting bus dwell time and number of on-board passengers data requires at least two well-trained observers on an articulated bus (Moreno González et al., 2012). Conventional manual technique collection techniques — such as field survey and in-vehicle checking — show vital limitations in frequency and sample size, resulting in potential biases on operation and planning decisions. The field still starves for advanced techniques to better collect operational information in a more efficient manner.

Figure 1.2: Physical appearance of some types of smart cards: Ezlink in Singapore, Yikatong in Beijing, EasyCard in Taiwan, Octopus in Hong Kong, Oyster in London, Opal in Sydney, SmarTrip in Washington DC and Suica in Tokyo.

The new electronic smart card systems, as implemented in Singapore and other cities around the world (see Figure 1.2 for some typical types of smart cards across the world), give us a new and much deeper insight into the operational and planning processes of public transport systems than ever before. The main purpose of the AFC systems is to make fare collection easier to both operators and users (Dorbritz et al., 2009; Pelletier et al., 2011). Operators are allowed to create some innovative and flexible fare schemes, which may take passenger transfer activities into account. For example, in Singapore the public transport operators use a distance-based fare scheme which integrates both bus and metro systems. Such a scheme is hardly applicable without the help of AFC systems. Moreover, another natural advantage of smart card system is that it speeds up the process of fare transaction, leading to less time spent at stops and in vehicles.

Although the the main purpose of introducing smart cards is for fare collection, it also produces large quantities of very detailed data recording spatial-temporal attributes of each boarding/alighting activity, which provides great opportunities in exploring and understanding travel behaviors and transit use patterns, even when the data are anonymous. At the meanwhile, the availability of such data has also greatly benefited transportation researchers, planners and policy makers to enhance transit service level, from daily operation to long term strategic planning. Both users and operators can benefit from taking full use of this valuable information. Smart card is expected to play an important role in building more advanced, innovative and reliable public transport systems. Highlighting their importance in understanding transit operation, recent academic studies on public transport systems also demonstrate an increasing interest in using smart card data. Pelletier et al. (2011) presented a good overview paper focusing on the use of smart card data in public transit.

1.2 Urban Transit Reliability

Given the growing dependency of urban mobility on public transport systems across the world, the role of public transit reliability becomes increasingly important in urban life, particularly in high-density metropolitan cities. Such a heavy dependency not only challenges the planning of transit systems, but also imposes enormous strains on service reliability, making service interruptions/disruptions hardly affordable. On the other hand, such a strong dependency also makes public transport systems more vulnerable than ever before; even limited service disruptions/interruptions could result in substantial productivity loss and widespread confusion. The unreliability of transit services exists at both small and large scales. Bus bunching for long services may double or triple the average waiting time for passengers. Taking the 16th December 2011 disruption in Singapore's metro network as an example, train services at 11 stations were disrupted for 5 h and more than 100,000 commuters were affected. Therefore, transit agencies and operators are required to pay more attention to service reliability and have a comprehensive understanding of their operational characteristics.

Despite previous efforts in the literature and practice guidelines in public transport operation, there are still plenty of open questions and research challenges arising from daily operation and remaining to be solved in more innovative approaches (Vuchic, 2005; Ceder, 2007). These challenges also provide us with new research opportunities to make full use of the emerging data sets. In this case, the smart card systems provide researchers with an ideal data set for building more appropriate models of transit operations and testing the performance of more advanced operation strategies. The research presented in this thesis aims to introduce the potential of smart card data in further understanding and modeling urban transit systems — including both bus and metro — and in particular developing methodologies and applications to improve transit service level.

In general terms, the reliability issues faced by agencies and operators are:

- limited knowledge about transit operation characteristics,
- insufficient interaction between demand and supply in both planning and operation, and
- lack of understanding/misunderstanding of passenger demand patterns and user behavior.

1.3 Research Scope and Objective

Previous studies have shown extensive attention on the methods to improve service reliability at the operational level in both theory and practice (e.g., Vuchic 2005; Ceder 2007; see Chapter 2 for a review). However, most studies focus either on the supply side or on the demand side. Without an understanding of the interaction between service operation and passenger behavior, it remains unclear how the strategic/tactical designs interact with service reliability and passenger perception. Before taking these strategies and planning/design into reality, it has long been assumed that they will provide services with higher-quality and enhance service reliability. As a result, our understanding of public transport operation characteristics and passenger behavior is still limited.

In practice, these problems/issues are difficult to solve without the support from comprehensive and fine-grained data sets. Given the large quantity and high quality of smart card data, the way to utilize this data set efficiently also emerges as a promising direction. Researchers now can better understand and plan urban transit systems with the help of such data. Recently, there has been a workshop in Japan which was dedicated to the better use of the emerging smart card data for transit service planning and operation (1st International Workshop on Utilizing Transit Smart Card Data for Service Planning). [1] It has provided researchers analyzing smart card data with a good venue for further continuous exchange. A comprehensive review of existing literature is provided in Chapter 2 and the overview sections in Chapters 3∼7.

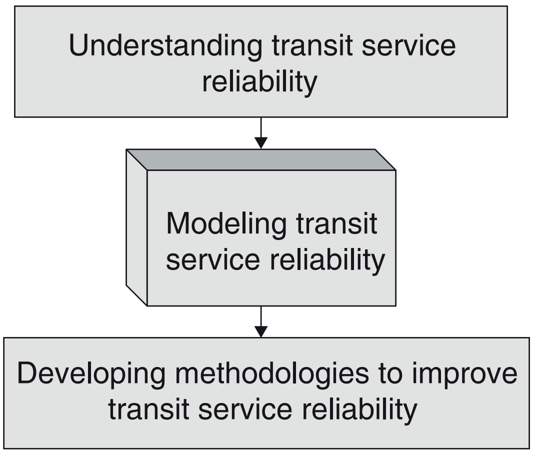

Figure 1.3: Hierarchical research approach

The overall objective of this thesis is to provide some new knowledge, understandings and operational strategies to transit agencies and service providers to enhance transit service reliability. Therefore, most of the topics presented in this thesis are built on real-world problems, which are unexplored but faced by agencies and operators daily, with a particular

[1] http://www.gu-rsp.org/smartcard/, Accessed October 10, 2014

focus on the three issues listed above. In order to achieve the objective, the thesis follows a sequential approach, trying to close some unexplored gaps in understanding service operations and to provide enhanced services. This research is conducted based on the framework shown in Figure 1.3, focusing on both bus and metro systems.

More specifically, this thesis is intended to provide data-driven tools and approaches to planners, researchers and decision makers and in particular authorities and operators in public transport, helping them to build reliable urban transit systems. By integrating the reliability issues listed in the above section and the smart card data in Singapore, this thesis studies the following research questions:

(a) Service operation characteristics: Understanding bus service reliability (Chapter 3), Estimating metro train loads and trajectories (Chapter 5) and Modeling passenger flow assignment in metro networks (Chapter 7).

(b) Interaction between demand and supply: Understanding bus service reliability (Chapter 3) and Designing demand-responsive metro timetables (Chapter 6).

(c) Passenger demand patterns and user behavior: Modeling bus boarding and alighting dynamics (Chapter 4), Estimating metro train loads and trajectories (Chapter 5) and Modeling passenger flow assignment in metro networks (Chapter 7).

Following the sequential approach of Figure 1.3, the detailed research scope in this thesis can be also divided into three parts shown in Figure 1.4.

1.3.1 Understanding transit service reliability

In order to characterize the existing demand trends, operational peaks, and unmet passenger demand, performance evaluation is required to measure service level, monitor operations, evaluate economic performance, administer the organization, develop service design standards, and increase community benefits (National Research Council, Transportation Research Board, 2010). This part is intended to develop methodologies and tools to process the smart card data, obtaining useful information for service performance evaluation and anomaly detection. Smart card data from bus system have a different structure from those of the metro system

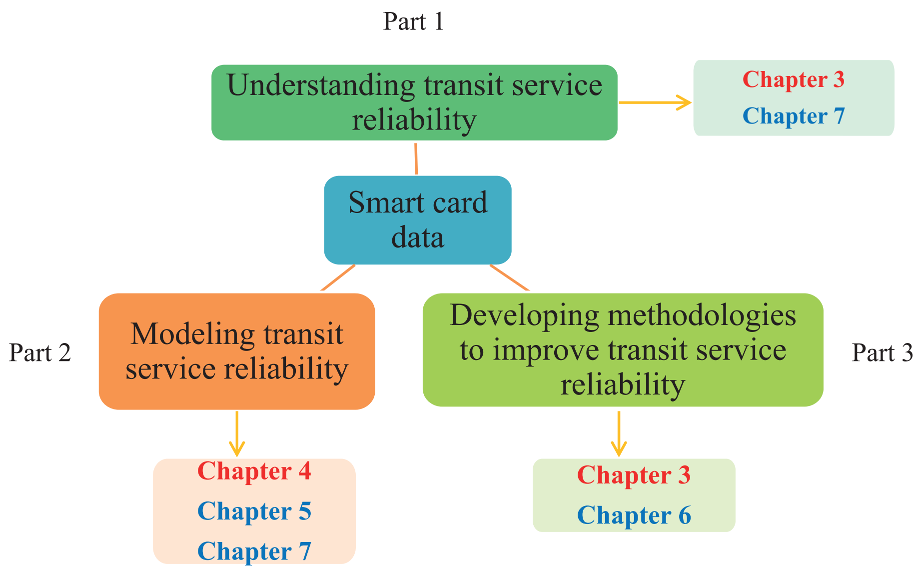

Figure 1.4: Thesis organization

(see Table 2.1 in Chapter 2). Therefore, we have to apply different approaches to process the data. For example, metro smart card data do not contain vehicle ID and this information is important to operators. This also becomes a critical research question in the field (Kusakabe et al., 2010). As a result, different performance indicators should be proposed to measure the service reliability of these two systems. Apart from understanding service reliability, this part is also intended to identify those factors causing service unreliability.

We focus on two field problems in this part: the first is on investigating and quantifying operational reliability of bus services, and the second is to characterize travel time reliability of metro services and build a sophisticated passenger flow assignment model. Using smart card transactions obtained from on particular bus service, we provide an exploratory study on bus service reliability in Chapter 3. The detailed boarding/alighting transactions are used to reconstruct operation log of each service, helping us to obtain vehicle trajectories and occupancy profiles. Travel time extracted from smart card data in metro systems is more complicated as it consists of not only in-vehicle time, but also access and egress time. In this case, it is difficult to obtain train operational characteristics from smart card data directly. To deal with this problem, in Chapter 7 we apply a Bayesian inference model to quantify the variability of station-to-station travel time in Singapore MRT network.

1.3.2 Modeling transit service reliability

This part is devoted to integrating the new knowledge we have learned from smart card data into the modeling of urban transit operation and passenger behavior. On one hand, we intend to propose more realistic mathematical models to explain how passenger demand interacts with service reliability. On the other hand, we are interested in building new formulation framework to better support the modeling of service operation.

We consider three modeling problems in this thesis. In Chapter 4 we try to examine the importance of vehicle configuration in determining bus dwell time and its variability. In doing so, we first estimate regression models by distinguishing boarding flows from alighting flows. Then, an integrated model is built and estimated to better capture the dynamics of passenger boarding and alighting behavior, and its interaction with on-board passengers. Such a model could help transit agencies and operators to find optimal vehicle type for a particular route. The latter two problems concentrate on metro operation. Despite the full spatial-temporal resolution of metro smart card data, it remains a challenge to distinguish each stage (access, waiting, on-board and egress) given that fare gantries are located at train stations instead of inside trains. In this part, we propose two models for metro operation:

- passenger-to-train identification and train trajectory/occupancy reconstruction;
- modeling passenger route choice behavior and flow assignment in a network level.

In Chapter 5, we reconstruct a full metro trip into four segments: access, waiting, on-board and egress, and use a regression model to quantify the time cost for each segment using travel time observed from those fastest passengers on each origin-destination pair (we assume that waiting time is zero for these users). Despite estimating travel time and its variability of each link Chapter 7 also presents a modeling framework for passenger flow assignment in a complex metro network. The key of this framework is to integrate passenger route choice model with travel time modeling by using a Bayesian inference approach.

1.3.3 Developing methodologies to improve service reliability

With the knowledge from understanding and modeling transit service reliability, the goal follows is to develop methodologies to improve transit service reliability. We aim at enhancing service quality by using advanced operation strategies to avoid service interruptions and disruptions as much as possible. In doing so, we need to have a comprehensive understanding about passenger demand distribution and try to satisfy this demand with limited public transport resources. In this part we discuss two problems on transit operation, on bus and metro systems respectively.

In Chapter 3 we propose a solution to cut long trunk bus services into segments by identifying optimal cutting point, where operators are allowed to add slack time and hold buses to avoid bunching. We measure the performance of this approach by conducting simulation experiments, finding that it is efficient in improving service quality and increasing commuter satisfaction. For metro operation, a dynamical timetable design problem is proposed and solved in Chapter 6. The key contribution of this approach is to establish more connection between passenger demand and service supply. The result shows that applying demand sensitive timetables will reduce passenger waiting time and then increase the total social welfare under the same operation cost.

1.4 Thesis Organization

The thesis consists of 8 chapters, which are organized as follows:

Chapter 1 introduces the background of transit reliability study using smart card data. The motivation and objectives are also introduced.

Chapter 2 provides a brief review of existing studies based on smart card data and reviews previous research on measuring transit reliability.

Chapter 3 presents an exploratory study on investigating the reliability of urban bus system empirically by measuring vehicle trajectory, occupancy and headway, and provides a demand based model to identify optimal stop for line splitting.

Chapter 4 describes the use of smart card data to study passenger boarding/alighting behaviour given different bus types/configurations.

Chapter 5 presents an approach to analyze smart card data and describe dynamic demand characteristics of one case mass rapid transit (MRT) service.

Chapter 6 proposes optimization models to solve timetable scheduling problems by using fine grained dynamic demand data.

Chapter 7 proposes an integrated Bayesian statistical inference framework based on large quantities of travel time observations from smart card data to characterize passenger flow assignment model in a complex metro network.

Chapter 8 draws the concluding remarks on the works from Chapter 3 to Chapter 7 and discusses future research topics.

Chapter 2

Literature Review

This chapter presents a survey of the literature on the use of smart card data in general public transport research and application with a focus on transit reliability studies. It reviews existing literature in a general way. For the following chapters on individual research topics, the overview of related studies will be provided separately in a more detailed manner. The review starts with introducing the application of smart card data in public transport research.

2.1 Smart Card Data in Public Transit

With the application of automated fare collection (AFC) systems by more and more cities (e.g., Singapore (CEPAS), London (Oyster), Tokyo (Suica) and Washington (SmarTrip); see Figure 1.2), revenue collection becomes easier to transit operators. A list of smart cards across the world can be found at http://en.wikipedia.org/wiki/List_of_smart_cards.[1] Although the general purpose for introducing such AFC system is to make transit fares collection more convenient, large quantities of detailed data recording passengers' boarding/alighting activities are generated at the meanwhile. Typically, the data stored for each tapping activity may include: date and time of the transaction, status of the transaction (boarding, alighting, and transfer), card ID, passenger type, service ID, service direction, station/stop ID and vehicle/driver ID (see Table 2.1 for the fields and their contents of CEPAS data in Singapore). The AFC system in Singapore was introduced in April 2002. The use of smart card system has

[1] Accessed October 10, 2014

Table 2.1: Fields and contents of CEPAS data in Singapore

Field	Description
Journey ID	A unique number for each transit journey. One journey may contain several trip segments.
Card ID	A unique coded number of each smart card (anonymized)
Passenger type	The attribute of cardholder (Adult, Senior citizen and Child)
Travel mode	Bus/Metro
Service No.	Bus route service number (e.g., 96)
Direction	Direction of bus route (1 and 2)
Bus registration Number	A unique registration number for each vehicle (e.g., '0999')
Boarding stop/station	A unique ID for boarding stop/station
Alighting stop/station	A unique ID for alighting stop/station
Ride date	Date of a trip (e.g., '2011-04-11')
Ride start time	Start (tapping-in) time of a trip (e.g., '08:00:00')
Ride distance	End (tapping-out) time of a trip (e.g., '08:00:00')
Fare	The fare paid
Transfer Number	All trips in one journey are labeled 0,1,2,$\cdots$

greatly improved the overall speed and efficiency of public transport systems. Commuters do not have to check fares in advance, as they can just present their cards and the system will calculate fares using service number, direction and boarding/alighting stop/stations to deduct payment from each card directly. The data set in Singapore records not only boarding but also alighting activities, with both stop/station information and time stamps. Using such a data set, one can reconstruct historical transit use patterns in an individual level.

Figure 2.1 shows how the system generates transaction records for each tapping-in/out activity. Essentially, the system first creates a temporary transaction when a user taps in on a bus or at train station, and then generates a full transaction in the database after the same user taps out.

One of the main purposes of this system is to decrease cash transactions, lowering the cost of handling cash and minimizing the traditionally disproportionate impact on ticket cost. After introducing the system, transit agencies and users enjoyed a successful switch from cash to smart card payment. Although cash payment is still available, payments made by smart card systems can enjoy fare discount for a single trip from 4% to 10% and additional transfer rebates, covering 97% of total transit trips in Singapore in the year 2008. The use of smart card system has greatly improved the overall speed and efficiency of public transit systems.

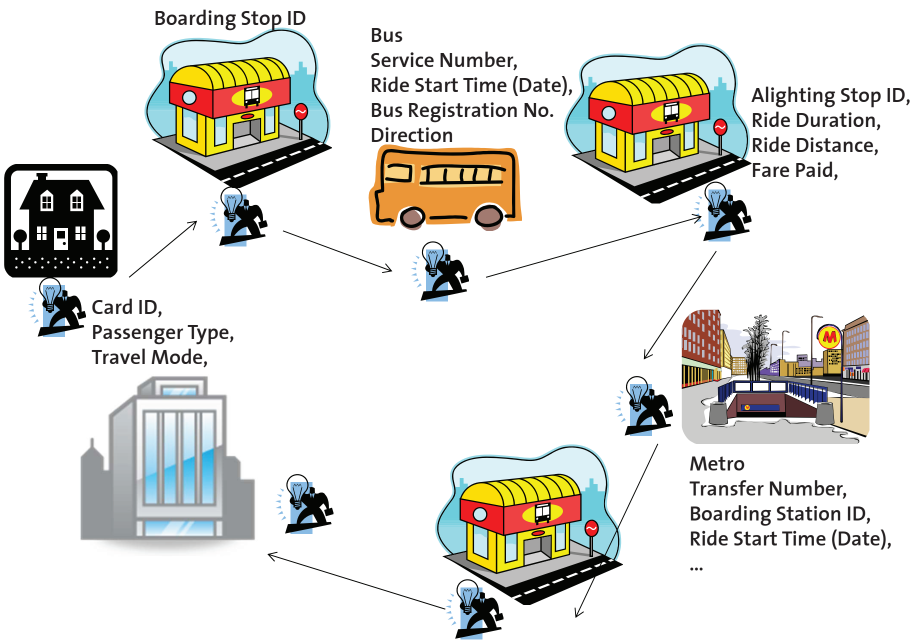

Figure 2.1: The information recorded in smart card transactions

Commuters do not have to check fares in advance, as they can just present their card and the system will calculate fares using service number, direction, and boarding/alighting stops to deduct payment from each smart card. Different from other smart card systems with no information about alighting (Barry et al., 2002; Munizaga and Palma, 2012), the system in Singapore records not only the boarding activities but also the alighting activities. When a user is tapping in or off from a bus, the timings, stop ID and user ID are recorded. Apart from the spatial-temporal records, the registration number of each vehicle and the passenger type (children, adult, senior citizens) are stored. Thus, given its rich content, the smart card data enables us to reconstruct the operation log of each bus.

Despite the privacy concerns of personal location and personal tracking (Clarke, 2001), the smart card data have received extensive attentions because of the huge potential in transit planning and operation. This section provides a general review on previous studies which utilize smart card data at different scales as summarized in (Pelletier et al., 2011). A comprehensive review of the use of smart card data in public transport research could be found in (Pelletier et al., 2011). Table 2.2 provides a general list of the application of smart card data in different scales and levels.

Table 2.2: The use of smart card data at different scales and benefits

Scale	Level	Benefits
Long-term	Strategic-level	understanding transit use patterns understanding individual behavior characteristics. network/route planning and adaptation uncovering travel behaviors supplementary/replacement of household surveys measuring network performance
Medium-term	Tactical-level	helping service adjustment estimating OD matrices linking trip segments to journeys modeling demand evolution measuring service load profile data fusion with AVL, APC, GPS, etc
Short-term	Operational-level	extracting operation log Measuring service level improving travel experience

2.1.1 Long-term: planning

In long-term scale (or at strategic level), smart card data have potential in better understanding transit use patterns. Travel behavior and transit use patterns of transit users are of major interests to researchers and transit agencies. In exploring these patterns, previous approaches are mainly based on household/field surveys. However, with the application of automated fare collection systems, the smart card data can actually provide increasing potential in further understanding travel behavior and transit use patterns at both individual and collective levels.

Bagchi and White (2005) employed personal smart card transactions to study the consistency of transit behavior over time. By grouping passengers according to the pre-defined user types, Agard et al. (2006) analyzed and compared transit behaviors/habits across different behavioral groups. They found that public transport users can be divided into four groups given their transit use behavior patterns, which are invariant of ticket types. Utsunomiya et al. (2006) took advantage of the personal information from smart card data by providing an announcement service to passengers, making it possible for users to follow alternative itineraries based on real-time service level and other travel information. Using smart card data collected over nine months, Morency et al. (2007) measured the variability and temporal dynamics of the usage of transit networks. Measures of spatial-temporal variability were defined and estimated to understand the periodic transit use patterns. Using the smart card data from Chicago rail, Mojica (2008) examined the travel behavior patterns by checking the relative proportions of bus commuters and rail commuters with a binary logit model, which is proposed to estimate user shift from rail to bus.

By using the age information of smart card holders, Eom and Sung (2011) analyzed travel behavior of the elderly and showed its temporal differences from young people in Seoul, South Korea. Furthermore, they found that the elderly are less willing to transfer between services compared with the young. By identifying transfer activities from smart card transactions of Seoul, the transfer patterns and transfer location choices are studied in Jang (2010).

The use of smart card data also shows endless potential compared with traditional household/field surveys. Trépanier et al. (2009b) compared smart card data with household survey data on bus use patterns and spatial/temporal distribution of bus trips. The study suggests that the accuracy and quality of survey data can be improved by incorporating smart card data. Chu and Chapleau (2010) also stated the advantages of passively collected data such as smart card transactions, which provide high-resolution information at both spatial and temporal scales. The authors also proposed a methodology to characterize monthly transit trips patterns with multi-day information.

2.1.2 Medium-term: application

As Figure 2.2 shows, three operations-planning categories are identified: (1) data collection, (2) analysis results and (3) relevant service elements. The studies on medium-term mainly focus on service adjustment by extracting and analyzing useful information from smart card data. The common approaches are listed as follows:

- create OD (Origin-Destination) matrices,
- create trip tables by linking stages with transfers, and
- model demand evolution.

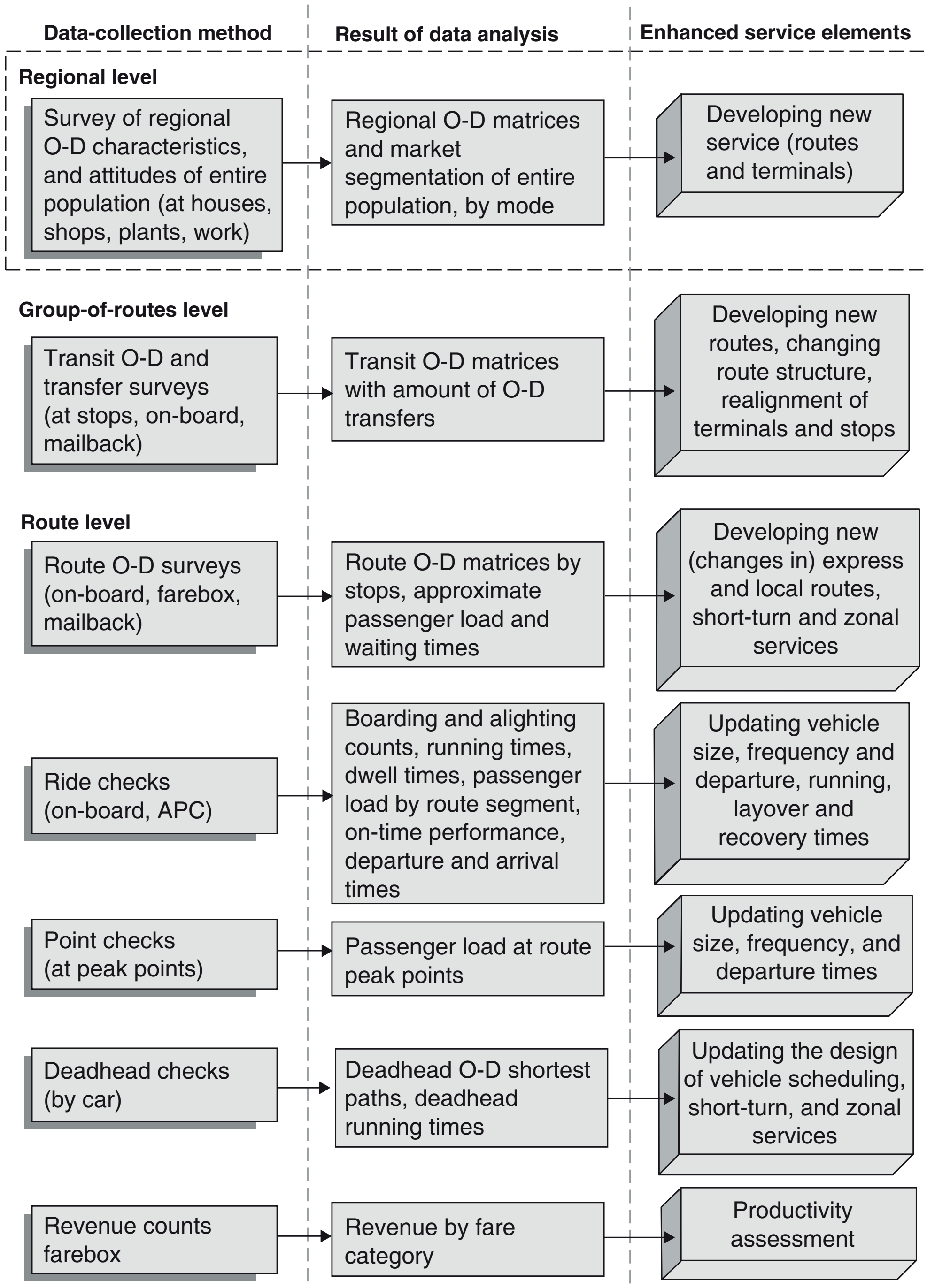

Figure 2.2: Conventional data collection methods and resultant analysis and service elements (adapted from Ceder (2007))

OD Matrix

The OD matrices are fundamental inputs for most transportation planning and operation analyses. However, using conventional physical surveys, it is always difficult to obtain a well-estimated OD table given limited sample size.

For public transport services, a route-level OD matrix plays an important role in estimating the loading profile of each service run and further adjusting service operation accordingly (Simon and Furth, 1985). To get such data, a common approach is to use on-board check to register each boarding/alighting activity. Compared with this labour intensive approach, the AFC system can also provide accurate boarding/alighting information, however, in a passive and more efficient way.

For those AFC systems without alighting information, it is important to make accurate inference of alighting stop for each individual record. Trépanier et al. (2007) first dealt with the unknown alighting location problem and proposed an algorithm to estimate the most probable alighting stop. Then, based on the detailed boarding/alighting information, the loading profile over the route for each service run can be estimated as well. This method is further improved in (Munizaga and Palma, 2012) in order to handle data from metro systems without direction information.

In terms of bus systems, it is also a primary task to infer the exact vehicle each passenger takes when vehicle information is not available in the data set. Bagchi and White (2004) employed personal trip data and proposed a model to identify the unique bus that a passenger may take from a pool of possible services, making statistics on each service run which could be used for further service adjustment (Bagchi and White, 2005). With the fusion with automated passenger count (APC) data and automated vehicle location (AVL) data, smart card data showed great potential to estimate OD matrices not only at a single route scale, but also at a network level for urban bus systems (Cui, 2006). Similarly, Farzin (2008) estimated bus OD matrix in Sãn Paulo, Brazil. To make an accurate estimation, the proposed processes combine three data sources together, including AVL data, AFC data and the profiles of bus stops.

The OD matrix can be directly obtained from smart card transactions for metro systems with both enter and exit controls (such as Washington Metropolitan, Singapore MRT, and London Underground). However, in terms of a entry-only metro system like Boston, Chicago and New York, the key for OD estimation is to identify the destination for each trip. Barry et al. (2002) developed a method to estimate the OD information based on a couple of rule-based assumptions, for instance: 1) most successive trips start at the destinations of previous trips, and 2) the last trip over one day ends at the origin station of the first trip of the next day. Similarly, Zhao et al. (2007) and Zhao (2008) worked on the entry-only metro system in Chicago. The authors took advantage of the patterns of an individual's consecutive transit trip segments, which are defined in a similar way as in (Barry et al., 2002). The authors also stated that the AFC system has the potential to provide richer information to better support decision making, however, with lower marginal cost. By considering the difference between egress and access activities, Chan (2007) estimated not only the OD matrix, but also various time cost such as walking times between gantries and platforms, waiting time at stations, in-vehicle travel time on train services, and in particular the interchanging cost from one line to another.

Trip Table

Smart card data also provides an opportunity to identify linked journeys, which occur when one travels from origin to destination using multi-services and multi-modes. In order to link trip segments to a whole journey, the transfer activities should be identified first. Since the AFC system records each transit trip by the corresponding tapping activities, it also enables researchers to study transfer activities in detail.

Based on data from magnetic cards — which is similar to a smart card — Hofmann et al. (2009) proposed a model to identify linked trips automatically at trip level. Barry et al. (2009) presented a case study on New York transit networks, including both bus and metro services. Since the AFC system in New York is an entry-only system, the authors first solved the destination inference problem and then identified the route and specific boarding/alighting stops for each transaction. If an individual took consecutive transit services, the corresponding multiple trip segments should be combined as a linked journey. Seaborn et al. (2009) also proposed a method to identify complete journeys from transactions of Oyster card data in London. The authors also provided additional information on route choices to transit users, which help travelers to minimize number of transfers in the whole journey. Combining smart card data with automated vehicle location (AVL) data, Gordon et al. (2013) tried to infer the journeys of all riders on a large public transit network have been built for analyzing passenger behavior. Using the proposed model, transfer activates between passenger trips of various public modes, and origin-destination matrices of linked intermodal transit journeys that include the estimated flows of passengers not using smart cards were constructed.

Similarly, Jang (2010) analyzed transfer activities based on data from Seoul. The author found that many transit users take advantage of the 30 min transfer interval to reduce their travel cost, resulting in irrational identifications.

Modeling Demand Evolution

Given its high spatial-temporal resolution, the smart card data also play an important role in modeling the evolution of transit demand over long term.

Utsunomiya et al. (2006) studied the day-to-day variation of transit demand to address the problem that whether different schedules should be applied given the variation of demand instead of a fixed schedule over all weekdays. Given that AFC system provides continuous stream of detailed data, Chu and Chapleau (2008) proposed a model to estimate the arrival time of each service run. Various information about transit demand can be extracted afterwards, such as spatial-temporal distribution of boarding activities, service loading profile and travel itinerary of each individual user. With the continuous stream of smart card data, a comprehensive transit demand profile can be drawn from the daily and seasonal demand evolution, contributing to future analyses such as route design, network adjustment and service scheduling. Taking the historical data in Seoul, Park et al. (2008) studied the trend of transit demand and created a future demand matrix for long-term transit planning. Chapleau et al. (2011) proposed a modeling framework of data fusion and presented the application of assessing service level and generating demand indicators. Asakura et al. (2012) studied the behavioral change of metro passengers using long-term smart card observations. The authors found that rail passengers are smoothly changing their travel behavior (departure time) to new service timetables. In a recent study, Kusakabe and Asakura (2014) developed a data fusion methodology to estimate and better understand behavioral attributes of passengers during monitoring their smart card transactions. The authors showed that the methodology can be applied to find and interpret passenger behavioral features observed in the smart card data, which had been difficult to obtain from each independent data set.

2.1.3 Short-term: operation and assessment

At the short-term scale, smart card data can be used to assess the performance of transit systems using various indicators. For instance, on supply side we may use schedule adherence, average waiting time, vehicle-kilometers, vehicle-hour and commercial speed as service level indicators, while on the demand side the indicators include person-kilometer, person-hour and average trip length (Trépanier et al., 2009a). Within an evaluation or assessment framework, these indicators and measures allow transit agencies to monitor service levels with available data collected during daily public transport operation. In fact, given the way that smart card data works, AFC can play as the replacement of automated vehicle location (AVL) and automated passenger counting (APC) systems (Hickman, 2001). For example, Chan (2007) estimated the reliability of journey time empirically and Uniman et al. (2010) showed the potential of using smart card data to quantify service reliability of London Underground.

By using data mining techniques, Morency et al. (2007) explored the variability of transit use patterns. From the authors' experiments, it is possible to calculate an individual's regularity indicators even little personal information is available. On one hand, this study shows the potential of smart card data on understanding individual human behavior and human dynamics, which are new research fields where smart card data may play an important role. On the other hand, it is suggested that the smart card data from each individual may help the owner of trip planning in return (Utsunomiya et al., 2006).

2.2 Smart Card Data in Transit Reliability

In view of commuters' increasing expectation for a more comfortable and efficient transit system, service enhancement programs are established to improve the overall bus service provision globally (Land Transport Authority, 2008). In terms of research, there are also a large number of studies focusing on transit reliability, in particular for bus systems.

Bus bunching is a universal phenomenon of public transport systems and a vital factor of determining service reliability. As first studied in Newell and Potts (1964), bus bunching is natural effect since service schedules cannot remain stable partially due to the uncertainty of the number of boarding and alighting of passengers and the variability in traffic conditions and hence travel time in between stops. Furthermore, the driving behavior of the bus captain is also considered as one of the factors leading to bus bunching (Strathman et al., 2002). One approach to address bus bunching and to maintain the service schedule is to add slack time into the schedule. However, too much slack time may cause the slowness of the buses and the reduction in service frequency (Daganzo and Pilachowski, 2011). In (Zhao et al., 2006), a model to determine optimal slack time to be inserted into the schedule is proposed by minimizing the expecting waiting times of the passengers. In many cities, the majority of typical urban bus services run at least in peak times with headway shorter than 15 minutes. In such a situation, the schedule-based strategy may cause additional on-board waiting time. To avoid this, service operators tend to adopt some other strategies, of which the most studied is the holding strategy (Abkowitz et al., 1986; Barnett, 1974; Eberlein et al., 2001; Hickman, 2001; Fu and Yang, 2002; Sun and Hickman, 2008; Xuan et al., 2011). Given its importance in daily operation, research on easing bus bunching is still very active nowadays. Here we only list some of them as examples and more literature on this topic could be found in Chapter 3, in which we also study bus control problem by identifying optimal control stops for long trunk services.

Previous studies on real-world transit reliability problems were mainly supported by survey data and other manually collected data (Turnquist, 1978; Turnquist and Blume, 1980). Over the last two decades, the field has seen an increasing interest and need in using automated collected data to better support the modeling of urban transit reliability (Furth and Muller, 2007). For example, the development of automated vehicle location (AVL) and automated passenger counting (APC) systems has facilitated researchers to monitor and improve service reliability at the operational level (Eberlein et al., 2001; van Oort et al., 2010; El-Geneidy et al., 2011). Although automated fare collection (AFC) system is more advantageous in terms of quantity and quality of the generated data, only a few studies have made use of smart card given the missing of real-time property. However, the large quantities of detailed time-stamped transaction actually shed new light on passenger demand and behavior modeling. We introduce a study on passenger boarding/alighting dynamics in Chapter 4.

Smart card data are playing an increasingly important role in enhancing urban transit service level and reliability at the operational level (e.g., Chan 2007; Uniman et al. 2010;

see Section 2.1.3). Despite the study on travel time reliability, smart card data also play an important role in answering some emerging research questions in rail operation. Kusakabe et al. (2010) studied passenger-to-train identification problem in metro network. Passenger demand information is valuable for designing service timetables and disruption prevention. However, in a close metro system where passengers only leave traces at fare gantries at boarding and alighting stations, passenger train choice is difficult to infer. The authors present a methodology and algorithm to infer passenger's train choice using long-term transactions. We study a similar problem in Chapter 5 using a different approach. This problem becomes more complicated at a network level since it is also difficult to infer passenger route choice with only travel time observations. Zhou and Xu (2012) and Zhu et al. (2014) studied flow assignment problem using smart card data, however, with different approaches. In (Zhou and Xu, 2012), the author developed a passenger route identification approach based on maximum likelihood boarding plan, which is similar to the approach in (Kusakabe et al., 2010). Zhu et al. (2014) focused on another aspect: using smart card data to calibrate a pre-defined passenger flow assignment model. The calibration approach employs a genetic algorithm-based framework with nonparametric statistical techniques. The authors concluded that the proposed approach performs better than conventional approaches and the calibrated model delivers more accurate flow assignment results. In this thesis, we also explore the passenger route choice inference problem in Chapter 7, together with the modeling of metro travel time reliability. Niu and Zhou (2013) studied the train timetabling problem under a dynamic passenger demand scenario and how services behave when passenger demand exceeds their designed capacity. The authors developed a genetic algorithm to optimize timetable scheduling for a single track and applied it on a real case with 13 train stations. This problem is also studied in this thesis in Chapter 6.

Chapter 3

Understanding Bus Service Reliability Using Smart Card Data

Chapter information

A conference paper based on this chapter was published in *12th Asia Pacific ITS Forum & Exhibition*: Lee, D.-H., Sun, L., Erath, A., 2012. Study of Bus Service Reliability in Singapore Using Fare Card Data, *12th Asia Pacific ITS Forum & Exhibition*, Kuala Lumpur, Malaysia.

A conference paper partly based on this chapter was published in *1st Symposium of the European Association for Research in Transportation*: Lee, D.-H., Sun, L., Erath, A., 2012. Determining optimal control stop to improve bus service reliability. *1st Symposium of the European Association for Research in Transportation*, Lausanne, Switzerland.

For public transportation service, schedule reliability is generally a central point in the service level agreement. However, bus bunching is a very common phenomenon in fleet operation, resulting in more waiting time for passengers. Based on smart card data, this chapter presents a case study on the reliability of one typical service route in Singapore. Characteristics such as headway distribution and average velocity are available from smart card data are employed for measuring service reliability and developing optimization tools for reorganizing bus routes. More importantly, real information from smart card data about boarding time, origin and destination stops of the trips is available for formulating a simulation scenario to test the performance of different control strategies based on real passenger demand. We are allowed to conduct simulation experiments on the observed passenger demand to compare bus service on the case route, which is characterized with relatively frequent services and featuring more than 70 stops. We propose two models to determine optimal holding/control stop, where buses are allowed to hold to avoid bunching. We examine the results of the two models based on real passenger demand data extracted from smart card data and then test their performance using the proposed simulation framework. Although the two models have different objectives, a consistent optimal solution is obtained.

3.1 Introduction and Overview

For public transportation service, schedule reliability is generally a crucial point in the service level agreement. Unreliable bus service can lead to longer waiting time and traveling time for passengers. However, bus services are born unstable due to various reasons. Generally, buses leave their departure station at regular intervals, namely the headway. But the intervals become irregular with buses traveling along the route (Barnett, 1974). Reasons can be summarized into two aspects: the first of which is the randomness of passengers' arrival at certain bus stops. When a bus falls behind its schedule, the headway with the preceding bus will become longer while the one with the following bus will become shorter. In other words, this may cause more passengers waiting at the approaching stop then result in more boarding time and make the bus fall further behind (Newell and Potts, 1964). The second reason is variability of travel time between stops owing to traffic congestion, signal control and the difference of bus captains' driving behavior.

The challenge of improving bus service reliability has been addressed by several researchers. In (Barnett, 1974), a headway threshold based control strategy was developed, which aimed at minimizing the waiting time of the passengers at bus stops and the delay of the on-board passengers. When the bus arrives at the stop with headway less than the threshold, it will wait until the threshold is attained. Otherwise, the bus will depart immediately when the headway becomes greater than the threshold.

In terms of bus route services with high frequency, because of the acceptable expected average waiting time, passengers have a tendency to arrive without a prearranged schedule. For this situation, headway based control strategies were implemented in (Abkowitz and Tozzi, 1986; Abkowitz et al., 1986; Abkowitz and Lepofsky, 1990). However, in these models, normally instead of actual data on the distribution of travel time and passenger demand, generic distributions that do not account for potential spatial correlation are employed. With the development of Intelligent Transportation Systems (ITS), real time data are available to service operators from automated vehicle location (AVL) systems, automated passenger counting (APC) and computer aided dispatching (CAD) systems (Eberlein et al., 2001; Zhao et al., 2003; Pilachowski, 2009; Daganzo, 2009a; van Oort et al., 2010). A model based on historical AVL data was also proposed to improve the service level (Horbury, 1999). In (Daganzo, 2009b) and (Pilachowski, 2009), models were proposed assuming that buses can adjust their velocity to maintain equal headway. To give a better picture, bus route service is explained as a system in which all buses are connected by springs and magnets with tension and attractive forces in (Daganzo, 2009a).

Meanwhile, analytic studies and mathematical models are conducted by some researchers. Mathematical models based on random process trying to minimize passenger waiting time at stops and additional on-board waiting time caused by bus holding (Osuna and Newell, 1972; Hickman, 2001; Zhao et al., 2006). In (Adebisi, 1986), headway variance was analyzed to provide more reliable services. In the field of practical application, a distributed architecture of bus holding was built with real time coordination taken into account (Zhao et al., 2003). In (Xuan et al., 2011), dynamic bus holding strategies were proposed to achieve schedule reliability and a comparison of different control methods was also conducted.

All the above control strategies and analytic studies can be summarized as holding strategies. To solve the problem on another aspect, stop-skipping strategies were implemented in (Suh et al., 2002; Fu et al., 2003; Sun and Hickman, 2005). Furthermore, a mixed model approach taking the bus capacity into account as well as holding and stop-skipping strategies was proposed in (Delgado et al., 2009). Simulation approaches are also conducted simultaneously. In (Turnquist and Blume, 1980; Koffman, 1978; Adamski and Turnau, 1998; Ding and Chien, 2001), different strategies are simulated to see how the buses run along a certain route. Some of simulations were conducted based on real-life bus services to give a more intuitive explanation and more realistic recommendations.

This remainder of this chapter is organized as follows: in Section 3.2, we introduce the smart card data and the case route studied throughout this chapter; in Section 3.3, we investigate the operation characteristics of the studied bus service, including headway distribution, operational speed and spatial-temporal occupancy profiles. In Section 3.4, we build two models in determining optimal control stop for buses to hold and avoid bunching. Section 3.5 presents the results of the proposed models based on demand data obtained from smart card transactions. Finally, we conclude our study, summarize our main findings and discuss future research directions in Section 3.6.

3.2 Data Analysis

3.2.1 Data preparation

The smart card based automated fare collection system was introduced in Singapore in April 2002 to provide simplified fare collection in public transportation as stored value contactless smart card. Today, smart cards are used island-wide for various purposes, such as public transportation, parking and road toll payment, and retail transactions. However, the most frequent application is still the payment method for public transportation. Cash payment is still possible for public transportation users, but subject to a higher charge rate, wherefore the smart card payment covers 96% of all the public transportation trips in Singapore (Prakasam, 2008). This makes the trip record data retrieved from smart card a highly comprehensive data source for research purpose.

The fare charge for each public transportation trip is calculated on trip distance, trip modes and passenger types. There are different charge rate for children, students, senior citizens and adults. Passengers have to tap their smart card on the reader when they enter or leave the MRT stations or boarding and alighting buses. When the passenger finishes a trip, a full record will be created which contains boarding time and alighting time, boarding station and alighting station, and the unique registration number of the bus taken by the passenger. The analysis is based on the smart card data recorded in one full week (from 11, April, 2011, Monday to 17, April, 2011, Sunday) in Singapore.

3.2.2 Case service route

In this chapter, the case service chosen to analyze the reliability of bus services is the busiest service according to the data set prepared. The service route under study, with 71 stops along the route and total length of 27.6 km, has the most trip records in the one week's data set.

The raw data in this study is based on single passenger trips. Generating detailed information of bus service like occupancy, velocity, arrival and departure time at each bus stop is not straightforward. To conduct the case study, the data needs to be processed in order to obtain bus-specific information such as arrival and departure time as well as occupancy.

3.3 Service Characteristics

3.3.1 Headway and distribution

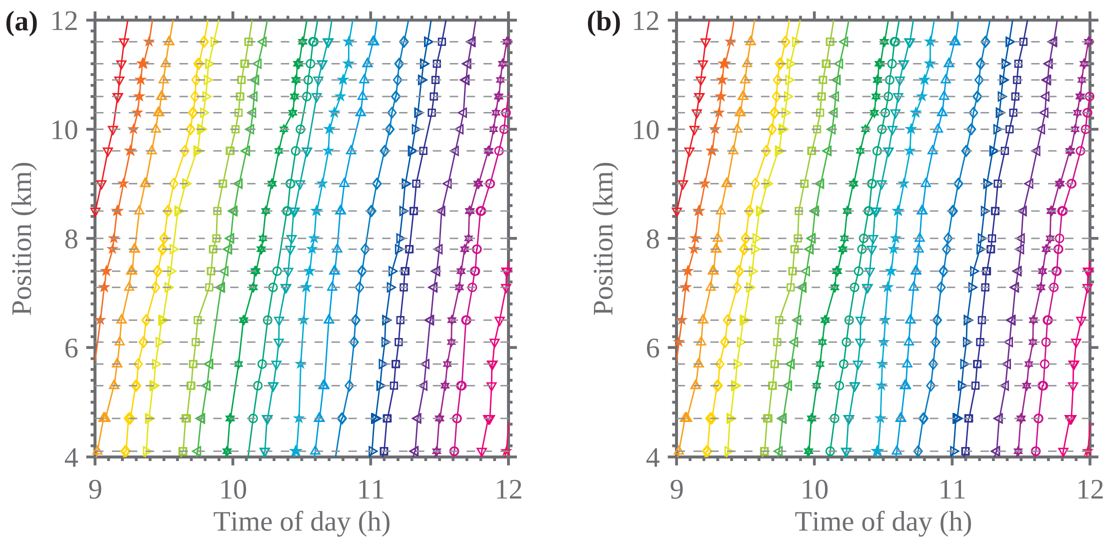

Figure 3.1: Bus Trajectories from the case route. (a), origin trajectories from smart card data. (b), processed trajectories with interpolation.

Considering the boarding and alighting process when the bus approaches and arrives at a certain bus stop, passengers will tap their card to leave before the bus arrives at the next bus stop. At the same time, the waiting passengers will board and tap after the bus arrival.

Therefore, it is reasonable to consider arrival time of bus as the boarding time record of the first passenger who boards. The departure time is considered as boarding time or alighting time of the last passenger who boards or alights. However, if there is no passenger boards or alights at the stop which means the bus passes the stop, no information is recorded. Based on this assumption and the location of certain bus stop, the spatial temporal point is recorded for the bus as long as there are passengers boarding or alighting at the bus stop. For the bus stops without records, the arrival and departure time are obtained based on linear interpolation. Figure 3.1 shows the trajectories of the case route from 9 a.m. to 12 p.m. in the morning, of which Figure 3.1(a) presents the original trajectory while Figure 3.1(b) presents the processed trajectory with interpolation at unrecorded points.

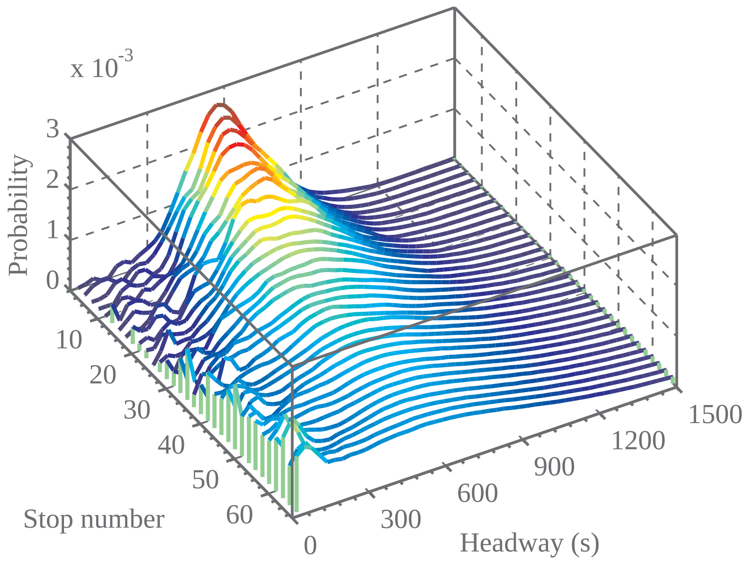

Figure 3.2: Headway distribution along the case route

As can be seen in Figure 3.1, the headways of buses passing certain bus stops are easily interpolated based on the trajectory. To have a more intuitive impression on how the headways change with the buses running along their route, the probability distribution of headways along the case route based on weekday records (11, April, 2011 to 15, April, 2011) are plotted in Figure 3.2. The buses were able to keep headways stable at the beginning segment, but with the buses traveling further, the distributions become more and more widely distributed. The headways increasingly diverge from the origin schedule.

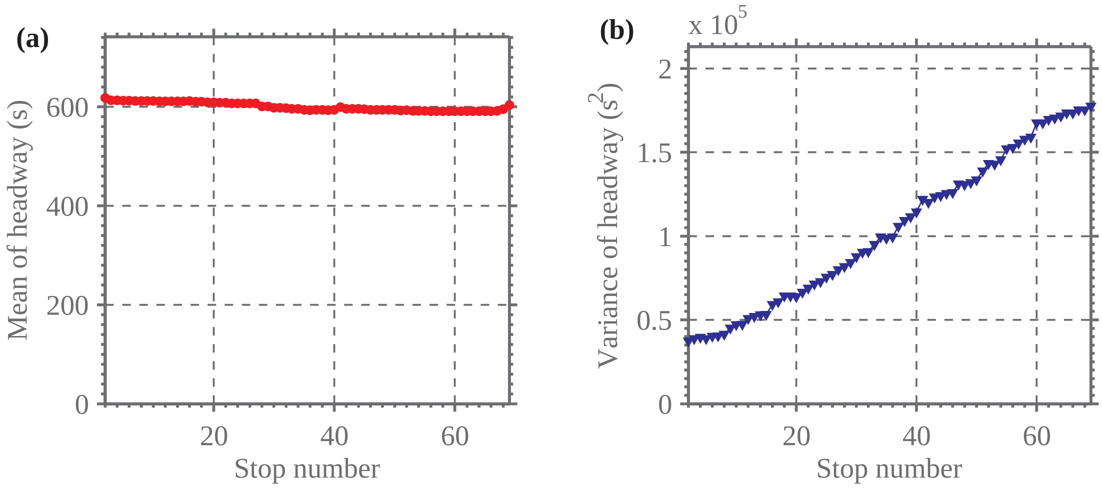

Figure 3.3: Mean and variance of bus headway along the case route

Figure 3.3 shows the change of mean and variance with the stop sequence, when considering the headway of each stop as a random variable. The mean values do not change substantially because of the scheduled operating time of the service. However, the variance almost continuously increases along the route, which means the headways become more irregular and passengers are facing more uncertainty of the service when the buses traveling forward (van Nes and van Oort, 2009). Assuming uniformly distributed arrival times of passengers at the bus stop, this pattern causes waiting times above the average mean value of headway as two buses arrive at the same time with one bus overcrowded and the other almost empty.

3.3.2 Commercial speed

Average velocity is another significant measurement of the service level, which can reflect the travel time spent on the bus. Figure 3.4 shows how the average velocity of the case route changes against time of day. The pattern of how velocity varies does not change very much from Monday to Friday. Therefore, it is reasonable to analyze the average velocity of weekdays together. The red line in Figure 3.4 summarizes the average velocity in 5 weekdays. It can be seen that the travel velocity remains fairly constant from early morning till 3 p.m., followed by a significant decrease of velocity till to 7 p.m. Afterwards, the velocity starts to increase again and reaches the highest value at midnight. Taken the real time traffic of Singapore into

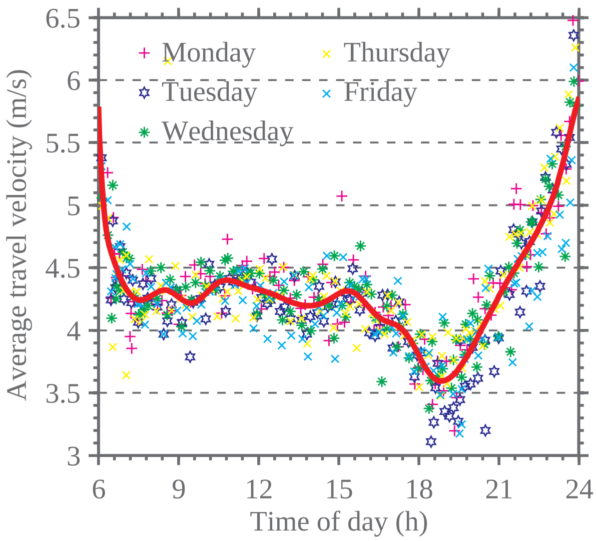

Figure 3.4: Average velocity over time of day

consideration, what has been shown in Figure 3.4 is correlated with the traffic condition, since 5 p.m. to 8 p.m. is the peak time of traffic in Singapore and there are so few passengers and cars in the night that the buses can travel at a very fast velocity. However, the morning peak of traffic seems not to influence the average speed of the service route under study.

3.3.3 Occupancy profile

By incorporating all the boarding and alighting transactions on each vehicle, we can get the occupancy profile at a any stop at certain time. For example, Figure 3.5 maps the spatial-temporal service occupancy profile on vehicle trajectories. We see clearly that bus bunching start to occur after 5 km and turn worse at 15 km. Due to bus bunching, we also observed an unbalanced service occupancy: the leading bus in a bunched cluster is usually full of passengers, while those following have less on-board passengers. This figure suggests that bus bunching may lead to substantial waste of service supply, making it even difficult for operators to respond to the increasing passenger demand nowadays.

In the next section we build two model to determine optimal holding stop, which allows operators to add additional slack time for each services run to avoid potential bus bunching.

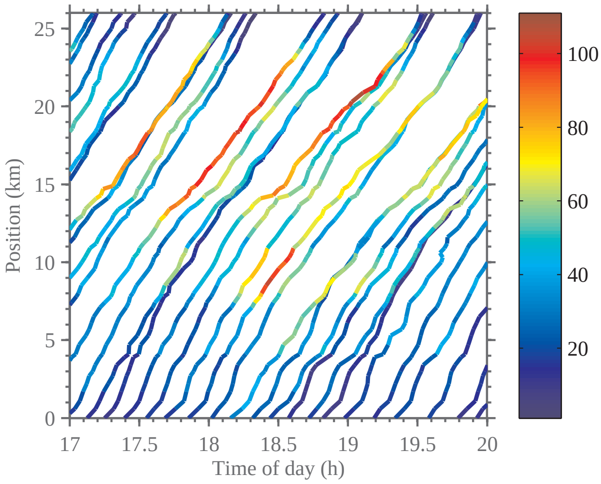

Figure 3.5: Spatial-temporal occupancy

3.4 Determining Holding Stop

Bus bunching is a common problem of public transport in cities and a vital factor of determining service reliability. The service schedule cannot remain stable because of both the uncertainty of the number of boarding and alighting of passengers, and the variability in traffic conditions and hence travel time in between stops. Furthermore, the driving behavior of the bus captain is also considered as one of the factors leading to bus bunching (Strathman et al., 2002).

One approach to alleviate bus bunching and to maintain the service schedule is to add slack time into the schedule. However, too much slack time may cause the slowness of the buses and the reduction in service frequency (Daganzo and Pilachowski, 2011). In Zhao et al. (2006), a model to determine optimal slack time inserted into the schedule is proposed by minimizing the expected waiting time of the passengers.

Different from the previous studies, we will not focus on how but where to control services and propose a methodology to determine the optimal position of the control stop along a service route. The application to a real scenario is demonstrated based on a simulation which is sourced by detailed data on effective traffic patterns for a bus line in Singapore. It builds on an study by Fu and Yang (2002), which concluded that control stops should have the following properties:

- a high level of boarding demand, and

- close to the middle of the service route.

The main contribution is a formalization and simulation-based implementations to find optimal control stops. To this means, two different models to determine the position of the control stop including demand patterns are presented.

3.4.1 Models to determine the holding stop

For a certain route service with M stops and N buses running on, the departure time of bus k at stop i is defined as $t_{i,k}$. For any stop i, the headway between bus $k+1$ and its preceding one (bus k) is determined by:

$$H_{i,k} = t_{i,k+1} - t_{i,k}, \tag{3.1}$$

where $i = 1, 2, \cdots, M-1$ and $k = 1, 2, \cdots, N-1$.

The number of passengers who board on stop i and alight on stop j is defined as $B_{i,j}$, which is the value from the OD matrix for the service.

In this study, if stop m is chosen as the control stop where buses will be rescheduled, the headway for stop m are set to be the same as the initial terminal (stop 1). If the a bus reach stop m within the headway interval, it will wait until the intended headway is reached, otherwise, an empty bus will depart from stop m. Under this assumption, determining a control stop is similar to the strategy of cutting a bus service into segments.

3.4.2 Waiting time-based model

This model tries to find the position of the control stop by minimizing average waiting time of all passengers. which includes both waiting time at the bus stop and the additional on-board waiting time for the passengers travel through the control stop.

If more than one bus arrives the control stop within the same interval, the passengers on the following buses are forced to transfer on the first bus without costing extra time to depart earlier.

The expectation of passenger waiting time of at a certain stop i is given by (Osuna and Newell, 1972):

$$E(w_i) = \frac{1}{2}E(H_i)\left(1 + \frac{Var(H_i)}{E^2(H_i)}\right) = \frac{1}{2}E(H)\left(1 + \frac{Var(H_i)}{E^2(H)}\right). \tag{3.2}$$

The second part of Eq. (3.2) refers to bus operation of a whole day. The expectation headway for any stop i is:

$$E(H_i) = E(H). \tag{3.3}$$

As mentioned in Section 3.3, in reality the variances of the headways increase almost linearly with stop sequence if no control strategy is imposed. The analytic mathematical model presented in Adebisi (1986) also shows that the main factors which influence headway variance are bus loading conditions and traffic conditions along the service route. In this study, the variability caused by changing in traffic conditions is not considered.

For one stop, the increase in variance from preceding stop is assumed to be in proportion to the number of boarding passengers. The headway variances at start of the route (stop 1) and terminal (stop M) are readily available for service operators, which are $Var(1)$ and $Var(M)$ respectively. Thus, headway variances at other stops can be calculated as:

$$Var(i) = Var(i-1) + \frac{Var(M) - Var(1)}{\sum\limits_{i=1}^{M-1}\sum\limits_{j=i}^{M} B_{i,j}} \cdot \sum_{j=i-1}^{M} B_{i-1,j}, \tag{3.4}$$

where $B_{i,j}$ represents the number of passengers who board at stop i and alight at stop j (i.e., the corresponding value in the OD matrix).

If stop m is chosen as the control stop, then it is assumed that $Var(m) = Var(1)$. For the following stops, the variance can still calculated by Eq. (3.4).

The total waiting time is the sum of three parts. Thus, the objective is to minimize the average waiting time γ:

$$\min \gamma = \gamma_1 + \gamma_2 + \theta \cdot \gamma_3, \tag{3.5}$$

where $\gamma_1 = \frac{\sum\limits_{i=1}^{m-1}\left(E(w_i)\cdot\sum\limits_{j=i}^{M} B_{i,j}\right)}{\sum\limits_{i=1}^{M-1}\sum\limits_{j=1}^{M} B_{i,j}}$, $\gamma_2 = \frac{\sum\limits_{i=m}^{M}\left(E(w_i)\cdot\sum\limits_{j=i}^{M} B_{i,j}\right)}{\sum\limits_{i=1}^{M-1}\sum\limits_{j=1}^{M} B_{i,j}}$, and $\gamma_3 = \frac{\sum\limits_{i=1}^{m-1}\left(\frac{E(H)}{2}\cdot\sum\limits_{j=m+1}^{M} B_{i,j}\right)}{\sum\limits_{i=1}^{M-1}\sum\limits_{j=1}^{M} B_{i,j}}$.

θ is the weigh factor and γ_3 is the additional waiting time to the the passengers who pass through stop m caused by bus holding at control stop. Previous studies suggest that passengers are more sensitive to at-stop waiting time than the riding time on bus using preference data, indicating that the value of weight factor should follow $\theta \in [0, 1]$.

Based on this objective function, the optimal control stops for both directions can be found. Same as (Lee et al., 2012), the arrival and departure time for every stop are estimated based on the smart card data records and interpolation of trajectories if there are no records.

3.4.3 Demand-based model

In this part, a simplified model which takes demand information (OD matrix) into consideration is proposed and discussed.

A bus service with stop m as a designated control stop, can be interpreted as two distinct route services. Intuitively, the control point should have the ability to have large direct flows in those new routes and try to reduce number of transfers.

The model is proposed based on actual demand patterns as observed by records of smart card fare collection data. δ_1, δ_2 and δ_3 represent the demand parameters of direct flow for previous stops, direct flow for after stops and flow passing the control point. Then, the objective function of this model is:

$$\max \delta = \delta_1 + \delta_2 - \delta_3, \tag{3.6}$$

where $\delta_1 = \frac{\sum_{i=1}^{m-1} \sum_{j=i}^{m-1} B_{i,j}}{m}$, $\delta_2 = \frac{\sum_{i=m}^{M} \sum_{j=i}^{M} B_{i,j}}{M-m+1}$, and $\delta_3 = \frac{\sum_{i=1}^{m-1} \sum_{j=m+1}^{M} B_{i,j}}{\sqrt{m(M-m+1)}}$.

3.5 Results and Analyses

The two proposed models are tested the same case service which has 71 stops in one direction and 74 stops in the other direction. This route has already previously been selected for the case study on service reliability, which provided the information on headway variability.

Waiting time-based model

In this case, variances for start and final terminal are $1 \times 10^4\ s^2$ and $22 \times 10^4\ s^2$ respectively. Since $\theta = 0$ means passengers ignore the additional waiting at control stops and $\theta = 1$ means that there's no difference between the on-board and at-stop waiting time. In the following analysis, θ is chosen as 0.2. Further analysis on the sensitivity of θ will presented in future works.

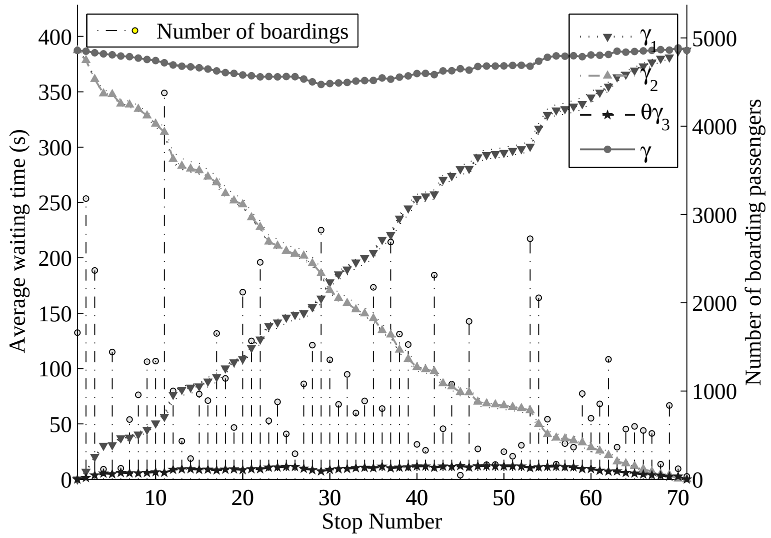

(a) Direction 1: West to East

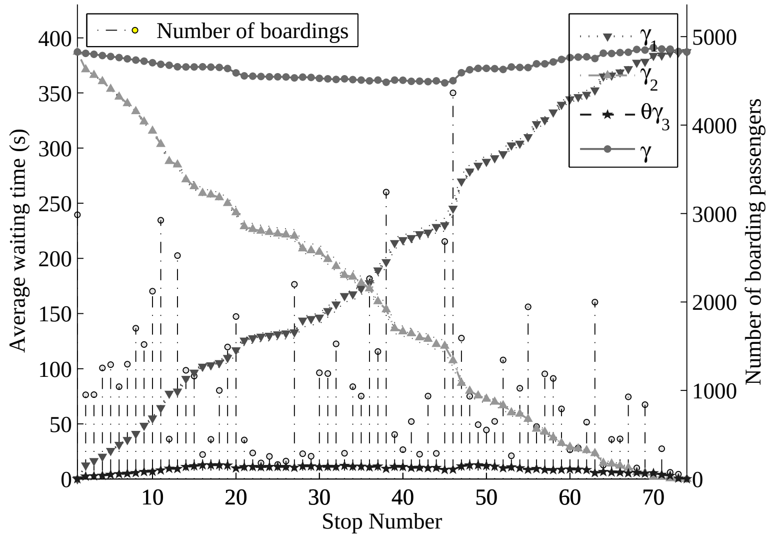

(b) Direction 2: East to West

Figure 3.6: The results on both directions from the waiting time-based model

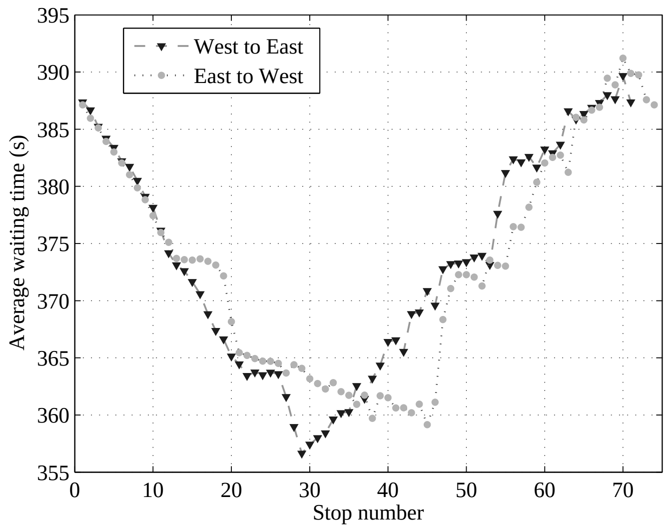

Figure 3.7: Waiting time against control stop for two directions

Figure 3.6 shows the result from the waiting time based model. The stem plots in both panels indicate the total number of boarding passengers at each bus stop. The final objective γ is shown as dotted-curves. Figure 3.7 shows the aggregated results of γ on both directions. We can see that stop 29 and stop 45 are the optimal control stop for the two directions, respectively. For such long bus services, a well-defined control stop could reduce average waiting time by about 10%. We next apply the same passenger demand data on the demand-based model.

Demand-based model

The demand-based model tries to identify a cutting stop, which can maximize the relative difference between direct trips and transfer trips. Figure 3.8 shows the result parameters calculated from the demand model. Same as Figure 3.7, the stem plots shows the total boarding demand at each bus stop. However, the y-axis in Figure 3.8 represents the objective value in Eq. (3.6). Therefore, the model actually identifies a balanced solution which tries to increase direct trips and reduce transfer trips simultaneously.

The objective of the demand-based model is different from the waiting time-based model; however, based on the value of δ, we have identified the same optimal control stops as the waiting time model.

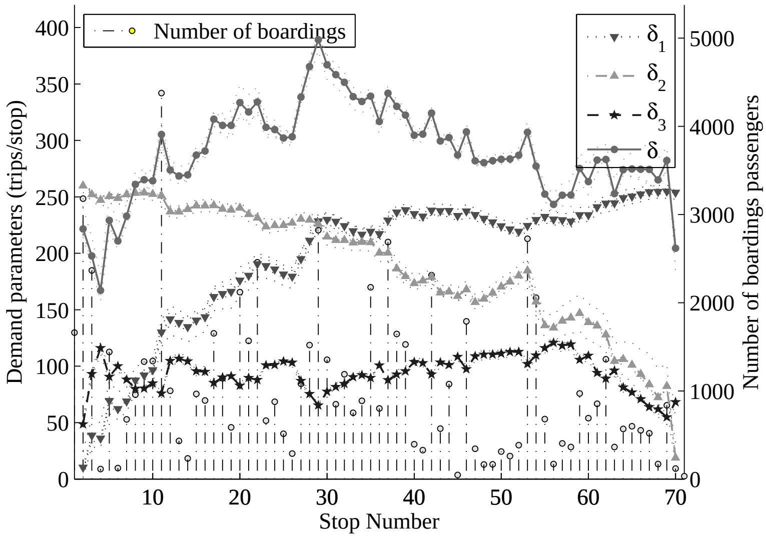

(a) Direction 1

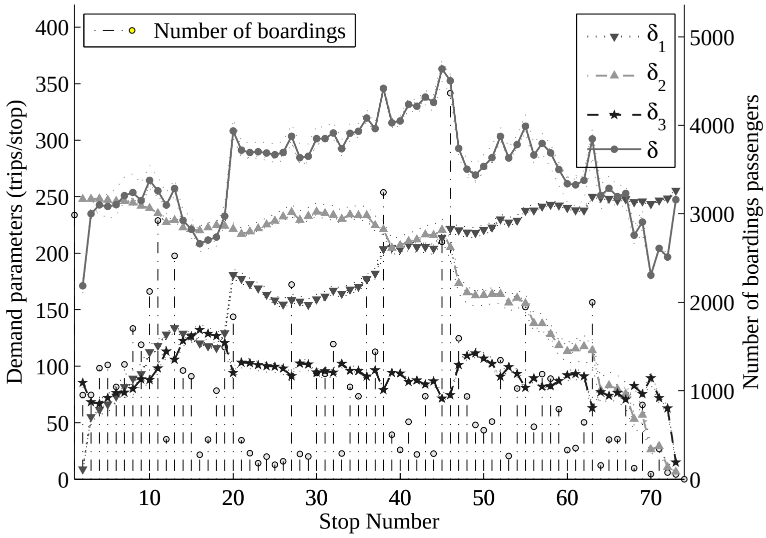

(b) Direction 2

Figure 3.8: Demand model

3.6 Summary

In this chapter, the study on bus service reliability is conducted based on smart card data to analyze the level of service of a typical route in Singapore. The smart data needs to be processed in order to obtain bus-specific information. The characteristics of a certain route were analyzed in terms of headway distribution and average travel velocity, from which it can be concluded that the unreliability increases for the chosen bus line quite linearly with increasing travel distance. Based on the analysis of the average velocity, it is also feasible to find how the traffic condition varies with time of day. For this selected route, the impact from evening peak is much more significant than the morning peak.

Two simple optimization models are proposed to determine the optimal control stop for a long bus service. Operators are allowed to add slack time at this control point to avoid bus bunching. Although the proposed models have different structures and objectives, the same optimal holding stops are identified with passenger demand data extracted from smart card transactions. We also assess the performance of the solution by conduction simulation experiments (comparing the scenarios with and without the control stops — i.e., stop 29 and stop 45 on two directions). Without inserting control stops, a fleet of 26 buses are needed. For the scenario with two control stops, the size of the fleet should be 27, i.e., one addition bus is needed compared with the original service schedule. Simulations also show that both of the control stops should have the capacity to store 3 empty buses.

In practice, for a service with two directions sharing the same route, it would be more easily to apply if the two control stops are close enough to each other. Regarding to the case service with a length of 27.6 km, stop 29 and stop 45 are located at 12.4 km and 12.3 km on direction 1 respectively. The distance between two stops is about 140 m which is adequately short to combine the control stops into a terminal. For future research, multi-services sharing the route will be considered to study the availability of building the terminal.

The study presented in this chapter is by no means complete, and the future research is needed in the following domains. First, more detailed simulations need to be developed to take more factors into consideration, such as variability of travel time between stop based on traffic condition for which historical data can be employed. Second, although bus bunching problems can be found in the simulation of the original service configuration and after cutting the bus line into two segments, there are still many factors in reality affecting bus service quality to be explored. They have the ability to expand or reduce reliability, such as the relevance of designated bus lanes, overlapping bus lines and precedence of buses at traffic lights. By enriching the detailed smart card data with information on traffic condition and organization of the transport infrastructure.

Chapter 4

Modeling Bus Boarding and Alighting Dynamics Using Smart Card Data

Chapter information

An article based on this chapter was published in *Transportation Research Part A: Policy and Practice*: Sun, L., Tirachini, A., Axhausen, K.W., Erath, A., Lee, D.-H., 2014. Models of bus boarding and alighting dynamics. *Transportation Research Part A: Policy and Practice* 69, 447-460.

Understanding the dynamics of boarding/alighting activities and its impact on bus dwell times is crucial to improving bus service levels. However, research is limited as conventional data collection methods are both time and labor intensive. In this chapter, we present the first use of smart card data to study passenger boarding/alighting behavior and its impact on bus dwell time. Given the nature of these data, we focus on passenger activity time and do not account for the time necessary to open and close doors. We study single decker, double decker and articulated buses and identify the specific effects of floor/entrance type, number of activities and occupancy on both boarding and alighting dynamics. A linear relationship between average boarding and alighting times and their respective standard deviations is also found, whereas the variability of boarding and alighting time decreases with the number of passengers boarding and alighting. After observing the cumulative boarding/alighting processes under different occupancy conditions, we propose a new model to estimate passenger activity time, by introducing critical occupancy — a parameter incorporating the friction between boarding/alighting and on-board passengers. We conduct regression analyses with the proposed and another popular model for simultaneous boarding/alighting processes, finding that the critical occupancy plays a significant role in determining the regime of boarding and alighting processes and the overall activity time. Our results provide potential implications for practice and policy, such as identifying optimal vehicle type for a particular route and modeling transit service reliability.

4.1 Introduction

The operating time of bus services comprises the driving time between stops and the dwell time at stops. Generally, the driving time between successive stops depends on the speed profile of the bus, the length of the link, and further factors such as signal control (Abkowitz and Engelstein, 1983). Driving time is modeled and estimated using a number of short-term traffic prediction methods and traffic control strategies. The other significant component of bus travel, the dwell time, is the duration of transit vehicle stopped for serving passengers (National Research Council, Transportation Research Board, 2010). Dwell time starts with the opening and ends with the closing of bus doors, allowing passengers to board and alight. Dwell time may cover a great proportion of total travel time, which shows the significance of boarding and alighting processes on bus operation. For example, Levinson (1983) found, for US operations observed from 1957-1980 in many cities, that dwell time made up about 20% of total travel time within urban areas and increased to 26% in the CBD on average, whereas Tirachini (2013b) reported that dwell time of around 23% of total travel time with on-board fare payments in Sydney.

An important issue that has received little attention in the literature is the estimation and analysis of the variability of bus dwell time, which has implications on bus operation and on the satisfaction of bus users, for whom it is valuable to have reliable public transport systems and predictable travel times. Unlike railway transit systems, for which dwell time is more controlled, the dwell time of buses has a higher variability owing to the demand variation in bus operation and generally less stringent operational constraints (Levine and Torng, 1994).

Additionally, there is the difficulty of buses to adhere to schedule due to traffic congestion or other factors. In fact, given the random nature of passenger turnover, dwell time is difficult to control even when the bus driver is experienced. As a result, the variation of dwell time is one of the major factors in the unreliability of bus operations, resulting in bus bunching and over-crowdedness (Newell and Potts, 1964; Strathman and Hopper, 1993). Apart from the randomness of demand, the dynamics of the boarding and alighting process also depend on various characteristics of the vehicles, such as the number and width of doors, the existence of steps to board and alight, the type of bus (single/double decker, rigid/articulated), the number of seats and space for standees, and the fare collection method (Guenthner and Hamat, 1988; York, 1993; Levine and Torng, 1994; National Research Council, Transportation Research Board, 2010; Dorbritz et al., 2009; Fernández et al., 2010; Tirachini, 2013a; Fletcher and El-Geneidy, 2013). Therefore, to model and estimate dwell time accurately at bus stops becomes one of the main challenges involved in predicting bus travel time.

A high variability of bus dwell times is likely to produce unreliable travel times, with negative effects for both bus operators and users, because operators have to adjust the length of slack times at terminals (Furth, 2000). Public transport users prefer reliable travel times (Bates et al., 2001; Hollander, 2006; Batley and Ibáñez, 2012), to the point that travel time variability influences users decisions on mode and route choice. Importantly, the social cost of unreliability in public transport might be significant, for instance, van Oort (2011) estimates a yearly cost of €12 million in the Hague, Netherlands, due to unreliable buses and trams. Therefore, a better understanding of travel time variability in all its components, including dwell time can be used in the operational and tactical planning of public transport operations and scheduling, and for the estimation of the economic and social benefits and costs of alternative systems of public transport service provision.

In this chapter, we analyzes passenger boarding and alighting dynamics at a microscopic user-by-user level by using individual transactions generated from the smart card-based automated fare collection (AFC) system of Singapore, in which passengers are required to tap on at the front door and suggested to tap off at the rear door(s) (Lee et al., 2012). As summarized in Pelletier et al. (2011), such data set provides new insights in reconstructing public transport operations at diverse scales, from strategic to tactical to operational management. To date, most studies utilizing smart card data focus on macroscopic characteristics such as adjusting services, designing networks, understanding demand variation and user habits, and measuring service performance, while the microscopic level is generally neglected. By constructing detailed bus operation logs we present detailed models of passenger boarding and alighting behavior under different occupancy levels and bus characteristics, and study their impact on bus dwell time. Note that such an operation log contains only passenger tapping-in/out activities, imposing an inherent limitation on our study: the time to open and close doors, which is also part of the dwell time, is unknown to us. Given the limitation of using smart card data as a proxy, we study the total passenger activity time between the first and the last tapping-in/out activities as a proxy which is called passenger activity time throughout this chapter.[1] The contributions of this chapter are twofold: First, we characterize the boarding/alighting dynamics (behavior) of users under different bus characteristics in a microscopic framework, allowing us to identify processes that have not been observed in previous dwell time studies. Second, we provide insights on the characterization of the variability of passenger activity time, an issue that can be analyzed in-depth with our smart card data. Implications for policy on bus service operation and planning follow in the conclusions.

The remainder of this chapter is organized as follows: in Section 4.2, we review existing studies on bus dwell time; in Section 4.3 the data employed in this study is described; in Section 4.4, we reconstruct the boarding/alighting processes and identify the boarding/alighting interval patterns for different types of buses. After observing the time-stamped boarding/alighting processes, in Section 4.5 we propose a new passenger activity time model for bus services on which passengers are required to board at the front door and suggested to alight at the rear door; the performance of the proposed model is analyzed in Section 4.6; and finally Section 4.7 summarizes the main findings of the study and provides the outlook for future work.

[1]Note that our analysis does not capture passenger activity time fully because if we have N passengers boarding or alighting, only $N-1$ intervals are observed: the time for the first boarding passenger and for the last alighting passenger are not computed.

4.2 Background

In exploring the determinants of bus dwell time, a number of studies have been conducted since 1970s (e.g., Kraft and Bergen 1974; Levinson 1983; York 1993; Weidmann 1994; Lehnhoff and Janssen 2003; Dueker et al. 2004; Fernández et al. 2010). The usual approach is the use of simple or multivariate regressions to relate dwell time to the number of passengers boarding and alighting, the number of passengers inside the vehicle, the number of doors and other variables. Most studies define dwell time as the time for boarding and alighting of passengers plus the time to open and close doors. Levinson (1983) modeled bus dwell time as a function of the total number of boarding and alighting passengers a bus in a bus stop:

$$Dw = t \times N + t_d, \tag{4.1}$$

where t is the average boarding or alighting time per passenger, N is the number of passengers including both boarding and alighting passengers, and t_d is the dead time spent on opening and closing the doors. Guenthner and Sinha (1983) also assumed that dwell time is governed by the number of total boarding and alighting passengers, and proposed a nonlinear model which contains two sub-functions for the number of passengers. Later Lin and Wilson (1992) developed linear and nonlinear dwell time models for light rail transit services using the number of passengers and standees as independent variables. Li et al. (2006) developed a binary choice model to study passengers' preference for the front or rear door when alighting and applied the model to estimate dwell time. Other authors have analyzed the influence on boarding and alighting times of several factors, including bus door width (Fernández et al., 2010), and bus floor height (Dueker et al., 2004; Fernández et al., 2010), lift operation (Dueker et al., 2004), alternative fare payment techniques (Guenthner and Hamat, 1988; Dorbritz et al., 2009; Fletcher, 2013; Tirachini, 2013), age of passengers (Tirachini, 2013) and crowding or friction effects among passengers boarding, alighting and on-board, (Lin and Wilson, 1992; Dueker et al., 2004; Milkovits, 2008; Tirachini, 2013a).

Taken together, the main stream of dwell time studies distinguish between sequential and simultaneous boarding and alighting. In a sequential model, all bus doors are sequentially used for both boarding and alighting, then dwell time is measured as:

Model I

$$Dw = a \times A + b \times B + t_d, \tag{4.2}$$

where A and B are number of boarding and alighting passengers, respectively. Correspondingly, a and b represent the marginal time for boarding and alighting per passenger. For simultaneous boarding and alighting when one bus door is used for boarding (usually the front door) and the remaining doors are used for alighting, dwell time is then estimated as the maximum of boarding time and alighting time:

Model II

$$Dw = max\{a \times A, b \times B\} + t_d, \tag{4.3}$$

where the notations are the same as Eq (4.2). These models have been applied in transit assignment models (Aashtiani and Iravani, 2002; Larrain and Muñoz, 2008) and agent-based simulations (Meignan et al., 2007).

Once a functional form for the dwell time function is proposed, the primary task is to estimate parameters for these models, and therefore, comprehensive data collection is necessary. However, this data collection is both time consuming and labor intensive, as commonly used techniques are on-board ride checking and on-stop observation. For example, the data collection in (Moreno González et al., 2012) required at least two well-trained on-board observers for an articulated bus. Therefore, most dwell time studies are limited by their sample sizes.

On the other hand, the behavior patterns of pedestrians are a key to understand the dynamics of crowds, in particular at transportation terminals and on transit vehicles (Weidmann, 1992; Helbing et al., 2005). However, the physical counting techniques fail to capture the dynamics of pedestrian behavior. To replace the physical surveying, video recording devices are employed firstly in micro-physical experiments, from understanding pedestrian walking behaviors (Daamen and Hoogendoorn, 2003; Helbing et al., 2005), to exploring vehicle boarding/alighting dynamics (Daamen et al., 2008; Rudloff et al., 2011). Laboratory experiments have also been used to estimate bus dwell times to analyze elements that are difficult to study in actual bus systems (Fernández et al., 2010). However, considering the human resources and the device costs, these experiments are usually expensive to conduct; therefore their application in non-laboratory contexts is limited.

Recently, with the development of automated vehicle location (AVL) and automated passenger counting (APC) systems, Rajbhandari et al. (2003) and Dueker et al. (2004) implement studies on dwell time with large datasets extracted from AVL and APC, which are used to estimate average boarding and alighting times with regression models. However, to date, there is no detailed analysis of boarding and alighting behavior at a microscopic passenger-to-passenger level, for which a system based on smart card transactions, is well suited as the exact time in which a person taps in and off is recorded, then passenger intervals are instantly recorded. Therefore, new opportunities to study boarding/alighting dynamics and dwell time at a microscopic level arise from the presence of smart card based automated fare collection systems.

4.3 Bus characteristics

Two data sources are used here to explore the nature of the dwell times. First, to uncover the patterns of boarding and alighting behaviors and in particular any friction effects from on-board passengers, the smart card data mentioned above is used. Note that since our data set is generated from smart card transactions, it lacks the dead time to open and close doors (which is also part of the dwell time), therefore we study the time interval between the first and the last boarding/alighting activities, which for simplicity will also be referred as dwell time throughout. The second database contains the detailed descriptions of the buses and is used to analyze the impact of different bus characteristics, such as the number of doors and the vehicle size.

The first data set is the smart card data from the public transport system in Singapore, containing transit trip transaction records over one full week, from 11 April 2011 (Monday) to 17 April 2011 (Sunday). The data were collected from more than 3.3 million anonymized smart card users across the whole city state. We select the records from 8 bus services over the full week, covering different operating companies and various bus models, the detailed characteristics of which are introduced next derived from a separate data source.

The second data set, which is a lookup dictionary with the registration number as its key, provides a detailed description of each bus. The content includes, but is not limited to, manufacturer, model, length, year of use, entrance type, exact capacity including both seating and standing passengers, engine model, and emission standard. This data set is available at SgWiki.[2] After extracting the detailed bus model information, the 13 different bus types are divided into 8 groups. Their features are given in Table 4.1.

Table 4.1: Bus type classification and detailed characteristics

Notation	Name	Floor D	Entrance S	Capacity Cap	Length [m]	Alighting doors
LL	Leyland Olympian 3-Axle	Double	Step	131	12	1
VL B9	Volvo B9TL	Double	Low floor	131	12	1
SC K230 VI	Scania K230 UB Euro VI	Single	Low floor	88	12	1
SC K230 V	Scania K230 UB Euro V	Single	Low floor	85	12	1
VL B10	Volvo B10M Mark IV	Single	Step	83	12	1
MB O405	Mercedes-Benz O405	Single	Step	85	12	1
MB OC500	Mercedes-Benz OC500LE	Single	Low floor	90	12	1
MB O405G	Mercedes-Benz O405G	Single	Step	132	17.8	2

Figure 4.1 shows the design and layout of Type 4 - Scania K230UB Euro V buses. The front door and rear door are strictly used for boarding and alighting, respectively. Two smart card readers are employed on both sides of each door.

4.4 Descriptive Analysis of Boarding and Alighting Behavior

In this section, we compare passenger's boarding and alighting behavior for different bus types by investigating the interval between successive boarding and alighting activities respectively. We record each *service* $\times$ *stop* with the number of boarding/alighting passengers, number of on-board passengers and the corresponding total passenger activity time for boarding and alighting. Thus, the data contains full operation logs along the service route. Note that buses do not stop when there is no boarding or alighting required at a stop.

[2]http://sgwiki.com/wiki/Buses, Accessed March 20, 2013.

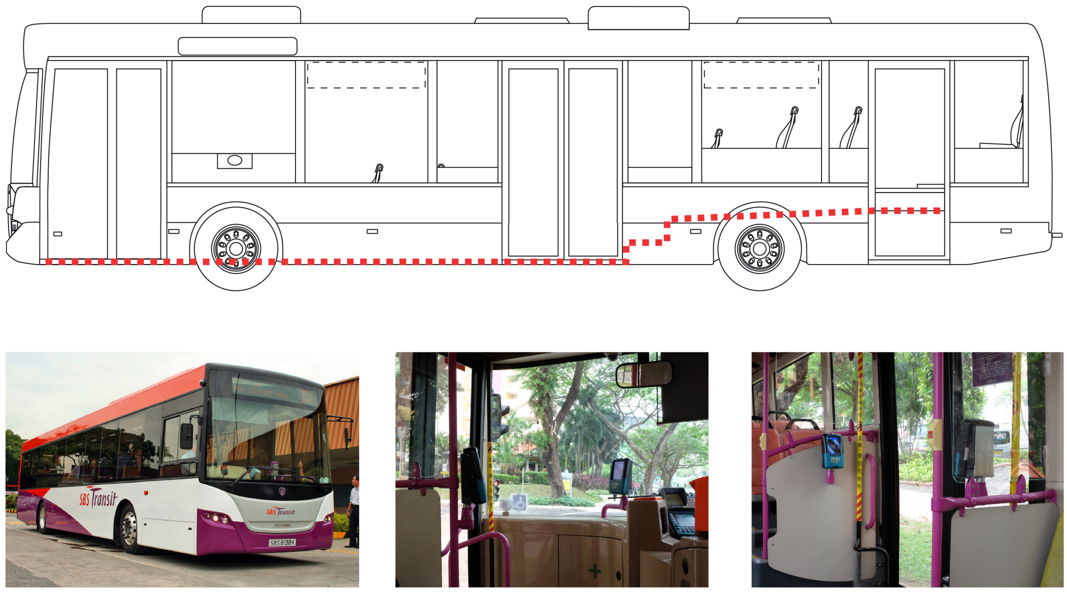

Figure 4.1: Layout of the Scania K230 single decker lower floor bus and location of smart the card readers (lower middle panel: front door; lower right panel: rear door)

4.4.1 Boarding behavior

Given two smart readers are deployed at each door, two queues may form when either boarding or alighting in our study. However, we miss information to map each transaction record to the corresponding smart card reader; and thus the interval h_B in this study describes the time interval between successive tapping-ins regardless of reader on which each transaction was generated (see Figure 4.1). In other words, the interval actually measures the inter-tapping-in time between successive transactions at the front door. Figure 4.2 shows the distribution of boarding intervals for different bus types. Since the front door is able to accommodate two users boarding at the same time, the minimum interval is 0 s. Note that some abnormal activities — e.g., passengers may take their card out after they board the bus — are also captured in such intervals, imposing increased heterogeneity in our observations. Nevertheless, such abnormal behavior indeed affects the boarding/alighting processes in practice, so we still take it into account in our analysis and model.

To explore the variation of boarding interval h_B, we first measure the distributions of h_B across the eight bus types. As expected, the distributions for different bus types share similar shapes because all buses have one door only for boarding. Figure 4.3 shows the trends of average boarding interval $\overline{h_B}$ against different number of boarding passengers during a stop.

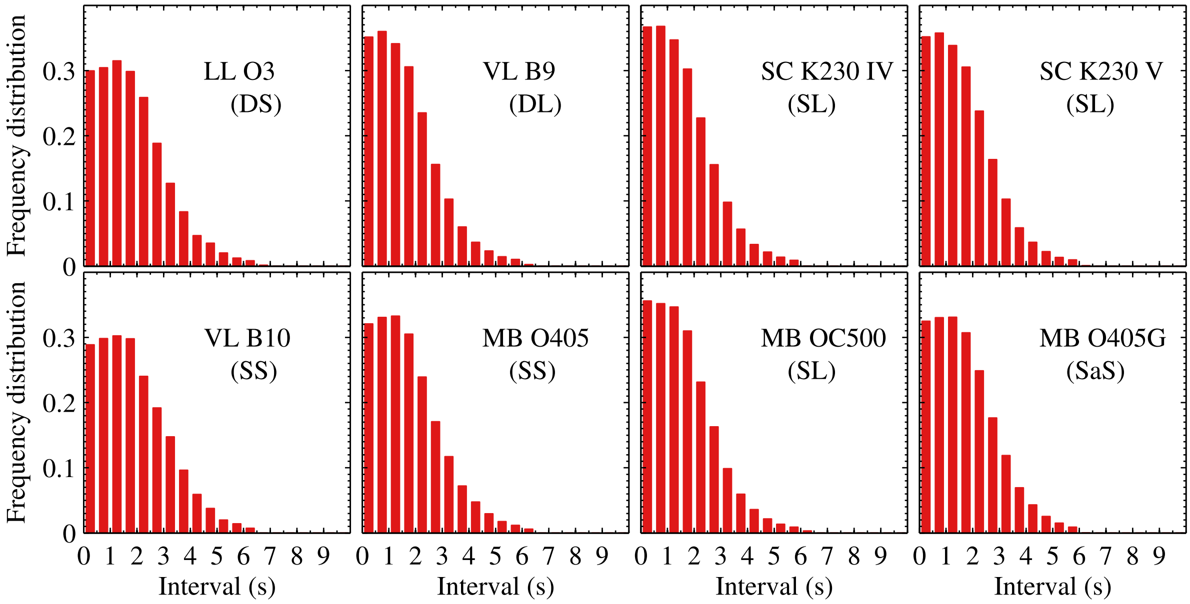

Figure 4.2: Distributions of boarding interval $P(h_B)$

Similar to the saturation flow at signalized junctions, we see that the variability of h_B is larger when fewer passengers board, and a more stable interval of around 2 s, needs some time to establish itself, indicating the lines with fewer, but more heavily used stops should be advantageous from an operational point of view and there exists marginal effect when number of boarding passenger is large.

Table 4.2: Statistics of boarding interval

Bus	Sample size	Mean [s]	Std Dev [s]
LL double decker, step	17,946	1.93	1.34
VL B9 double decker, low floor	22,817	1.76	1.27
SC K230 VI single decker, low floor	144,752	1.72	1.25
SC K230 V single decker, low floor	129,198	1.76	1.26
VL B10 single decker, step	19,758	2.02	1.39
MB O405 single decker, step	64,123	1.86	1.34
MB OC500 single decker, low floor	59,386	1.68	1.22
MB O405G articulated-single decker, step	115,396	1.83	1.28
Total	573,376	1.78	1.27

The statistics on the boarding headways of different bus types are given in Table 4.2. For the eight bus groups, the average boarding time per passenger ranges from 1.68 to 2.02 s, with standard deviations between 1.22 and 1.39 s. Considering each group as an observation

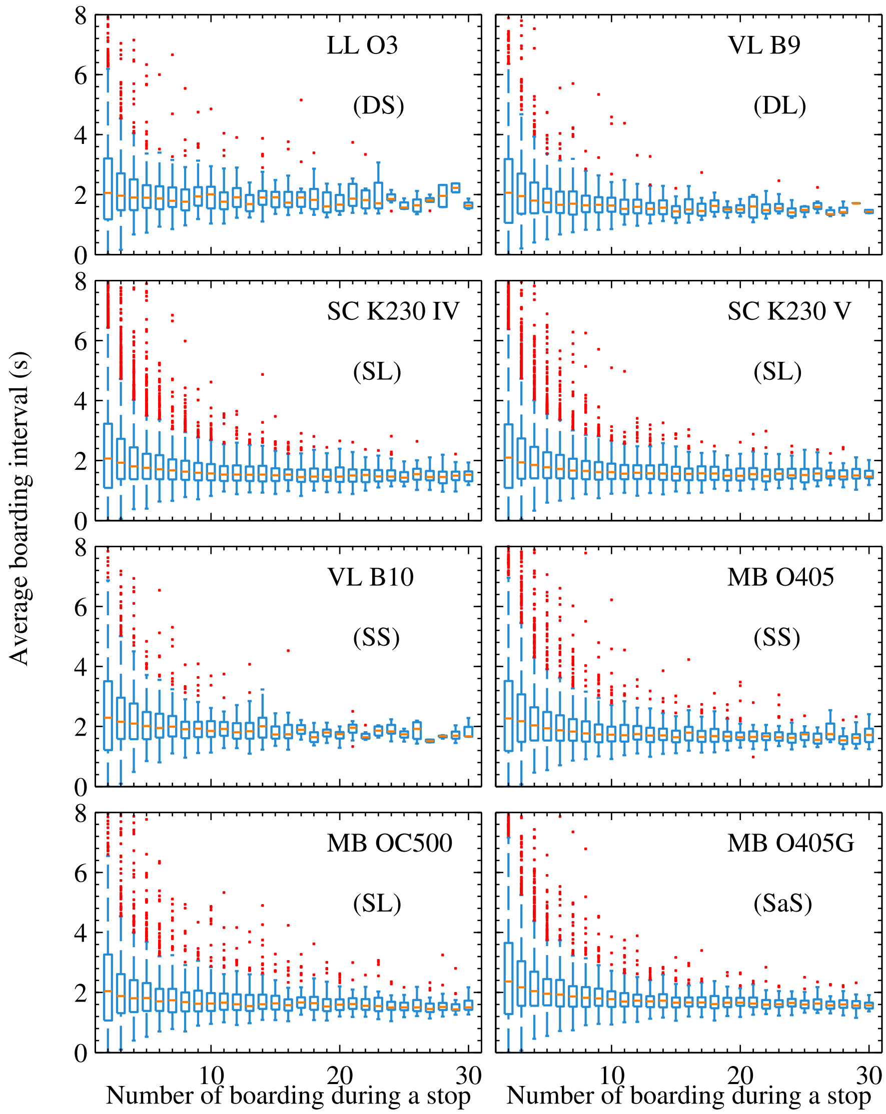

Figure 4.3: The trend of average boarding interval $\overline{h_B}$ against number of boarding passengers during a stop

it stands out that there is a linear correlation between the mean and standard deviation of boarding times:

$$Std(h_B) = 0.50 \times h_B + 0.39, \tag{4.4}$$

with $R^2 = 0.95$ (see Figure 4.4). This implies bus configurations with slow boarding times also have a greater variability in boarding, and consequently, in travel times, which has undesirable effects on bus operations and is negatively valued by users.

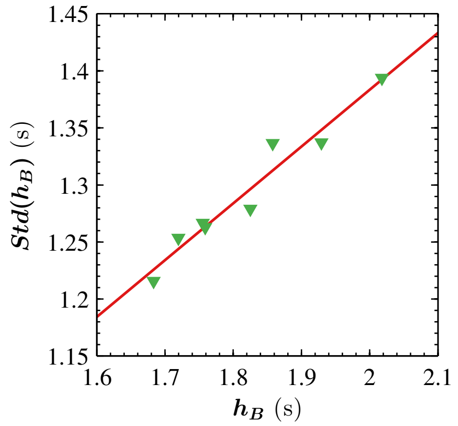

Figure 4.4: Bus types: h_B and $Std(h_B)$

Other studies found a mean boarding time for on-board smart card validation of 2 s/pax, e.g., Bus Rapid Transit Systems in China (Wright and Hook, 2007) and for uncrowded conditions in Santiago de Chile (Fernández et al., 2008). Due to data limitations, previous studies have been unable to trace the relationship between the mean and the standard deviation of boarding time, as done in Figure 4.4.

In terms of entrance types, we find that buses with low floor entrance performed better in terms of average boarding time. On the other hand, we find single decker buses are superior to double decker buses, which have larger average boarding headways.

To further address the impact of bus characteristics on boarding interval, we used a regression model to measure average cost of each boarding b activity using the following parameters: intercept (β_B), the marginal effect of additional boarding (β_{Bs}), the contribution of floor type (β_D), entrance type (β_S) and occupancy (β_{Oc}) on each boarding activity:

$$\begin{aligned} T_B &= (B-1) \times b + \varepsilon \\ &= (B-1) \times (\beta_B + \beta_{Bs} \times (B-1) + \beta_D D + \beta_S S + \beta_{Oc} On/Cap) + \varepsilon, \end{aligned} \tag{4.5}$$

where $T_B = t^B_{last} - t^B_{first}$ is the total time for boarding for each *service* $\times$ *stop*, B represents number of boarding passengers and thus $B-1$ is number of recorded activities, D and S are dummy variables indicating bus types:

$$D = \begin{cases} 1 & \text{double decker} \\ 0 & \text{single decker} \end{cases}, \; S = \begin{cases} 1 & \text{step entrance} \\ 0 & \text{low floor entrance} \end{cases}. \tag{4.6}$$

Cap represents vehicle capacity, On/Cap ($[0,1]$, number of on-board passengers/capacity) indicates occupancy before boarding and alighting and ε is the residual or unexplained variance.

Table 4.3: Regression analysis of total boarding time

Parameter	Description	Unit	Estimate	SE	t-stats	p-value
β_B	Intercept	s/pax	1.951	0.003	648.05	0.000
β_{Bs}	Number of activities	s/pax^2	-0.017	0.000	-259.13	0.000
β_D	Double decker	s/pax	0.047	0.007	7.21	0.000
β_S	Step entrance	s/pax	0.156	0.003	57.02	0.000
β_{Oc}	Occupancy	s/pax	0.340	0.008	48.78	0.000
Adjusted R^2	0.914		Observations		61555	

Table 4.3 shows the regression result of Eq. (4.5) using total boarding time observed with more than one passengers for all types. The average time without considering specific vehicle attributes is about 1.95 s/pax. We find that number recorded activates have a negative impact on average boarding time, which is in accord with Figure 4.3, suggesting that the average boarding interval decreases as the number of boarding passengers increases within our range of observations. Step entrance increases average boarding times significantly by 0.156 s. Double decker buses also show a statistically significant influence on boarding behavior; however, the effect is small (0.047 s) as passengers can continue boarding while passengers that boarded ahead are walking in the aisle or upstairs. Note that occupancy has significant negative impact on boarding flows, as they incur more friction within the vehicles, delaying the boarding processes. On the other hand, vehicle capacity diminishes boarding time significantly, as larger capacity may reduce the in-vehicle friction. Taken together, despite number of boarding passengers, the boarding processes is affected by the entrance type and occupancy: although boarding time is largely covered by the time spent on swiping smart cards and waiting for transaction responses, low floor with large capacity still offers better user experience since passengers do not have to walk up steps, in particular for senior citizens.

4.4.2 Alighting behavior

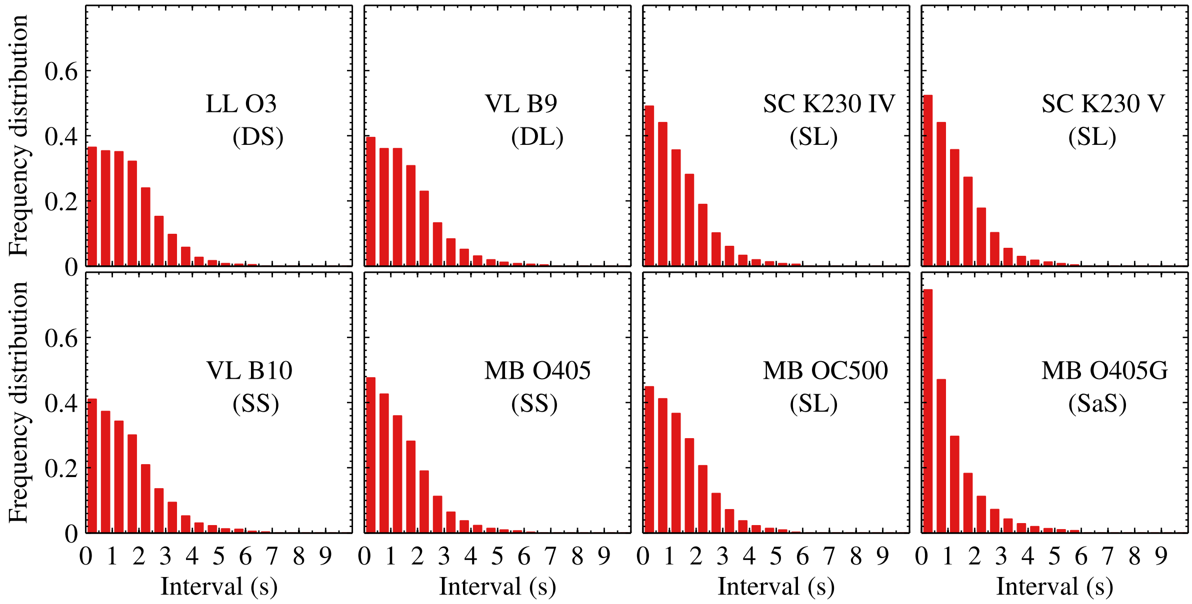

Figure 4.5: Distribution of alighting interval $P(h_A)$

Analogous to the definition of boarding interval, alighting interval h_A is defined as the time interval between two successive tapping-offs. Figure 4.5 shows the distributions of alighting interval for the different bus types. Unlike the boarding activities, significant heterogeneity is observed in alighting. It should be noted that the distribution of articulated bus (MB O405G) is substantially different from others in Figure 4.5 as they have two doors for alighting, therefore shorter intervals are observed. The detailed statistics are listed in Table 4.4. Observations in which passengers tap out before the bus arrives at the stop were removed, thus, the sample size of alighting interval is smaller than that of boarding. The average alighting time per passenger varies from 1.26 s to 1.78 s. Overall the average alighting time is about 0.30 s shorter than the average boarding time (1.48 s vs 1.78 s per passenger).

As in the case of boarding, the standard deviation of alighting times is also positively correlated to its mean, as shown in Figure 4.6 (the regression does not include articulated buses - MB O405G). In this case, a linear relationship is not as clear as that of boarding with $R^2 = 0.73$:

$$Std(h_A) = 0.53 \times h_A + 0.45. \tag{4.7}$$

Table 4.4: Statistics of alighting headway

Bus	Sample size	Mean [s]	Std Dev [s]
LL double decker, step	8810	1.78	1.30
VL B9 double decker, low floor	11305	1.75	1.32
SC K230 VI single decker, low floor	69388	1.54	1.25
SC K230 V single decker, low floor	63039	1.50	1.26
VL B10 single decker, step	9682	1.78	1.37
MB O405 single decker, step	36846	1.52	1.22
MB OC500 single decker, low floor	34647	1.48	1.14
MB O405G articulated-single decker, step*	64736	1.26	1.23
Total	298453	1.48	1.23

*Given there are two doors used for alighting in articulated bus, the value here is not the defined alighting headway anymore.

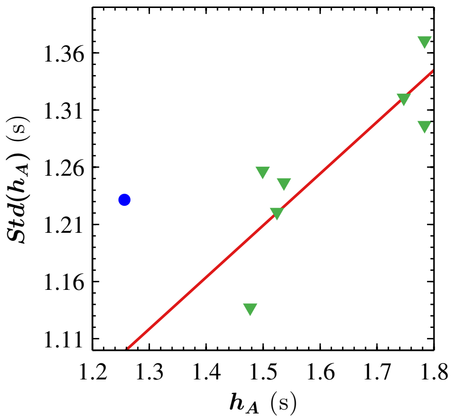

Figure 4.6: h_A and $Std\ (h_A)$ for different bus types (blue circle represents MB O405G)

Similarly, to address the impact of bus characteristics on alighting interval, we estimated a regression model to measure average time of each alighting activity a using: intercept (α_A), the diminishing marginal effect of additional alighting (α_{As}), the contribution of floor type (α_D), entrance type (α_S) and occupancy (α_{Oc}) on each boarding activity:

$$\begin{aligned} T_A &= (A-1) \times a + \varepsilon \\ &= (A-1) \times (\alpha_A + \alpha_{As} \times (A-1) + \alpha_D D + \alpha_S S + \alpha_{Oc} On/Cap) + \varepsilon, \end{aligned} \tag{4.8}$$

where $T_A = t^A_{last} - t^A_{first}$ is the total time for boarding for each $service \times stop$, $(A-1)$ is the number of recorded alighting activities.

Table 4.5: Regression analysis of alighting headway

Parameter	Description	Unit	Estimate	SE	t-stats	p-value
α_A	Intercept	s/pax	1.691	0.006	261.74	0.000
α_{As}	Number of activities	s/pax^2	-0.014	0	-66.04	0.000
α_D	Double decker	s/pax	0.217	0.009	24.4	0.000
α_S	Step entrance	s/pax	0.016	0.005	3.09	0.002
α_{Oc}	Occupancy	s/pax	-0.082	0.019	-4.41	0.000
Adjusted R^2	0.879		Observations		23083	

Given that the alighting process on an articulated bus is considerably different from other types, we did not take the observations on those buses into account. Table 4.5 shows the regression result of Eq. (4.8). The average time across all bus types is about 1.69 s/pax. We also find that number recorded activates have a negative impact on average boarding time, diminishing the effect of additional alighting for 0.014 s less, similar to the value of β_{Bs}. The effect of step entrance is significant but small, increasing average alighting time by 0.016 s. The results are in accord with York (1993), which compared buses with one, two and three entrance steps in London, finding that more steps does increase average alighting times. However, double decker buses do show a statistically significant and great influence on alighting behavior. This suggests that on double decker buses, passengers are more likely to wait upstairs until the bus comes to a full stop before they start walking downstairs on the narrow steps to alight, as usually observed in double decker buses in Singapore. Occupancy also plays a significant role. Different from what we find for boarding process, a high occupancy actually speed up the alighting process. This might be due to passengers feeling crowded or due the pressure from other alighting passengers. Taken together, the alighting process is dominated by the entrance type, occupancy, and in particular double decker. Therefore, it follows that the impact of steps on both boarding and alighting need to be studied in each specific context, taking into account differences due to number and height of steps, and width and location of doors.

In Singapore, it is also observed in the field that, apart from the mentioned effects, both boarding and alighting queues can come to a halt owing to random events, such that when passengers forget to prepare their smart cards before their boarding/alighting. On the other hand, crowding inside vehicles is also likely to lengthen boarding and alighting. In such situations, the dwell time model (II) (Eq. (4.3)) fails to capture any friction effect amongst passengers. Therefore, a new passenger activity time model is proposed below given the above findings.

4.5 Modeling Passenger Activity Time for Restricted Flows

The friction among boarding, alighting and on-board passengers has shown its importance in determining bus dwell time in the literature (Lin and Wilson, 1992; Dueker et al., 2004; El-Geneidy and Vijayakumar, 2011; Fletcher and El-Geneidy, 2013; Tirachini, 2013a). However, the factors resulting in such friction were not studied given the lack of microscopic passenger activity observations. In this section, we try to explore such friction by analyzing the cumulative boarding, alighting and on-board curve over time. Then, models for passenger activity time (without considering the time to open and close doors) are estimated and analyzed.

Boarding and alighting processes can be treated as pedestrian flows with the smart card reader as their checkpoint. Given the mentioned dynamics, boarding passengers might form a stable flow when the interval is less than a certain level. Thus, using the time-stamped passenger activities, we can find how the number of boarding and alighting passengers varies with time during a stop. In Figure 4.7, we show four types of cumulative boarded, alighted and on-board curve over time identified from SC K230 VI single decker, low floor buses. To separate boarding and alighting flows, the cumulative alighting curve is shown on the negative axis. Time is referenced by setting the first activity time (either boarding or alighting) as zero. Thus, both the cumulative boarding and alighting curves increase with time (note that the alighting curve is also increasing, but it is projected on the negative axis). Given that the number of on-board passengers is available in our data, we can also plot the cumulative on-board passengers. Thus, for example, panel [1] shows a process with 34 on-board passengers before the bus stopped, 46 boarding passengers and 4 alighting passengers. We can see that total activity time is mainly determined by boarding activities whereas alighting activities happened simultaneously. We call such process 'boarding dominates'. Total time of such processes could be estimated using Eq. (4.5), determining boarding time as total activity time ($Ac = T_B$). Similarly, panel [2] shows an 'alighting dominates' process (on-board 61, boarding 0, and alighting 61) and we may estimate activity time as $Ac = T_A$ using Eq. (4.8). When number of boarding and alighting processes happen simultaneous, total activity time is determined by the longer process (see panel [3], boarding process is slightly longer than alighting). Such cases exist when the number of on-board passenger is not large and the corresponding total activity time is the longer process ($Ac = \max\{T_B, T_A\}$). However, if a bus is almost full before it stops, the boarding flow is delayed and frictions between boarding and alighting flows should be considered. We show such a process with on-board 61, boarding 32 and alighting 45 in panel [4]. Given the large occupancy when opening doors (61 on-board passengers), the boarding process was delayed for 28 s. In this case, alighting happens first, and boarding starts after the number of on-board passengers is less than certain level (about 35 in this case). We call this value as 'critical occupancy' Cr hereafter.

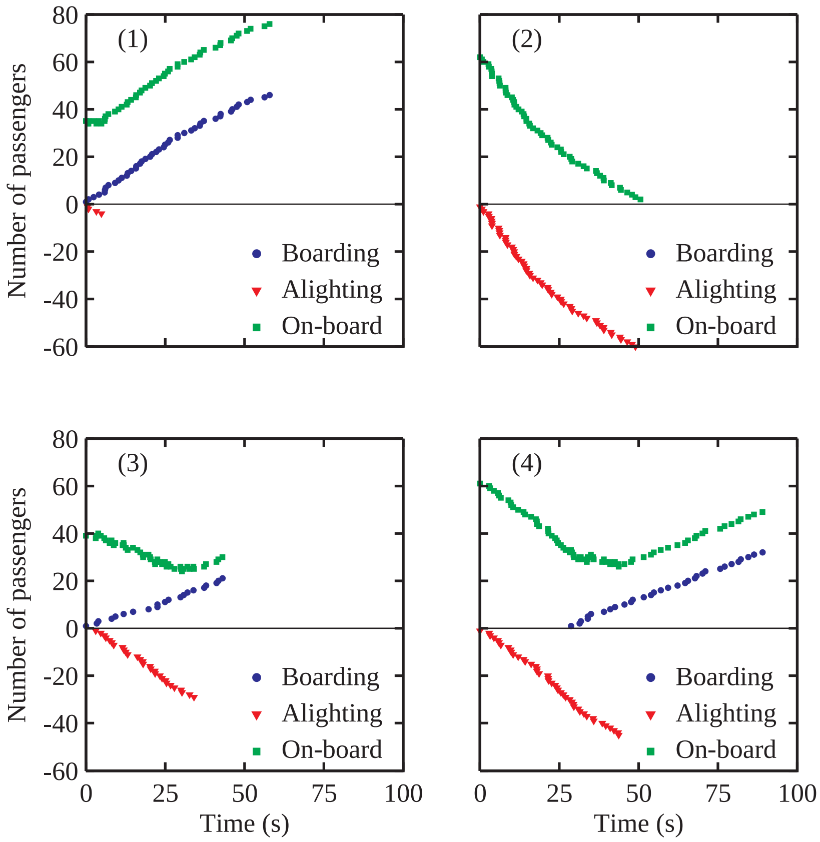

Figure 4.7: Boarding/alighting flow and instantaneous on-board passengers (SC K230 VI single decker, low floor)

Therefore, we can see that passenger activity time is determined by three variables, i.e., the number of passengers boarding B, alighting A, and on-board On. Based on the patterns observed in Figure 4.7, we assume that both boarding time and alighting time is in linear with the number of activity passengers respectively, and propose a new model that considers both boarding/alighting dynamics and the interactions of on-board passengers (note that the recorded total passenger activity time is the interval between first and last-nth activities, so only $(n-1)$ intervals are taken into account):

$$Dw = \begin{cases} b \times (B-1) & \text{pattern (1)} \\ a \times (A-1) & \text{pattern (2)} \\ \max\{b \times (B-1), a \times (A-1)\} & \text{pattern (3)} \\ \max\{b \times (B-1) + a \times (On-c), a \times (A-1)\} & \text{pattern (4)} \end{cases}, \tag{4.9}$$

where B and A denote the number of boarding and alighting passengers respectively, and On represents the number of on-board passengers. All together, Eq. (4.9) can be summarized as the combined dwell time model III (see also Figure 4.8):

Model III

$$Dw = \max\{b \times (B-1) + a \times (\max(On-c, 0)), a \times (A-1)\}. \tag{4.10}$$

4.6 Analysis and Results

Given the operation scheme is simultaneous boarding and alighting, we compare model II with the new model III for the activity time based on the large quantity of observations extracted from the smart card data. To insure the consistency of the two models, we ignore the recovery time to open and close doors and only model passenger activity time (Ac) determined by the first and last boarding/alighting. Thus, given the formulation of model II, total activity time is determined by the longer process between boarding and alighting:

Model II[3]

$$Ac = \max\{(B-1) \times b, (A-1) \times a\} + \varepsilon, \tag{4.11}$$

[3]Note that the time for first activity (either boarding or alighting) is not captured in the smart card data

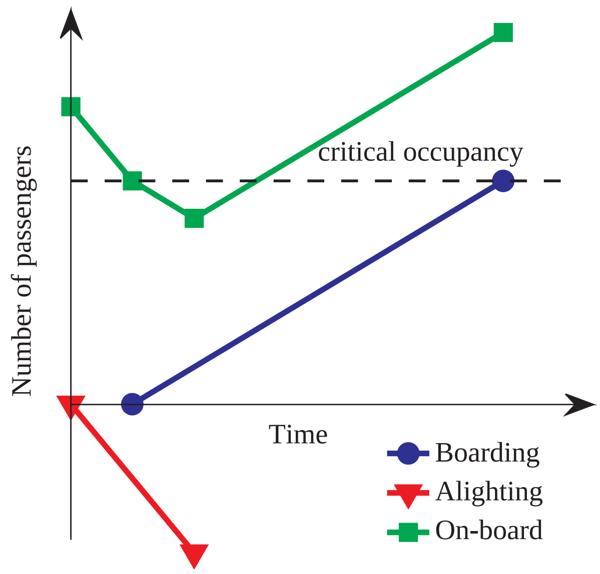

Figure 4.8: Temporal cumulative curves of boarded, alighted and on-board passengers for restricted flows

where $b = \beta_B + \beta_{Bs} \times (B-1) + \beta_D D + \beta_S S + \beta_{Oc} Oc$ and $a = \alpha_A + \alpha_{As} \times (A-1) + \alpha_D D + \alpha_S S + \alpha_{Oc} Oc$. In model III, we assume that critical occupancy is in proportion with the total capacity, $Cr = \gamma Cap$. Thus, model III can be demonstrated in a similar way Eq. (4.11). However, note that boarding happens only when load is lower than critical occupancy Cr, so the average boarding time should be revised as:

$$b = \beta_B + \beta_{Bs} \times (B-1) + \beta_D D + \beta_S S + \beta_{Oc} \gamma Cap. \tag{4.12}$$

And the average alighting time before load reach Cr is different from should be:

$$a' = \alpha_A + \alpha_{As} \times (On - Cr) + \alpha_D D + \alpha_S S + \alpha_{Oc} On/Cap. \tag{4.13}$$

Taken together, the regression model III is formulated as:

$$Ac = \max\left\{(B-1) \times b + (\max(On - \gamma Cap, 0)) \times a', (A-1) \times a\right\}. \tag{4.14}$$

Regression models are estimated for Eq. (4.10) (model III) and Eq. (4.11) (model II). Similar to the estimation of boarding/alighting processes, we only include observations in which either number of passengers boarding or number of alighting per bus stop are greater than or equal to 2 ($B \geq 2$ or $A \geq 2$). Table 4.6 summarizes the descriptive results of the observed data at each $service \times stop$ used in regression analysis. We used MATLAB Statistical Toolbox to do the regression, which uses Levenberg-Marquardt least squares algorithm to estimate models II and III (Seber and Wild, 2003). In applying the Levenberg-Marquardt algorithm, we first set the initial values of different parameters based on their physical representation. By doing so we try to make the algorithm converge to our expected values rather than local optimal. Different indicators show the quality of these two models.

Table 4.6: Descriptive results of observed data

	unit	mean	MIN	MAX
Activity time Ac	s	16.95	2.03	255.06
Number of boarding passengers A	pax	7.12	0	79
Number of alighting passengers B	pax	3.83	0	74
Number of on-board passengers Oc	pax	21.68	0	99

We set the initial value for critical occupancy as 0.5. Initial values for other parameters are set as the previous estimates in the regression on boarding and alighting separately. The regression results are shown in Table 4.7. Given the absence of in-vehicle friction (see Figure 4.7, panel [4]), model II gives a high estimate of upper decker on boarding time (0.33 s/pax), which is clearly higher than the estimate in Table 4.3 (0.05 s/pax). Moreover, occupancy is estimated to increase alighting time, showing an opposite effect to the separate model on alighting (Table 4.5) and our intuition. Although we have a lower coefficient of determination in model III, the results are more reasonable than model II in terms of factor contribution compared to previous separate models. By introducing critical occupancy as one parameter in model III, we find that the effect of initial occupancy becomes not significant (p-value=0.616). The critical occupancy is estimated as 63% of total capacity for all bus types, and its contributions becomes very significant in the regression analysis. The marginal effects of boarding and alighting activities (i.e., the quadratic terms β_{Bs} and α_{As}) are also identified to be significant, both reducing the total activity time in the range of our observations. In additional, when taking all data into consideration, the effect of upper decker on boarding becomes not significant, indicating that upper decker can be a good choice when most on-board passengers alight together. Taken together, the proposed model III performs well in relating the physical characteristics of vehicles to the boarding/alighting and on-board friction dynamics observed from the smart card data set.

Table 4.7: Results of regression analysis on activity time model II and III

Parameter	Description	Unit	Estimate	SE	t-stats	p-value	Estimate	SE	t-stats	p-value
			model II				model III			
β_B	Intercept	s/pax	2.009	0.005	403.13	0.000	2.050	0.117	17.47	0.000
β_{Bs}	Number of recorded activities	s/pax^2	-0.016	0.000	-128.39	0.000	-0.010	0.000	-66.40	0.000
β_D	Double decker	s/pax	0.332	0.009	3.79	0.000	0.080	0.061	1.30	0.192
β_S	Step entrance	s/pax	0.186	0.005	36.80	0.000	0.167	0.007	24.51	0.000
β_{Oc}	Occupancy	s/pax	0.359	0.012	29.30	0.000	-0.001	0.002	-0.50	0.616
α_A	Intercept	s/pax	1.889	0.013	149.41	0.000	1.969	0.015	135.76	0.000
α_{As}	Number of recorded activities	s/pax^2	-0.023	0.000	-58.41	0.000	-0.012	0.000	-27.08	0.000
α_D	Double decker	s/pax	0.235	0.017	14.09	0.000	0.285	0.019	14.86	0.000
α_S	Step entrance	s/pax	0.087	0.009	9.46	0.000	0.075	0.011	7.09	0.000
α_{Oc}	Occupancy	s/pax	0.329	0.035	9.30	0.000	-0.371	0.039	-9.46	0.000
γ	Critical occupancy	1	-	-	-	-	0.633	0.002	381.11	0.000
	Number of observations	41618	R^2	0.870			R^2	0.844		

4.7 Summary

The new electronic smart card systems, as implemented in Singapore, give us a new and much deeper insight into the operational processes of bus boarding and alighting than ever before: more observations, more variance across bus types, and wider range of operating conditions.

Having reconstructed the operations for each combination of service per stop, we were able to describe and then model the three processes of interest here: boarding, alighting and (total) passenger activity time (without the door opening and closing times). We provided explanations for the different performance based on our understanding of the operational characteristics. Boarding is consistently slower than alighting by about 0.3 s. It becomes clear that single decker buses with low floor entrance speed up the boarding processes. Although the upper deck also shows a statistically significant effect in slowing down the boarding process, its contribution is trivial comparing to step entrance. However, in terms of alighting, the upper deck does play a significant role in delaying the alighting for more than 0.2 s per activity, as the steep stairs discourage passengers to walk down until the bus has come to a complete stop. The quadratic terms are found to determine both boarding time and alighting time significantly, indicating that average boarding/alighting interval decreases as the number of activities increases, which shows a diminishing marginal effect. In other words, on average the boarding and alighting is faster, when demand is greater in total, as observed in the marginal diminishing effect parameter (β_{Bs} and β_{As}). Interestingly, the occupancy before boarding/alighting starts is found to lengthen the boarding time but shorten the alighting time significantly. Other operational factors such as peak/off-peak demand differences and weather are not taken into account in this chapter; however, they may influence passenger behavior as well. These would be interesting future research questions.

The joint model of passenger activity times we proposed here shows clearly, that vehicle occupancy determines the regime of the two processes and the overall activity time. Beyond a critical occupancy level of about 60% of the total bus capacity, the internal friction prevent passengers from boarding, as the alighting passengers have to reduce that critical level of occupancy for the boarding process to properly start. The conventional dwell time models for simultaneous boarding/alighting — which is model II in this chapter — failed to observe and take such effect into account.

Our data are limited to a regime where the front door and rear door are primarily used for boarding and alighting, respectively. In crowded conditions, however, it is common that travelers alight trough both doors while boarding is only allowed through the front door to assert fare collection. Therefore, no conclusion can be drawn on the effectiveness of such boarding and alighting scheme and compared to other setups. Although the use of smart card data shows its advantages, we failed to account for other vehicle configuration and human factors, such as whether a particular vehicle is friendly to wheelchairs, bicycles, and strollers without doing a comprehensive field survey. Similarly, we did not account for potential stop configuration effects such as availability of a bus bay and crowdedness on the waiting platform. Passenger attributes — such as age and gender — also play a crucial role in determining boarding/alighting dynamics; however, such information is only available from a field survey. Furthermore, the techniques only enable us to observe passenger activity time, hindering us from identifying service interruption, disruptions, scheduled delays, gap time to enter the traffic again, and on-stop traffic controls which may cause abnormal dwell time observations. Thus, a potential direction is to combine survey data and smart card data together in interpreting passenger behavior patterns. In the studied transport system of Singapore, during the boarding and alighting processes each passenger needs to swipe the ticket over the card reader. This is also a source of variability as some passengers have the smart card prepared for swiping while others needs first to find it in their pockets, imposing heterogeneity on our analysis. This opens up further research questions to address the practical questions on how to improve the situation with the given bus fleet. First, it would be interesting to see whether and when the boarding and alighting process could be sped up and variability reduced, by installing additional card readers at the bus stop so that passengers could tap in and out the system outside the bus. Second, for stops where either preliminary boarding or alighting regimes dominate, it might make sense to allow boarding or alighting through all doors to increase the flow. For practical application, the regularity of such scheme in terms of time of the day and bus stop is crucial as one would need to communicate with passengers in advance when boarding or alighting through both doors is allowed (Jara-Díaz and Tirachini, 2013). To this end, however, a multi-week passenger transaction data set would be needed to account for the various potential sources of demand variability such as special events, public holidays, school holidays and weather conditions.

Our results have a number of potential implications for practice and policy. First, the relationship between passenger activity time duration and bus capacity can be incorporated into models on optimal bus size; such relationship should be taken into account when deciding if having rigid, articulated or up-decker buses. Double-decker does not slow boarding, but it does do so for alighting. These buses might be good choice when demand is high and most passengers alight at a particular bus stop, for example commuting buses collecting workers from different housing locations to the same working location. Step entrance increases boarding time significantly, while it does not deley alighting processes much.

Second, the variability of boarding and alighting times have likely but unknown effects on bus interval variability, and consequently, on increasing waiting times. Together with traffic congestion and demand heterogeneity, dwell time variability increases the risk of service unreliability (Vuchic, 2007; Strathman and Hopper, 1993). The correlation between dwell time variability, service reliability and bus bunching needs further scrutiny, in particular, on determining how they interact to influence optimal bus headway, optimal bus stop spacing and control strategies such as bus holding (Hickman, 2001; Strathman et al., 2002). This is particularly urgent when the existing operations are characterized by high unreliability and a large mix of different bus types. Finally, the results of boarding and alighting dynamics models can directly be applied to calibrate large-scale, agent-based transport simulation such as MATSim (http://www.matsim.org)[4] or Transims (https://code.google.com/p/transims/)[5] which allows us to evaluate how different bus types and deployment schedules impact service quality and reliability.

[4] Accessed October 9, 2014
[5] Accessed October 9, 2014

Chapter 5

Estimating Metro Train Loading Profile and Trajectories from Smart Card Data

Chapter information

A conference paper based on this chapter was published in *ACM SIGKDD International Workshop on Urban Computing*: Sun, L., Lee, D.-H., Erath, A., Huang, X., 2012. Using smart card data to extract passenger's spatio-temporal density and train's trajectory of MRT system, *ACM SIGKDD International Workshop on Urban Computing*. ACM, pp. 142-148.

Mass Rapid Transit (MRT) systems are the most important public transportation service modes in many large cities around the world. Hence, its service reliability is of high importance to government and transit agencies. Despite taking all the necessary precautions, disruptions cannot be entirely prevented but what transit agencies can do is to prepare to respond to failure in a timely and effective manner. To this end, information about daily travel demand patterns are crucial to develop efficient failure response strategies.

In this chapter, we present a methodology to analyze smart card data collected in Singapore, to describe dynamic demand characteristics of one case mass rapid transit (MRT) service. The smart card reader registers passengers when they enter and leave an MRT station. Between tapping in and out of MRT stations, passengers are either walking to and fro the platform as they alight and board on the trains or they are traveling in the train. To reveal the effective position of the passengers, a regression model based on the observations from the fastest passengers for each origin destination pair has been developed. By applying this model to all other observations, the model allows us to divide passengers in the MRT system into two groups, passengers on the trains and passengers waiting in the stations. The estimation model provides the spatial-temporal density of passengers. From the density plots, trains' trajectories can be identified and passengers can be assigned to single trains according to the estimated location.

Thus, with this model, the location of a certain train and the number of on-board passengers can be estimated, which can further enable transit agencies to improve their response to service disruptions. Since the respective final destination can also be derived from the data set, one can develop effective failure response scenarios such as the planning of contingency buses that bring passengers directly to their final destinations and thus relieves the bridging buses that are typically made available in such situations.

5.1 Introduction and Overview

Rapid transit systems are increasingly becoming the most important mode of public transportation in many large cities around the world owing to its faster velocity, higher reliability, and larger capacity, as compared with other transport modes. Understanding the demand characteristics of such systems is central to the public transport agencies and operators, so as to manage and improve their services. During a typical weekday, the demand of the bus and rapid transit systems have distinct spatial-temporal characteristics, which have been captured using smart card data, as shown in (Munizaga and Palma, 2012) and (Park et al., 2008) respectively. Park et al. (2008) studied the demand characteristics of different public transport modes, in particular the rapid transit system, based on the smart card data records in Seoul, South Korea.

The implementation of an automated fare collection (AFC) system allows public transport agencies to collect large quantities of data, recording passengers activities with detailed time and space information. It has been recognized that there are large potential benefits of using this data to improve public transport planning and operation (Pelletier et al., 2011). As a result, an increasing number of researchers have been using such data to analyze public transport systems characteristics and passenger behaviors. Bagchi and White (2005) have demonstrated the feasibility of obtaining turnover rates, trip rates and the proportion of linked trips from smart card data, which can be further used to adjust such services. For some entry-only smart card systems, trip destination information is not recorded but needs to be imputed. Different methodologies haven been proposed to estimate the origin-destination pairs and alighting time (Munizaga and Palma, 2012; Barry et al., 2002). Jang (2010) has studied the travel time and transfer activities in Seoul, South Korea using smart card data, which provides a comprehensive travel time map and basic understanding of transit services. By analyzing smart card data collected in Outaouis, Canada, Agard et al. (2006) have identified different trip habits based on the pre-defined user types and variabilities of trips against time. Utsunomiya et al. (2006) pointed out that demand pattern varies with day in week, therefore, different operation schedules should be provided for each day. Some researchers also focus on data processing methods and aim to get more meaningful information from smart card data. In (Chu and Chapleau, 2008), different types of analyses are conducted to support further planning purposes. Potential usage and challenges have also been highlighted. Lee et al. (2012) used smart card data from Singapore which contains detailed boarding/alighting activities to conduct an analysis on bus service reliability, including trajectories, occupancy of buses and in particular the headway distribution along the route since bus bunching occurs at times. Based on this approach, different operating strategies can be applied and tested in a simulation environment with passenger demand as inputs.

To date, information dedicated to identify passenger locations within a MRT system based on smart card data remains scant. Identifying trajectories and occupancy of trains is significant to transit agencies in order to improve the service level by designing timetable, adjusting velocity and increasing/decreasing dwell time at stations, however, these information is difficult to obtain from the operators' point of view. This is different from data generated from bus systems, as rapid transit data records do not feature any time information regarding when passengers board or alight from a train, which leads to difficulties in describing the trajectories and occupancy of trains. Fortunately, smart card data provides us the opportunity to extract this information. In this present study, smart card data is used to extract the spatial-temporal demand variation of the MRT system.

In the light of smart card records of passengers' tapping in and tapping out of the system, a model has been proposed to detect different travel time elements. This model can be regressed based on the assumption that the observations with the least duration between each origin and destination pair record over a given day travel through the system has no waiting time. The regressed parameters can then be employed to indicate the most probable location of every passenger, which further results in a realistic description of passengers' spatial-temporal density and trains' trajectories.

5.2 Case study: EW services

The smart card data used in this study was collected by a fare collection system, kindly provided by the Singapore Land Transport Authority (LTA). The smart card is Singapore's single largest contactless stored value smart card system and is mainly used for payments on public buses and MRT trains since April 2002. For this study, only records with both boarding and alighting stops being on the East West MRT line are selected since it is the most busiest rapid transit service in Singapore, as shown in Figure 5.1.

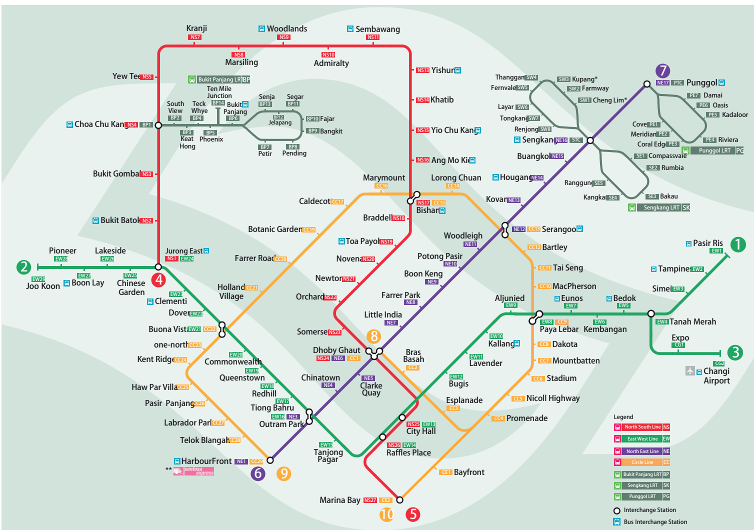

Figure 5.1: MRT and LRT system map in Singapore in 2011

Compared with other smart card data sources stated in (Munizaga and Palma, 2012) and (Trépanier et al., 2007), the most significant advantage of the smart card dataset is that it contains precise timing and location information for both boarding and alighting. Hence, transfer information can also be derived. This serves as a basis to generate information on load profile, spatial-temporal variation, and the waiting time of passengers.

In the smart card based fare collection system, the fare charge is calculated based on travel distance, trip mode and different passenger types, so any other information describing these three characteristics can be obtained from the data set.

This present study is conducted based on smart card records of one entire week in April, 2011 provided by the Land Transport Authority (LTA) of Singapore. To test the presented methodology of identifying spatial-temporal density and train trajectories, a one day sample is used.

In this study, the East-West (EW) MRT service, which is known as the green line, is chosen to investigate the demand characteristics and test the proposed strategies in order to identify passengers' spatial-temporal density and trains' trajectories. This service has 29 stations moving in both directions. Figure 5.1 shows the general map of MRT and LRT (Light Rapid Transit) systems in Singapore. The case study examined is service that is on the green line, but the two stations on the extension line leading to Changi Airport are not included.

For this study, records of the time taken for passengers to tap in and tap out are used, along with boarding and alighting stations, and passenger types. Other information such as the locations of stations along the routes and characteristics of stations are obtained from supplementary information provided by Land Transport Authority of Singapore.

5.3 Demand Pattern

In this section, travel demand patterns based on the data extracted from smart card data are described. With the help of the smart card data, it is possible to estimate how many passengers are in the MRT system at a given time t, for each station. To this end, records with tapping in time, known as $t_{in} < t$ and tapping out time $t_{out} \geq t$ are identified as passengers in the MRT system.

Figure 5.2 shows the number of passengers at each station during the course of the day, for train services in both directions, on a Monday in April 2011. It is observed that the demand for each direction has its own characteristics and both have significant morning and evening peaks.

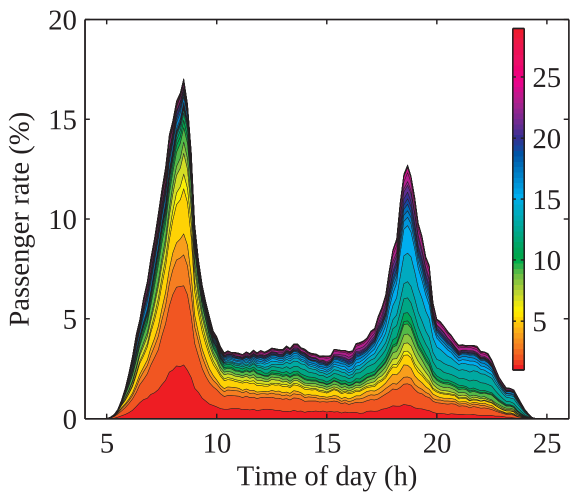

(a) EW1-EW29

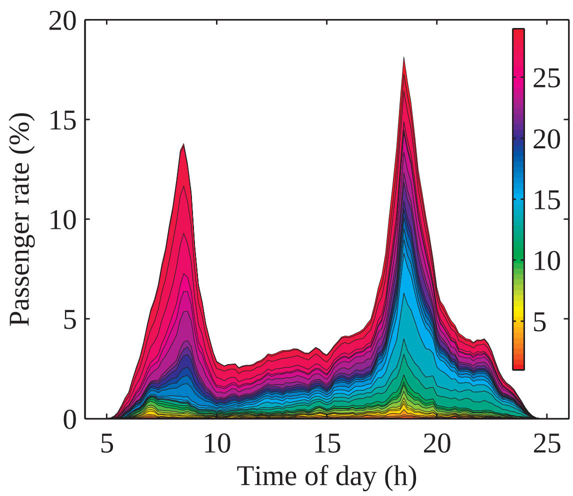

(b) EW29-EW1

Figure 5.2: Demand characteristics on EW line

Figure 5.2 shows a distinct morning peak at 8:30 am for both directions. Likewise, the evening peak can be observed at 6:30 pm. The different shapes of the two graphs indicate significant commuting in both directions with the morning commute direction from EW1 to EW29 being somewhat more distinctive.

It can be seen as well that in the morning peak, most of the demand originates from the first and last few stops along the line, while in the evening peak, most of the demand departs from the middle section of the line/service. In fact, this pattern maps effectively with land usage in Singapore. The predominant residential locations are located along the outskirts of Singapore and the work locations are centralized at the middle part of the city. During a typical weekday, most of the trips generated in the morning and evening peaks are commuters who travel to their work locations and back home respectively.

Such demand characteristics provide a basic understanding of an MRT service and the travel demand patterns of commuters over a typical weekday. The characteristics can be helpful to fine tune demand responsive train schedules or to define a more reliable strategy regarding the operation of MRT services.

5.4 Passenger Travel Time and Location

5.4.1 Travel time

Unlike the bus system, the MRT boarding and alighting times of individual passengers cannot be extracted directly. The tapping in and tapping out of their smart card takes place at the ticket gantry of the MRT station which is typically located on another floor of the station, typically one level below the entrance of station. Therefore, we cannot assign passengers to single trains directly. To make this information available to transit operators, a model describing passenger's movement between tapping in and tapping out would be required. In this study, such a model is proposed.

Figure 5.3 shows the typical activities for an MRT train ride. The trip begins with passenger tapping in at the ticket gantry. The passenger then makes his/her way to the platform, boards a train to travel on his/her journey, alights, and ends the journey by tapping out at another ticket gantry at his/her final destination. The waiting time can be calculated as the interval between passenger's arrival at the platform and upon boarding the train. In the smart card data set, the exact time of tapping in and tapping out are recorded. The interval between these two activities is the total time which a passenger spends in the MRT system. However, as stated,

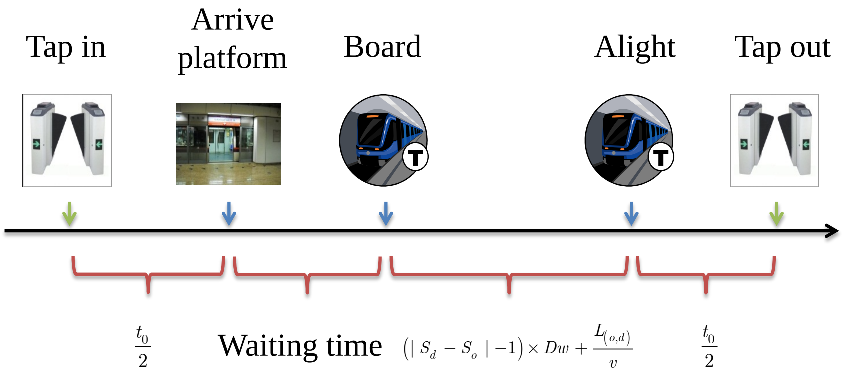

Figure 5.3: Activity chain of a typical subway trip

the boarding time and alighting time can not be obtained directly because of the uncertainty in the length of waiting time. This however needs to be imputed.

From all the passengers having the same origin and destination pair, the passenger with the minimum travel time can be located. In this study, the travel velocity of trains is assumed to be constant, therefore, the passenger with the minimum travel time also has the minimum waiting time. Due to the large quantity of data used in this study, the waiting time of these fastest passengers are assumed to be zero, which means that the passengers can board a train immediately upon arriving at the platform.

The time interval between boarding and alighting is assumed to comprise two parts. First, the total running time between every two adjacent stations, and secondly the total dwell time at internal stations. From this, a general travel time model can be formulated as follows:

$$T - T_w = t_0 + (|S_d - S_o| - 1) \times Dw + \frac{L_{(o,d)}}{v}, \tag{5.1}$$

where T_w is the waiting time while t_0 comprises two parts, the time spent tapping into the station to the time when a passenger arrives at the platform, and the time spent alighting from the train to tapping out of the station. S_o and S_d are the index of the stations, thus $|S_d - S_o| - 1$ is the number of stations a passenger has passed, excluding the origin and destination stations. Dw is the average dwell time at each station, which is assumed to be a constant value for all stations without considering the boarding and alighting demand. $L_{(o,d)} = |D(d) - D(o)|$ is the distance from the origin station to the destination station and v is the velocity of the trains. Thus, in this proposed model, only T_w, Dw and v are unknown.

Based on the minimum travel times for each origin-destination pair, this travel time model can be estimated with the fastest passengers who generally have $T_w = 0$. In this regression analysis, the minimum travel time records with an origin same as destination are removed so that the size of the regression data for both directions is $N^2 - N = 812$. The results of this is a travel time model are shown in Figure 5.4 and Table 5.1.

Table 5.1: Regression result of travel time model

Parameters	Value	t stat	p value
$t_0(s)$	109.75	48.5787	0.0000
$Dw(s)$	65.76	61.4119	0.0000
$v(m/s)$	21.63	61.8186	0.0000
R^2		0.9981	

The regression results indicate that dwell time at stations is about 65s and that the travel velocity of trains is about 22m/s, which are in accordance with effective values. Figure 5.4 shows the observed travel time for the fastest passengers from smart card data set and the predicted travel time based on the proposed model.

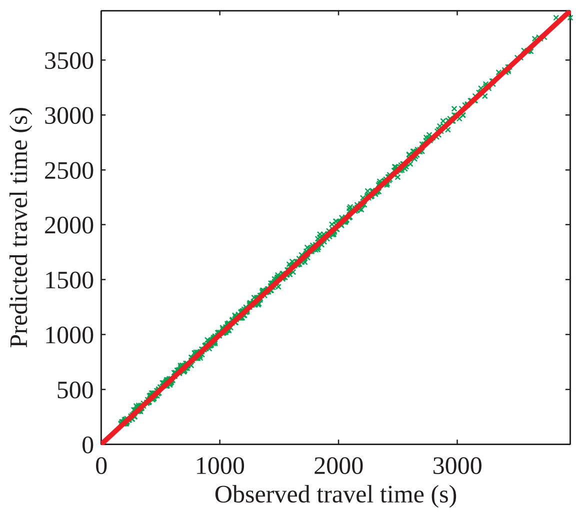

Figure 5.4: Predicted versus observed travel time for the fastest passengers

5.4.2 Determining location

Given the variability of the platform waiting time and availability of records of both the tapping in and tapping out of the smart card, it would be wise to use the latter for determining the passengers' location. Based on the previous travel time model, a passenger's location L at certain time t for two directions can be described by following Eq. (5.2):

$$T_a - t = \begin{cases} \frac{D(d)-L}{v} + (|S_d - S_n| - 1) \times Dw + \frac{t_0}{2} & \text{if } D(d) \geq L \\ \frac{L-D(d)}{v} + (|S_d - S_n| - 1) \times Dw + \frac{t_0}{2} & \text{if } D(d) < L \end{cases}, \tag{5.2}$$

where T_a is the time when a passenger taps out of the station, and n, S_n are the number of stations which the passenger has journeyed through and the location of that station respectively. In Eq. (5.2), t_0 is likewise divided equally into two parts, so only $\frac{t_0}{2}$ is considered for determining the passenger's location based on the tapping out smart card record.

The temporary location of any passengers boarding at station k traveling in direction 1 (fulfilling $D(d) > D(o)$) can then be described by Eq. (5.3).

$$L(k) = \left(t - T_a + (|S_d - k| - 1) \times Dw + \frac{t_0}{2}\right) \times v + D(d). \tag{5.3}$$

To distinguish between passengers waiting on a platform an travelling on a train, Eq. (5.4) is proposed. For all the possible stations in $o, \cdots, k, \cdots, d$, if the first station k^* can be found which satisfies Eq. (5.4), the permanent estimated location of the passenger is $L(k^*)$, where $P(k^*)$ is the location of station k^*:

$$L(k^*) - P(k^*) \geq 0. \tag{5.4}$$

For the opposite direction, the same method can be applied assuming that the passenger has just passed station k, then the temporary estimated location of this passenger is

$$L(k) = \left(T_a - t - (|S_d - k| - 1) \times Dw - \frac{t_0}{2}\right) \times v + D(d). \tag{5.5}$$

Then, for all the possible stations in $o, \cdots, k, \cdots, d$, if the first station k^* can be found which satisfies Eq. (5.6), the estimated location of the passenger is $L(k^*)$, where $P(k^*)$ is the location of station k^*.

$$P(k^*) - L(k^*) \geq 0. \tag{5.6}$$

5.4.3 Waiting passengers

Based on the location model in Section 5.4.2, if for all the possible stations $o, \cdots, k, \cdots, d$, no station k^* satisfies Eq. (5.4), it must be assumed that the passenger is in the MRT system but not on a train which, according to the travel time model, means that the passengers is either on the way to the platform or waiting there.

In other words, based on location estimation procedure the demand in the subway system can be consciously categorized into two groups: passengers who are on board the trains and passengers who are waiting for their trains.

Figure 5.5 shows the number of waiting passengers and on board the trains for both directions.

Compared with Figure 5.2, Figure 5.5 provides time-volume relationship for both trains and platforms. This serves as a basis for the spatial-temporal density model presented in the next section. Furthermore, for any point in time and any station, the number of passengers located at the respective station can be derived, which is crucial in the event of train breakdowns or evacuations, in order to determine an effective response strategy.

5.5 Spatial-Temporal Density and Trajectories

Section 5.4 describes the data processing to determine passenger's locations based on the proposed travel time model. In this section, the results of applying the described method using the smart card data records of a Monday in April 2011. The travel time model has been regressed with the travel time of the fastest passengers with the same data set. These two models make it possible to extract the spatial-temporal density of passengers on-board a train. Furthermore, the trajectories of trains can also be identified based on the spatial-temporal density figure.

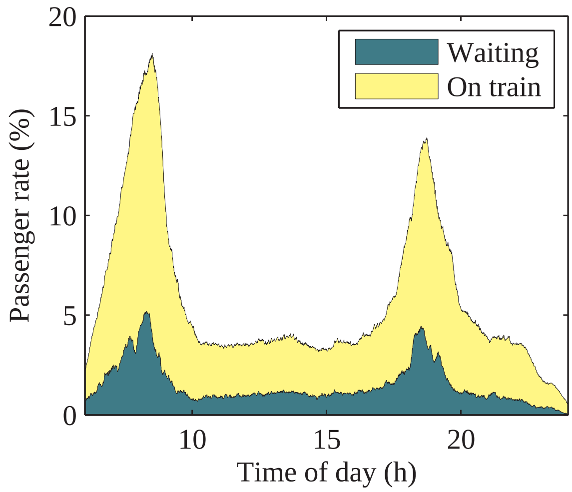

(a) EW1-EW29

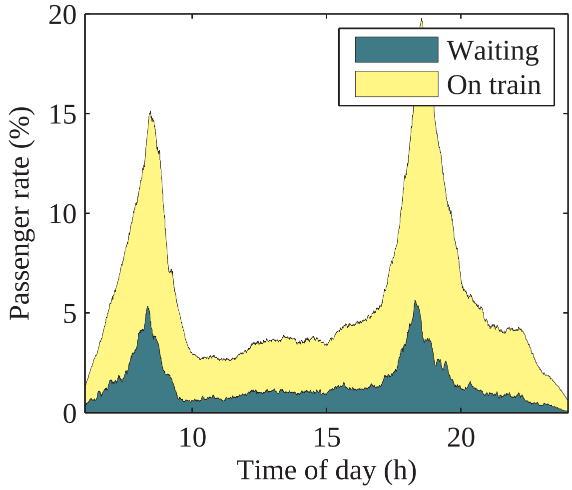

(b) EW29-EW1

Figure 5.5: Demand of waiting and on-board passengers on EW line

Based on the location estimation model, for all the passengers on-board as shown in Figure 5.5, their locations at any time t can be determined. As a next step, the spatial-temporal density relationship can be constructed using the estimated number of passengers within a certain length interval. Figure 5.6 shows the spatial-temporal density of passengers, from 7 a.m. to 9 a.m. in the morning and 12 p.m. to 2 p.m. in the afternoon respectively for one direction, in intervals of 100 m and 30 s. The colors indicate the passenger density who are on-board a train at a certain time and location. Intuitively, the location estimating model will work better for passengers with less travel time for each origin-destination pair, because there would be more variations for longer travel times for certain origin-destination pair, such as the cumulative difference in dwell time and velocity.

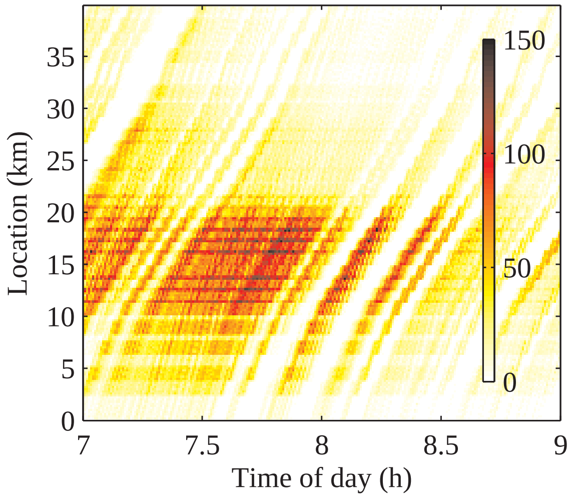

(a) EW1-EW29,7 a.m.—9 a.m.

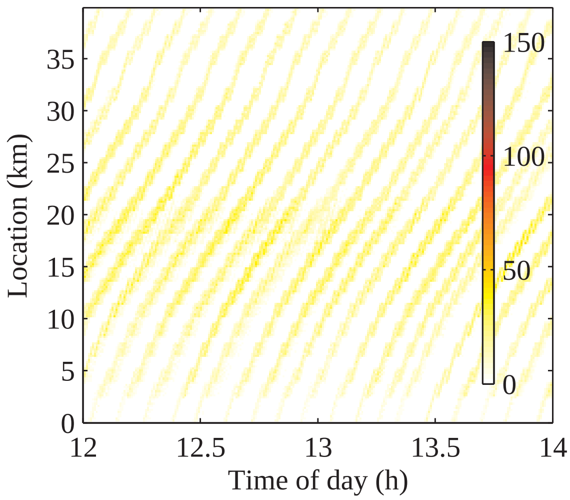

(b) EW1-EW29,12 p.m.—2 p.m.

Figure 5.6: Spatial-temporal density of passengers on EW line($pax/100m$)

Despite some decentralization in the density figure due to non-observed variability, distinct spatial-temporal relationships can be detected as well. This applies especially to graph (a) which plots the density distribution for midday. However, for peak hours, as depicted in graph (b), the assignment to single trains does not appear to be so straightforward. Here, additional information such as effective train operations on a given day or at least the trains schedule would help to consolidate decentralized density observation to individual train trajectory.

After such a procedure, passenger loading profile could be determined for every train along the entire Ease-West line. Such information is ideally suited to serve as a basis for developing failure response strategies. Since origin and destination pairs for every observation are known, one could use such data in the event of service disruption for the route planning of contingency buses which would act as a substitute for the disrupted train service. Currently, such buses typically run along the interrupted track section, and serve as bridge services. However, depending on the demand patterns and spatial distribution of the final destination, other strategies such as direct buses to highly frequented destinations might provide better service for affected passengers. Because of the very limited time for replacement service planning after an incident, failure response plans need to be prepared in advance and be readily available in the event of an incident. Compared to a system based on real-time information, the retrospective nature of this study is therefore advantageous. However, given the changing demand patterns over a day, a series of different service dispatch plans would need to be prepared to suit the prevailing demand conditions at a given point in time optimally.

5.6 Summary

In this chapter, the demand characteristics of the case study of one MRT service was investigated using smart card data collected in Singapore, with the objective of identifying effective commuter loadings for every train service.

A travel time model has been proposed by reconstructing a typical MRT trip into segments. The model was regressed using the data collected from the fastest passengers for each origin-destination pair. Based on the regression results, a location estimation model was developed to distinguish between passengers traveling on trains and waiting on platforms.

The location estimation model was then applied to all MRT train passengers. Based on the resulting spatial-temporal density plot, it appears feasible to group observations together to individual train trajectories. Such information in turn, has great potential to improve current disruption response plans. Optimizing demand responsive failure response plans based on origin destination demand data, however, is a complex and extensive problem, especially since a multitude of such plans would need to be prepared given the demand fluctuations over a day. Further research would therefore need to focus on developing heuristics that allow one to generate failure response efficiently.

The proposed model can be improved by accounting for station specific access and egress times t_0 given the different layouts of MRT stations. In terms of applying this to real world scenarios, the scope of the analysis needs to be extended from a single line to the whole MRT network which would require consideration of transfers. We will conduct a further study in the future.

Chapter 6

Designing Demand-driven Timetables for Metro Services Using Smart Card Data

Chapter information

An article based on this chapter was published in *Transportation Research Part C: Emerging Technologies*: Sun, L., Jin, J.G., Lee, D.-H., Axhausen, K.W., Erath, A., 2014. Demand-driven timetable design for metro services. *Transportation Research Part C: Emerging Technologies* 46, 284-299.

Timetable design is crucial to the metro service reliability. A straightforward and commonly adopted strategy in daily operation is a peak/off-peak-based schedule. However, such a strategy may fail to meet dynamic temporal passenger demand, resulting in long passenger waiting time at platforms and over-crowding in trains. Thanks to the emergence of smart card-based automated fare collection (AFC) systems, we can now better quantify spatial-temporal demand on a microscopic level. In this chapter, we formulate three optimization models to design demand-sensitive timetables by demonstrating train operation using equivalent time (interval). The first model aims at making the timetable more dynamic; the second model is an extension allowing for capacity constraints. The third model aims at designing a capacitated demand-sensitive peak/off-peak timetable. We assessed the performance of these three models and conducted sensitivity analyses on different parameters on a metro line in Singapore, finding that dynamical timetable built with capacity constraints is most advantageous. Finally, we conclude our study and discuss the implications of the three models: the capacitated model provides a timetable which shows best performance under fixed capacity constraints, while the uncapacitated model may offer optimal temporal train configuration. Although we imposed capacity constraints when designing the optimal peak/off-peak timetable, its performance is not as good as models with dynamical headways. However, it shows advantages such as being easier to operate and more understandable to the passengers.

6.1 Introduction

With the increasing amount and range of urban mobility, making public transport more efficient has become a primary task for many cities. Owing to its greater capacity, higher speed and increased reliability, rail-based metro systems, such as Singapore's "Mass Rapid Transit" (MRT), the London Underground and the Tokyo Metro are particularly important to a metropolis. To improve service quality and reduce passenger waiting time, recent studies demonstrate an increasing interest in designing efficient operation strategies — such as adjusting train speed dynamically, increasing or decreasing the dwell time at stations and designing new service timetables — to improve metro service reliability. Of all these approaches, timetable design has been accepted as the most straightforward and effective solution.

To provide user-centric public transport services, the principle of timetable design is to meet passenger demand, reduce passenger waiting time and avoid overcrowding as far as possible (Ceder and Wilson, 1986). Without an in-depth understanding of temporal demand patterns, operators' straightforward and commonly adopted strategy is a peak/off-peak-based schedule, where two types of service frequencies are set for peak and off-peak time, respectively. For example, the MRT system in Singapore operates at double frequency during morning and evening peaks. This strategy is easy to apply and performs well when supply is sufficient; however, given that passenger demand is not steady even during off-peak time, waiting time under fixed headway is still unbalanced when passenger arrival rate varies with time. On the other hand, under congested conditions or strong temporal demand heterogeneity, passengers might be unable to board a full train and they have to wait for another train. In these cases, the peak/off-peak timetable may fail to meet the temporal demand with limited supply. Furthermore, ignoring such demand dynamics may result in minor disruptions and poor service reliability. Thus, understanding the temporal demand variation and adjusting service frequency dynamically become crucial, since commuters are sensitive to their daily travel itineraries even at the minute level. Instead of assuming passengers will adjust their behavior to the service given, transit operators must better understand the nature of demand dynamics and design demand-sensitive timetables to meet greater demand with capacity-limited train services (Ceder, 2007; Niu and Zhou, 2013), reducing the risk of disruptions and attracting more ridership (Jin et al., 2013, 2014).

Lacking detailed passenger demand data, previous research works on scheduling mainly focused on an idealized transit system (de Palma and Lindsey, 2001; Newell, 1971; Osuna and Newell, 1972), while only a few noted the importance of passenger demand dynamics (Ceder, 1984, 1986; Ceder et al., 2001). Thanks to the emergence of smart card-based automated fare collection (AFC) systems (normally on-board registration for bus systems, while off-board registration at fare gantries for metro services), we can now extract the spatial-temporally stamped journey information on an individual level from days to weeks, helping us to better understand demand variations.

In this chapter, we present three optimization models for demand-driven timetable design. The first does not take train capacity as a constraint, while the second and the third allow for limited capacity constraints. The contributions of this chapter are twofold; first, we propose three demand-driven timetable design models, the results of which can be further used as operational guidelines and benchmarks; second, we use smart card data to conduct an in-depth analysis of daily transit demand pattern variation and obtain detailed spatial-temporal service loading profiles.

The remainder of this chapter is organized as follows: in the next section, we review previous studies on timetable design problems and the use of smart card data in transport modeling; in Section 6.3, we introduce our single-track timetable design problem and set out three different formulations; in Section 6.4, we employ a metro line in Singapore as a case and analyze the corresponding demand variation. Using the performance of the proposed models, we demonstrate the balance of different parameters against timetables in Section 6.5; finally, we summarize our main findings and discuss future work in Section 6.6.

6.2 Background

Previous studies on timetable design can be divided into two categories:

(1) Network timetable design problem; and

(2) Single track timetable design problem.

A network timetable design problem attempts to set up a timetable for multiple services in a connected transit network. The most common objective is to minimize transfer cost through transit coordination and synchronization among different routes. These problems have been investigated extensively on both bus networks (Ceder et al., 2001; de Palma and Lindsey, 2001; Ibarra-Rojas and Rios-Solis, 2012; Rapp and Gehner, 1976; Ting and Schonfeld, 2005) and metro networks (Caprara et al., 2002; Liebchen, 2008; Wong et al., 2008). Essentially, the motivation for synchronization arises from services with longer headway and higher reliability; transit services in rural areas might be a good example illustrating these characteristics. In this case, passenger waiting time can be reduced by increasing the simultaneous vehicle arrivals at transfer points. In other words, when timetables are independent (without synchronization), missing a connection will result in long delay.

In this chapter, we treat the demand-driven timetable design as a single track scheduling problem. This issue was first introduced to urban bus systems as setting service frequency. Furth and Wilson (1981) proposed a model to find optimal headway by maximizing social welfare, which included both ridership benefit and waiting-time savings. The corresponding constraints were total subsidy, fleet size and occupancy levels. However, due to lack of data, the importance of time-dependent demand was not addressed and frequencies were assumed to be constants during peak and off-peak time, respectively. To characterize the time-dependent nature of transit demand and take crowding cost into account, Koutsopoulos et al.

(1985) extended this model using a non-linear programming model. With the development of data collection techniques, Ceder (1984) first addressed the importance of ridership information and stated that service frequency should correspond to temporal passenger demand. This study summarized and analyzed four data collection techniques and evaluated their efficiency, using a frequency-setting problem, suggesting that a comprehensive load profile (ride check) is always superior to stop check (point check). However, the cost of such a ride check is much higher setting service because of the labor-intensive manual data collection. In a follow-up study, Ceder (1986) introduced an alternative approach for timetable design, with the objective of maximizing the correspondence of vehicle departure times with dynamic passenger demand. To evaluate the contribution of automated data collection system (ADCS) techniques, an automated procedure for efficiently setting bus time timetables was demonstrated. Given the nature of time-varying demand, Ceder et al. (2001) proposed a scheduling model to replace constant headway by making transit vehicles even-loaded.

Compared to bus systems, a metro system is more reliable regarding operation speed, dwell time at stations and service regularity, providing a better field to simplify service-scheduling problems. Chang and Chung (2005) considered both flexibility of service rescheduling and the process of defining timetables, providing a quick response in service regulation and constructing new timetable when an incident occurs. To control irregularity caused by stochastic variations in passenger demand and traffic conditions, a real-time control strategy was introduced to maintain headway regularity by minimizing total headway variance Ding and Chien (2001). This strategy was further tested by simulating a LRT (Light Rapid Transit) service in Newark, New Jersey. The vehicle holding problem was formulated as a deterministic quadratic program for a loop network with equal scheduled headways (Eberlein et al., 2001). Peeters and Kroon (2001) proposed a method to design an optimal cyclic passenger-rail timetable, in which trains depart at the same minute every hour. By applying the periodic event-scheduling problem in a graph model (Serafini and Ukovich, 1989), Liebchen (2008) designed a timetable with shorter passenger waiting time. This timetable has been implemented on the Berlin subway system in daily operation and it is reported that both passengers and transit operators profit from this timetable. Kaspi and Raviv (2012) proposed an integrated line planning and timetabling framework with the objective of minimizing operation cost and passenger cost, which includes waiting time at both origins and transfer stations. However, for a single track timetabling problem on frequent metro services with high demand — in particular during peak hours — the primary objectives are to meet the high demand by train services with limited capacity and to reduce passenger waiting time as much as possible (Niu and Zhou, 2013). In this situation, ensuring that passengers can board a train becomes operators' primary task and understanding the variation of passenger demand becomes crucial.

The implementation of smart card-based AFC system has generated large quantities of high-quality data, recording passenger activities with detailed time and location information. It offers a comprehensive profile on passenger demand variation. It has been publicly recognized that the potential benefit of smart card data on improving public transport planning and operation is enormous (Pelletier et al., 2011). In fact, AFC can replace automated passenger counting (APC) system by recording both passenger tapping-ins and tapping-outs, helping us obtain accurate load profiles for both bus service (Lee et al., 2012) and metro service (Sun et al., 2012). Smart card data offers us an excellent opportunity to identify the demand pattern for both spatial and temporal variation.

6.3 Timetable Design Problem

In this section, we first present a detailed description of the demand-driven timetable design problem for single track metro services. Assumptions are proposed based on operational characteristics. Then, we demonstrate three mathematical programming models to design demand sensitive timetables:

- Model (A): trains without capacity constraints (optimal design)
- Model (B): trains with limited capacity (optimal operation)
- Model (C): trains with limited capacity (optimal peak/off-peak)

6.3.1 Modeling framework

To explore temporal variation patterns of passenger demand, we first measure the rate of metro trips on a typical weekday. Figure 6.1 shows the demand variation of the whole EW line in Singapore from April 11th, 2011 to April 15th, 2011 (including both directions; averaged across weekdays), together with the temporal service headway extracted from *Google Maps*. In contrast to the pre-defined constant headway in peak and off-peak time, we see that passenger demand exhibits a significant degree of temporal variation. In this case, the metro system may suffer from greater total waiting time resulting from unbalanced passenger demand and fixed service headway. When demand is further increased, some passengers may be left behind if a coming train is full. Therefore, an optimal timetable should better meet dynamic passenger demand and reduce total waiting time, particularly when supply is limited. Our motivation is to make service timetables consistent with time-dependent passenger demand; our approach is to determine service departure times dynamically to minimize total passenger waiting time.

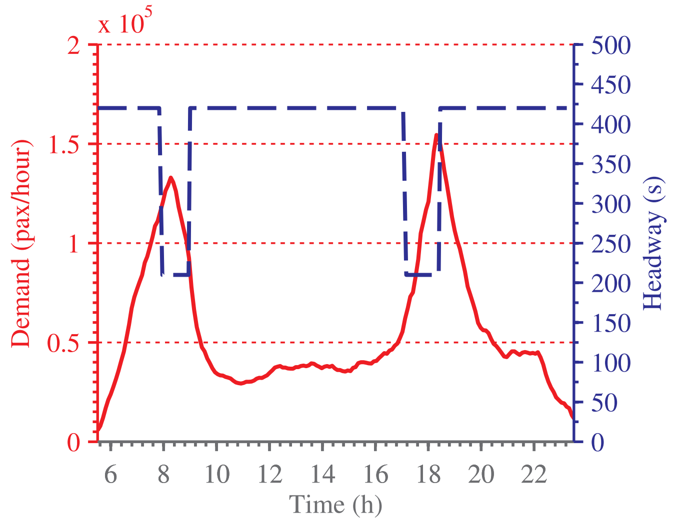

Figure 6.1: Demand and headway variation of the EW line over time of day

In a previous study, Sun et al. (2012) proposed a regression model to extract train trajectories as a first step in describing demand patterns and modeling of service operations. The result also demonstrates service reliability of the EW line of Singapore's MRT system; the extracted train trajectories are parallel with each other. Therefore, in the context of reliable operations (trains operated at same speed and without disruption), the timetable design problem is to plan train departure time from its terminus. Next, we use Figure 6.2 to simplify train operation processes for convenience of formulation.

When train services are operated with high reliability, headway between two successive trains should be steady from the departure terminal to the final destination, resulting in identical trajectories across all runs (Sun et al., 2012). In this case, train trajectories can be approximated by a straight line in a spatial-temporal panel (see Figure 6.2(a)). Although trains depart in continuous temporal scale, we model train departure times as discrete values to simplify this problem. In fact, formulation with discrete decision variables is more applicable and convenient for real-world operation as well. For example, the so-called "clock-face" headways are easy to memorize and operate (Ceder, 2007):

- 6 minute interval: vehicles depart at 0, 6, 12, 18, 24, 30, $\cdots$, 60 min in an hour.
- 10 minute interval: vehicles depart at 0, 10, 20, 30, 40, $\cdots$, 60 min in an hour.
- 15 minute interval: vehicles depart at 0, 15, 30, 45, 60 minutes in an hour.

Therefore, continuous time can be rescaled to discrete values given a pre-defined interval. In cases where headways are even shorter and vary over time, the interval can be defined as the greatest common divisor of headways in a similar way. Hence, time can be rescaled to discrete values as well. For example in Figure 6.2(a), trains depart from the terminus at the time $t = \{1, 3, 8, 17, \cdots\}$. However , the unit of time interval can be any values, such as 30 s, 1 min, or 2 min, depending on operating requirement.

Thus, passengers at the terminus can also be grouped into time intervals given their entering times. However, considering that it takes time for trains to travel from one station to another (the operation offsets shown in Figure 6.2(a)), passengers entering different stations at the same time do not share the same attribute; they may not board the same train. To better model passenger demand based on train operation, we need to rescale time correspondingly for each station. Inspired by the concept of 'moving time coordinate' (Newell, 1993), we propose the concept of equivalent time to synchronize train operation and passenger demand collectively. For any station s_i, its equivalent time is defined as the exact

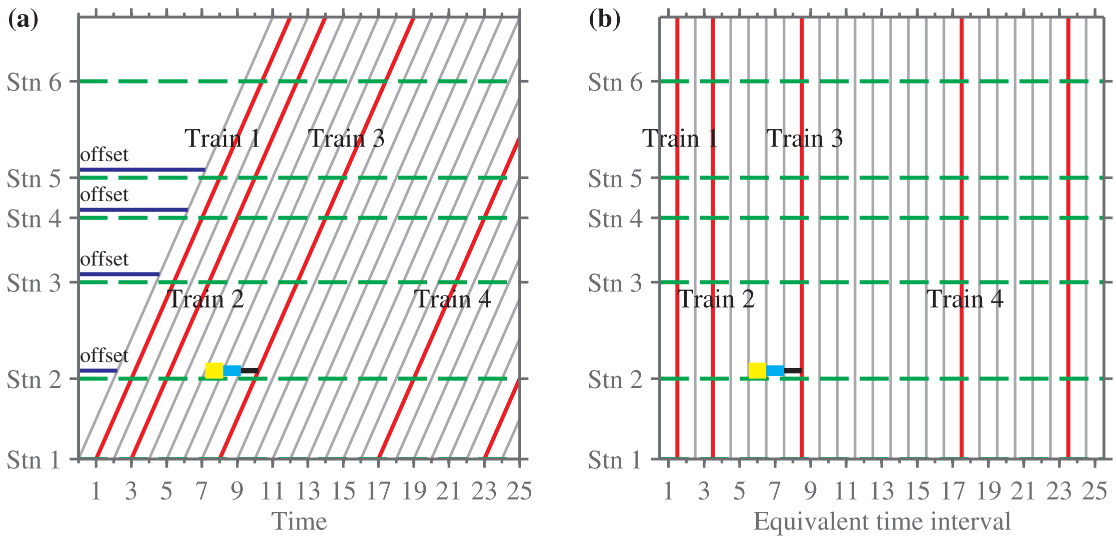

Figure 6.2: Descriptions of discrete departure time and equivalent time interval

time minus its operation offset (see Figure 6.2(b)). Through this transformation, we can redefine the passenger demand as a two-dimensional matrix — B_s^u — representing the number of passengers entering station s at equivalent time interval u.

Thus, train service operation can be simplified into a discrete process. Taking Figure 6.2(b) as an example, passengers in B_2^6, B_2^7, and B_2^8 may board Train 3, which runs at the end of equivalent interval 8.

6.3.2 Assumptions and operational constraints

Given the previous problem description, we make the following assumptions:

Assumptions

A1 Reliable services: Trains run at the same speed and dwell time, their trajectories are identical. This is a major assumption to simplify service operation processes explained in the previous section. It is also a strong one, since train services are not always punctual to timetables given various disturbances. For the case in Singapore, metro systems are automatically or semi-automatically operated, making themselves more resilient to disturbance by adjusting speed and dwell time in real-time. This assumption was tested in a previous study (Sun et al., 2012), where we find that trains can be operated regularly in disruption-free scenarios from the observed identical trajectories.

A2 Uniform arrival: For any station s, passengers arriving at equivalent interval t are distributed uniformly, which is proposed to simplify measurement of total waiting time. A number of service reliability studies suggest that this assumption is reasonable for transit service with short headway (such as metro services). However, passengers may have prior knowledge about service timetables when frequency is low and they tend to adjust their departure time accordingly (Furth and Muller, 2006). The operation constraints are identified before we formulate the model. We introduce the following operation constraints:

Constraints

C1 Discrete departure time: trains are restricted to depart at the end of equivalent interval t.

C2 Operation cost: number of daily services is fixed.

C3 Operation safety: headway should not be less than the minimum requirement.

C4 Service level: all passengers should be accommodated within a certain time, such as 20 minutes.

C5 Last service: departure time of the last service is pre-defined.

6.3.3 Model formulation

We now formulate mathematical programming problems that determine the departure time of each service. To measure passenger waiting time, we first define the set of waiting profiles p based on equivalent time intervals:

p**:** if passengers who enter stations in interval u board the train service departing at the end of interval t $(t \geq u)$, their waiting profile is defined as $p = t - u + 1$ (see Figure 6.3 for description).

Given the uniform arrival assumption, passengers have an average wait time $p - 0.5$ (in number of equivalent intervals) if they choose waiting profile p. Assuming the designed timetable should serve every passenger in time, i.e., Constraint C4, the set of waiting profile should be upper bounded. Taking all assumptions and constraints, we formulate the timetable

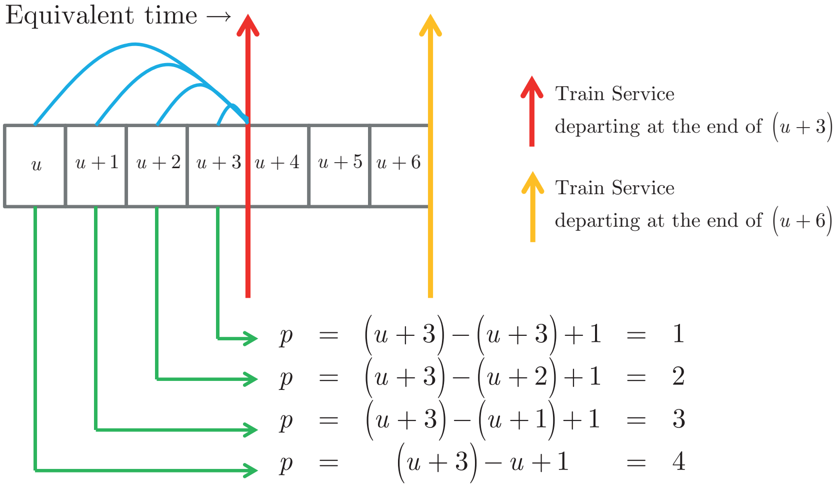

Figure 6.3: Description of waiting profile p

design process as an optimization problem minimizing passengers' total waiting time. Before presenting the formulations, we first define the following notations.

Notation

The following sets, indices, and parameters are used:

Sets:

T**:** set of equivalent time intervals. $T = \{1, 2, \cdots, T_n\}$.

S**:** set of stations, excluding the final destination. $S = \{1, 2, \cdots, S_n\}$.

P**:** set of waiting profiles. $P = \{1, 2, \cdots, P_n\}$.

Indices:

t**:** index of equivalent time intervals for train services. $t \in T$.

u**:** index of equivalent time intervals for passengers. $u \in T$.

s**:** index of metro stations. $s \in S$.

p**:** index of waiting profiles. $p \in P$.

Parameters:

T_n**:** number of equivalent time intervals.

S_n**:** number of metro stations, excluding the final destination.

K_n**:** number of daily train services.

P_n**:** number of waiting profiles.

B_s^u**:** demand profile, representing number of passengers arriving at station s in equivalent time interval u.

$N_{\max}$**:** maximum service headway, in number of equivalent intervals.

$N_{\min}$**:** minimum service headway, in number of equivalent intervals.

Model (A)

Here we assume that trains have unlimited capacity. In other words, a train can carry all passengers waiting for it. Given the reliable service assumption, as long as passengers arrive at a station in the same equivalent interval u, they will share the same waiting profile (i.e., the average waiting time of passengers groups B_s^u $\forall s \in S$ is the same.). In this model, we define two sets of decision variables:

Decision variables:

$x_t :\in \{0,1\}$, $\forall t \in T$**:** 1 if a train departs from terminal at the end of equivalent interval t; and 0 otherwise.

$y_{u,p}$, $\forall u \in T$, $\forall p \in P$**:** the proportion of passengers entering stations in equivalent interval u choosing waiting profile p.

Given the uniform arrival assumption, the average waiting time w^u of passenger entering at equivalent u can be calculated as:

$$w^u = \sum_{p \in P} y_{u,p} \, (p - 0.5). \tag{6.1}$$

By defining total passenger demand in equivalent interval u across all stations as $B^u = \sum\limits_{s \in S} B_s^u$, the timetable design problem is formulated in the following mathematical programming:

[Model (A)]

$$\min \sum_{u \in T} B^u w^u, \tag{6.2}$$

subject to:

$$x_t \in \{0,1\}, \quad \forall t \in T \tag{6.3}$$

$$\sum_{t \in T} x_t = K_n \tag{6.4}$$

$$\sum_{t \in [t_1,t_2]} x_t \leq 1, \quad t_2 = t_1 + N_{\min} - 1, \forall t_1, t_2 \in T \tag{6.5}$$

$$\sum_{t \in [t_1,t_2]} x_t \geq 1, \quad t_2 = t_1 + N_{\max} - 1, \forall t_1, t_2 \in T \tag{6.6}$$

$$x_{T_n} = 1 \tag{6.7}$$

CA1

$$0 \leq y_{u,p} \leq 1, \quad \forall u \in T, \forall p \in P \tag{6.8}$$

CA2

$$\sum_{p \in [1, \min(T_n - u + 1, P_n)]} y_{u,p} = 1, \quad \forall u \in T \tag{6.9}$$

CA3

$$x_t \geq y_{u,p}, \quad t = u + p - 1, \forall t \in T, \forall p \in P \tag{6.10}$$

Objective function (6.1) minimizes the total waiting time over all passengers. Constraints (6.2)~(6.7) correspond to the pre-defined operational constraints C1-C5. Constraint (6.8) and (6.9) ensure that all passengers are assigned waiting profiles. $p \in [1, \min(T_n - u + 1, P_n)]$ guarantees that the size of waiting profiles is reduced for passenger arriving after $u = T_n - P_n$. Constraint (6.10) guarantees consistency between boarding passengers and train services; if there are passengers assumed to board at the end of interval u, there must be one train serving people at that equivalent time (see Figure 6.3). Taken together, Model (A) is formulated as a mixed integer programming (MIP) problem.

A strong assumption of this model is that trains have unlimited capacity and passengers can always board the first coming train. In other words, this result provides us the optimal timetable only if service capacity is sufficient to carry all the waiting passengers. Nevertheless, if we consider the current metro operation as a feasible case with few people unable to board due to the capacity constraint, Model (A) still has the potential to design a more dynamical timetable compared to the peak/off-peak schedule. Furthermore, Model (A) may provide implications on the optimal time-dependent service capacities. By applying the optimal timetable on the current demand, we may get the maximum occupancy in temporal scale, helping us identify best train configurations over time of day. For example, in order to provide more space for standees and to increase the total capacity using the same number of train cars, operators usually run coaches with fewer seats in peaks hours in Singapore.

However, when demand further increases or temporal heterogeneity becomes more significant, Model (A) may fail to capture the additional waiting time caused by passengers left behind by a full train, particularly during peak time. To address this limitation, we extend Model (A) to take these capacity constraints into account.

Model (B)

To model limited service capacity and its consequences, the following additional parameters are introduced:

Parameters:

CAP**:** service capacity (number of on-board passengers should not exceed CAP).

$B^u_{s,d}$**:** temporal demand profile indexed by both boarding station and alighting station, representing number of passengers entering station s in equivalent interval u with destination d. By dividing $B^u_s = \sum_{d \in S} B^u_{s,d}$ in Model (A) using destinations, we are able to quantify the spatial occupancy of each train.

Decision variables:

$x_t :\in \{0, 1\}$**:** 1 if there is one train serving at the end of equivalent interval t; and 0 otherwise.

$y^s_{u,p}$**:** The proportion of passengers entering station s in equivalent interval u choosing waiting profile p. This variable is an extension of $y_{u,p}$ in Model (A), since passengers at different stations no longer share similar attributes. If the surplus capacity of the first coming train is limited, only part of the waiting passengers can board the train; the rest have to wait for the following service. For the example shown in Figure 6.4, 90% of the waiting passengers who entered station k at u to $u+3$, can board on the first train. Therefore, $y^s_{u,p}$ is a continuous value within $[0,1]$ in this model.

q^s_t: occupancy of train services departing at the end of t at station s ($s \in [1, S_n - 1]$) after alighting and boarding.

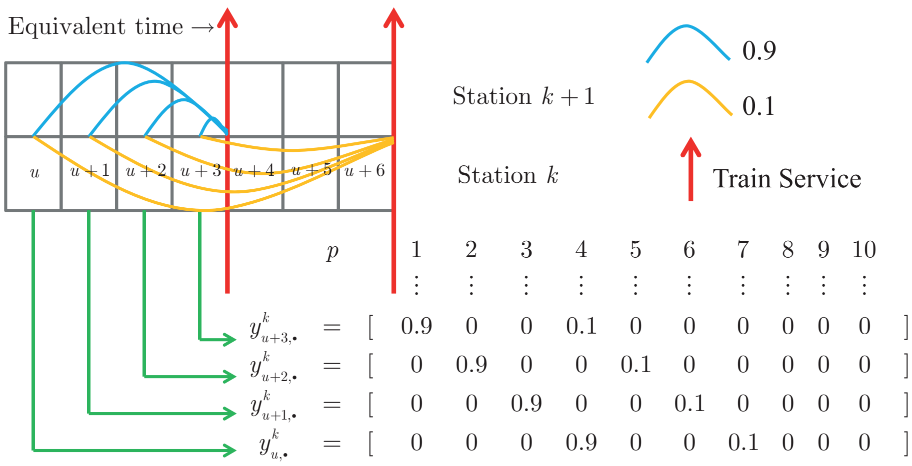

Figure 6.4: Description of $y^s_{u,p}$ ($\cdot$ means all waiting profiles $p \in P$ ($P_n = 10$))

Because of capacity constraints, passengers arriving in u no longer share the same waiting profile, as they might be unable to board if the coming train is full. Hence, the average waiting time of passenger group B^u_s is calculated as:

$$w^u_s = \sum_{p \in P} y^s_{u,p} \, (p - 0.5). \tag{6.11}$$

Then, the capacity incorporated timetable design problem is formulated as:

[Model (B)]

$$\min \sum_{s \in S} \sum_{u \in T} B^u_s w^u_s, \tag{6.12}$$

where $B^u_s = \sum_{d \in S} B^u_{s,d}$.

subject to:

$$x_t \in \{0,1\}, \quad \forall t \in T \tag{6.13}$$

$$\sum_{t \in T} x_t = K_n \tag{6.14}$$

$$\sum_{t\in[t_1,t_2]} x_t \leq 1, \quad t_2 = t_1 + N_{\min} - 1, \forall t_1, t_2 \in T \tag{6.15}$$

$$\sum_{t\in[t_1,t_2]} x_t \geq 1 \quad t_2 = t_1 + N_{\max} - 1, \forall t_1, t_2 \in T \tag{6.16}$$

$$x_{T_n} = 1 \tag{6.17}$$

CB1

$$0 \leq y^s_{u,p} \leq 1, \quad \forall s \in S, \forall u \in T, \forall p \in P \tag{6.18}$$

CB2

$$\sum_{p\in[1,\min(T_n-u+1,P_n)]} y^s_{u,p} = 1, \quad \forall s \in S, \forall u \in T \tag{6.19}$$

CB3

$$x_t \geq y^s_{u,p}, \quad t = u + p - 1, \forall s \in S, \forall t \in T, \forall p \in P \tag{6.20}$$

CB4

$$q^s_t = \begin{cases} \sum\limits_{u\in[\max(1,t-P_n+1),t]} \sum\limits_{d\in[2,S_n]} B^u_{1,d} y^1_{u,t-u+1} & s = 1, \forall t \in T \\ q^{s-1}_t - \sum\limits_{u\in[\max(1,t-P_n+1),t]} \sum\limits_{o\in[1,s-1]} B^u_{o,s} y^o_{u,t-u+1} + & \\ \qquad \sum\limits_{u\in[\max(1,t-P_n+1),t]} \sum\limits_{d\in[s+1,S_n]} B^u_{s,d} y^s_{u,t-u+1} & \forall s-1, s \in S, \forall t \in T \end{cases} \tag{6.21}$$

CB5

$$q^s_t \leq CAP, \quad \forall s \in S, \forall t \in T \tag{6.22}$$

Objective function (6.12) minimizes the total waiting time. Constraints (6.13)∼(6.17) correspond to the pre-defined operational constraints. Additional constraints CB1 ∼ CB5 are due to the following:

Constraint (6.18) and (6.19) ensure that all passengers are assigned waiting profiles. Constraint (6.20) guarantees consistency between boarding passengers and train services as well; if there are passengers supposed to board at the end of interval u, there must be one train serving people at that equivalent time (see Figure 6.4). Constraints (6.21) quantifies the spatial-temporal occupancy. Constraint (6.22) corresponds to the limited capacity, ensuring that occupancy is not more than capacity. Similar to Model (A), Model (B) is also a MIP; however, the problem is much larger, considering that the decision variable $y_{u,p}$ has been increased for one dimension to $y^s_{u,p}$ and additional constraints regarding service capacity have been added.

Optimal capacitated peak/off-peak timetable

We also introduce another model to find optimal peak/off-peak timetable. We define two additional parameters:

Parameters:

N_{Peak}: headway (in number of intervals) in peak periods.

N_{Off}: headway (in number of intervals) in off-peak periods. To avoid too much imbalance between peak and off-peak services. We let $N_{Off} < 3N_{Peak}$.

This model has the same decision variables and objective function as Model (B).

[Model (C)]

$$\min \sum_{s \in S} \sum_{u \in T} B^u_s w^u_s, \tag{6.23}$$

.

subject to Constraints (6.13), (6.14), (6.17), (6.18), (6.19), (6.20), (6.21), (6.22) and:

$$x_{t+N_{Peak}} + x_{t+N_{Off}} \geq x_t, \forall t, t+N_{Peak}, t+N_{Off} \in T. \tag{6.24}$$

$$\sum_{t \in [t_1, t_2]} x_t \leq 1, \quad t_2 = t_1 + N_{Peak} - 1, \forall t_1, t_2 \in T. \tag{6.25}$$

Constraint (6.24) ensures that headway should be chosen as N_{Off} of N_{Peak}. On the other hand, we need to also avoid both peak and off-peak headways being selected at the same time. In doing so, we can simply impose another constraint:

$$x_{t+N_{Peak}} + x_{t+N_{Off}} \leq 1, \forall t, t+N_{Peak}, t+N_{Off} \in T \tag{6.26}$$

, when $N_{Off} \neq 2N_{Peak}$. If $N_{Off} = 2N_{Peak}$, Constraint (6.26) should be removed as both $x_{t+N_{Peak}}$ and $x_{t+N_{Off}}$ can be 1 during peak period.

Note that this model does not limit the number of transitions between peak and off-peak strategy. However, given the strong temporal demand pattern, we do expect the model to provide timetables with a consistent peak/off-peak structure.

6.3.4 Complexity analysis

The metro service timetable design problem without capacity consideration is equivalent to the one-dimensional *Facility Location Problem* (Love, 1976) where all facilities and customers are all restricted to a Euclidean line: trains and passengers correspond to facilities and customers, respectively; the train departure decision corresponds to the facility location selection; the passengers' waiting time corresponds to the distance from demand points to facility locations; the amount of passengers corresponds to the weighting factor of demands. The unique feature of the metro timetable design problem is that demands can be only assigned to facilities with larger coordinates along the line since passengers can only board trains after their arrival. To solve the uncapacitated version of the location problem on a line, Love (1976) proposed a dynamic programming algorithm, which can be easily adopted to solve the uncapacitated metro service timetable design problem with minor adjustment. Thus, the uncapacitated metro service timetable design problem can be solved in polynomial time.

Similarly, if we consider a special case of the capacitated metro service timetable design problem where the minimum or maximum headway consideration is not considered, the resulted problem is equivalent to the capacitated *p-Facility Location Problem* on a real line (Brimberg et al., 2001). The authors proved that the addition of capacity constraints for facilities renders the problem to be NP-hard. Thus, the train service timetable design problem with capacity consideration is also NP-hard.

We simply employ standard solvers (e.g., CPLEX) to solve the uncapacitated and capacitated metro service timetable design problems (Model (A), (B) and (C)), as computational experiments show that both models can be solved within acceptable time.

6.4 Case Study

So far, we have formulated three different MIPs on the single-track timetable design problem. To test performance of the proposed timetable design formulations, we conduct a case study based on one MRT line in Singapore. In this section, we first introduce the smart card transaction data and then briefly discuss the case line.

6.4.1 Data preparation

Compared to entry-control system, such as in Outaouais Region, Canada (Trépanier et al., 2007) and Santiago, Chile (Munizaga and Palma, 2012), this AFC system in Singapore records both entry and exit information, making the data source highly comprehensive for research purposes. To better understand the demand variation of metro services, we employ one week's smart card transactions from April 11th, 2011 to April 17th, 2011. The data recorded both bus and MRT trips. A full trip record can be represented as a tuple (id, t_o, l_o, t_d, l_d), suggesting that passenger id departed from origin station/stop l_o at the time t_o and arrived at destination station/stop l_d at the time t_d. This information enables us to obtain the input parameters $B^u_{s,d}$ for the timetable design problem.

6.4.2 Case: the EW line

We chose one line from the MRT system in Singapore as an example. To convert real time to the defined equivalent time interval, we applied the travel time regression model in (Sun et al., 2012) to estimate the offset for each station. The results are provided in Table 6.1.

Table 6.1: Time offset table for estimating demand over equivalent time

Station	1	2	3	4	5	6	7	8	9	10	11	12
Offset [s]	0	178	309	492	646	806	922	1039	1160	1291	1408	1525
Station	13	14	15	16	17	18	19	20	21	22	23	···
Offset [s]	1637	1749	1870	1982	2118	2239	2370	2491	2608	2739	2884	···

6.4.3 Passenger demand

Smart card data has been used to study transit macroscopic demand patterns and their variation by many researchers. For example, Agard et al. (2006) analyzed smart card data collected from Outaouais Region, Canada and identified different trip habits and variability based on pre-defined user types. Utsunomiya et al. (2006) found that the demand pattern varied with day of the week, especially for weekdays and weekends. Therefore, transit operators are urged to use different schedules from day to day. Park et al. (2008) investigated and characterized the demand pattern of different transport modes in Seoul, South Korea. However, we need to measure the temporal demand $B^u_{s,d}$ in microscopic detail. In order do so and characterize the variability of B^u_s from day to day, we first distinguish two types of metro trips:

Full trips: Both entry and exit stations are on the selected service line.

Partial trips: Only part of the metro trip is on the selected line. (At least one station is not on the line.)

Therefore, the demand matrix B^u_s is the combination of full and partial trips. As opposed to bus systems, the tapping-in time is registered at fare gantries instead of on transit vehicles, making it easy for us to obtain the temporal demand. However, for partial trips, we have to identify which segments of the selected line the passenger has traveled, and then add this part on to the full trip demand.

To solve this problem, we apply the MATSim agent-based transport simulation toolkits to reconstruct the daily scenario (MATSim, 2013). To find the segment these passengers traveled (s and d on the subject line), partial trips are simulated on the whole metro network. Using travel time as utility, we find that about half of the trips on the selected line are full trips and the other half are partial trips. After combining these two demand sources, we begin to estimate the final temporal demand B^u_s.

Using the calculated time offsets and directed/transfer trip information, we estimate each element in the temporal demand B^u_s. Figure 6.5 plots the average demand profile for different stations over weekdays. As can be seen, demand is smooth and steady for most times of day; however, significant morning and evening peaks emerge at most stations.

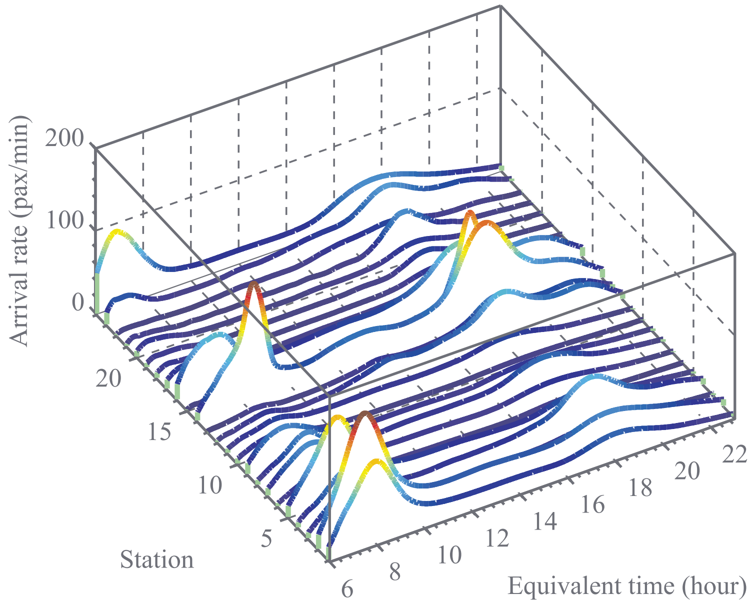

Figure 6.5: Passenger demand over equivalent time

6.4.4 Demand variation

To explore the day-to-day variation of passenger demand, we use cosine similarity to measure the spatial-temporal variation of both boarding demand and on-board demand. First, for boarding demand, after filling the demand matrix $B_s^u\,(\forall s, \forall u)$ for each day, the boarding demand similarity between day i and day j is defined as:

$$Sim_B\,(i,j) = \frac{\sum\limits_{s\in S}\sum\limits_{u\in T} b_{s,u}^{i} b_{s,u}^{j}}{\sqrt{\sum\limits_{s\in S}\sum\limits_{u\in T}\left(b_{s,u}^{i}\right)^2}\sqrt{\sum\limits_{s\in S}\sum\limits_{u\in T}\left(b_{s,u}^{j}\right)^2}}, \tag{6.27}$$

where $b_{s,u}^{i} = \frac{B_s^u(i)}{\sum\limits_{s}\sum\limits_{u} B_s^u(i)}$ is distribution of boarding demand at day i. Therefore, the value of similarity is between 0 and 1. The more similar the two matrices are, the nearer to 1 Sim_B is.

Based on the demand data, we calculate Sim_B during weekdays. Table 2 shows the cosine similarity of both boarding demand and on-board demand with equivalent interval length $\Delta\tau = 1\,\text{min}$. Note that all values of weekday boarding demand similarity are larger than 0.95, indicating a strong similarity between each day; day-to-day demand variation is tiny and negligible. The analysis shows that daily transit demand on the selected line exhibit a strong degree of homogeneity.

Table 6.2: Cosine similarities of boarding demand and of on-board demand

Sim_B	(Mon)	(Tue)	(Wed)	(Thu)	(Fri)	(Sat)	(Sun)
(Mon)	-	0.97	0.97	0.96	0.96	0.76	0.68
(Tue)	0.97	-	0.97	0.96	0.96	0.76	0.68
(Wed)	0.97	0.97	-	0.97	0.96	0.76	0.69
(Thu)	0.96	0.96	0.97	-	0.96	0.77	0.69
(Fri)	0.96	0.96	0.96	0.97	-	0.80	0.73
(Sat)	0.76	0.76	0.76	0.77	0.80	-	0.92
(Sun)	0.68	0.68	0.69	0.69	0.73	0.92	-

Hence, for convenience, we use an average demand profile over weekdays to test the proposed models' performance in the following analysis.

6.5 Results and Analysis

In this section, we evaluate the performance of these three models based on the case line introduced in previous section. We consider two cases here: Case 1 is a major problem, covering the entire metro line across whole operation time; Case 2 is a minor problem confined to the morning peak, consisting of only 15 stations. The detailed parameters of these two cases are listed in Table 6.3. We first use Case 1 to compare the overall performance of Model (A), (B) and (C).

Table 6.3: Input parameters of case studies

Parameter	Case 1	Case 2
$\Delta\tau$	1min	1min
T_n	1021 (6:00 – 23:00)	181 (6:00 – 09:00)
S_n	24	15
K_n	165	40 [35-55]
P_n	20 (maximum waiting time 20 min)	20 (maximum waiting time 20 min)
$N_{\max}$	10 (maximum headway 10 min)	10 (maximum headway 10 min)
$N_{\min}$	2 (minimum headway 2 min)	2 (minimum headway 2 min)
B_s^u	obtained by averaging weekday demand	obtained by averaging weekday demand
CAP	2000 pax/service	2000 [1900-2500]

All computation experiments were conducted on a PC with an Intel Core i7 3.40GHz with 16 GB RAM. The proposed Models (A), (B) and (C) are coded in CPLEX solver 12.5, using the standard configuration of CPLEX solver, which usually employs the Branch-and-Bound algorithm for MIP models. Table 6.4 summarizes the computational costs of these three models using both the major and minor cases.

Table 6.4: Computational results of Model (A) and (B)

Running time [sec]	Case 1 (Major)	Case 2 (Minor)
Model (A)	1.17	0.20
Model (B)	≈36000.00	161.17
Model (C)	≈36000.00	-

6.5.1 Optimal results

As the length of peak period headway and off-peak headway are parameters in Model (C). Based on the constraints on headway $N_{min} \leq N_{Peak} < N_{Off} \leq N_{max}$ and $N_{Off} < 3N_{Peak}$, the parameter set of (N_{Peak}, N_{Off}) is $\{(2,3), (2,4), (2,5), (3,4), (3,5), (3,6), (3,7), (3,8), (4,5), (4,6), (4,7), (4,8), (4,9), (4,10), \cdots\}$. We tested all possible combinations of (N_{Peak}, N_{Off}), finding that those feasible are (3,8), (4,7), (4,8), (4,9), (4,10) and (5,7). In all these cases, the model provides consistent peak/off-peak timetables with four transitions. The least waiting time is obtained when $N_{Peak} = 4$ and $N_{Off} = 8$.

To explore the variation of optimal timetables from these models, we plot the temporal headway by calculating the difference between sequential departure times for three scenarios in Figure 6.6(a): (1) peak/off-peak, (2) optimal solution of Model (C), (3) optimal solution of Model (A) and (4) optimal solution of Model (B), respectively. As can be seen in Figure 6.6(a), timetables (3) and (4) display more consistence with temporal passenger demand compared to (1) and (2). The figure also helps us distinguish the optimal solutions from each other. Owing to capacity constraints, we see clearly that timetable (4) operates more trains than timetable (3) during morning peaks.

To estimate the desired occupancy (when no passengers are left behind) of train services, we map passenger demand $B^u_{s,d}$ on timetable (1) and (3), respectively, to calculate the corresponding spatial temporal occupancy of each train. We determine the maximum occupancy of a train departed at the end of t as $Q_t = \max_{s \in S} \{q^s_t\}$ and use it to measure the importance of capacity constraints for all the three timetables (Figure 6.6(b)). Obviously, Q_t

is always less or equal to 2000 for Model (B) and (C) (see the second and the bottom inset of Figure 6.6(b)). However, we found that Q_ts of both timetable (1) and (3) exceed 2000 during morning and evening peaks, suggesting that the passenger demand at these equivalent intervals may not be met effectively if service capacity is fixed at 2000, resulting in additional waiting time when some passengers are left behind.

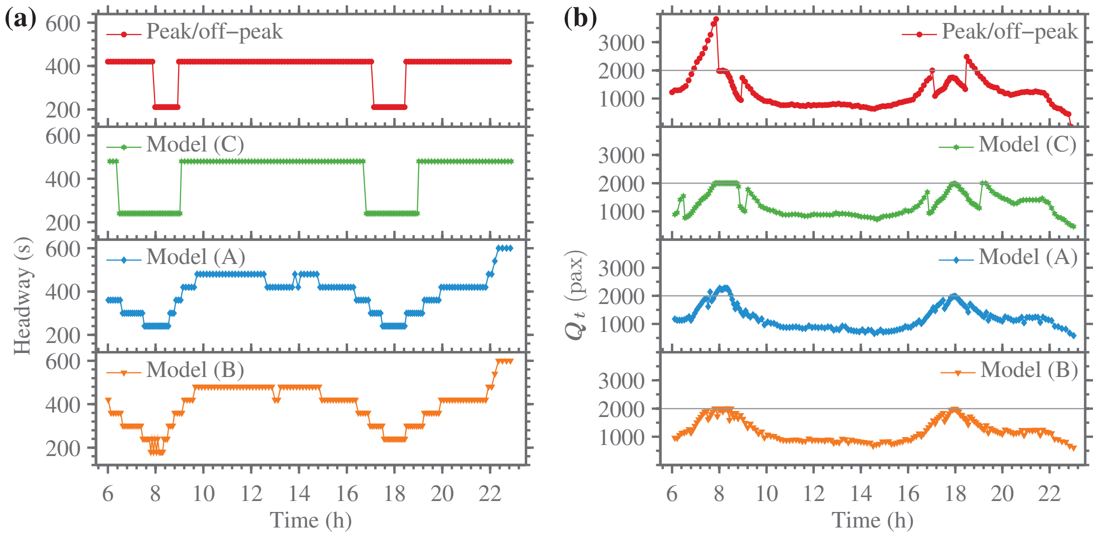

Figure 6.6: Headway profile and maximum occupancy from peak-based schedule, Model (C), Model (A) and Model (B)

To measure the actual/congested waiting time W'_u of timetable (1) and (3), we calculate the spatial occupancy of each train based on $B^u_{s,d}$ by tracking parameter ρ^u_s, demonstrating the ratio of left-behind passengers. To quantify ρ^u_s, we first map the tested timetable on the same panel as in Figure 6.2(b) and assume that left-behind passengers and new arriving passengers have the same chance to board on the coming train when occupancy reaches capacity. Then, the ratio ρ of left-behind passengers over all waiting passengers for each station and each train can be calculated. The estimation of ρ^u_s also helps us measure the total waiting time $W_{s,k}$ for Train k at Station s. In general, $W_{s,k}$ consists of waiting time of boarding passengers $W^1_{s,k}$ and left-behind passengers $W^2_{s,k}$. Taking Station 2 in Figure 6.2(b) as an example, if no passengers are left by Train 2, passengers who arrived in equivalent interval 4-8 have the same chance to board train 3, with total waiting time measured as $W^1_{2,3} = \sum_{u=4}^{8} (1-\rho)\, B^u_{s,\cdot}\, (8-u+0.5)$, where $B^u_{s,\cdot} = \sum_{d\in S} B^u_{s,d}$. Next, we can move the passengers left behind $\rho B^u_{s,\cdot}$ $(4 \le u \le 8)$ to $B^9_{s,\cdot}$ and charge them with full waiting time as: $W^1_{2,3} = \sum_{u=4}^{8} \rho B^u_{s,\cdot}\, (8-u+1)$. By applying this procedure iteratively, we can measure both spatial-temporal occupancy and total waiting time under capacity constraints simultaneously.

Table 6.5: Waiting time under different scenarios

	Timetable	W'_u [min]	Left-behind (pax)
(1)	Peak/off-peak	4.277 (+46.3%)	147,434
(2)	Model (C)	3.232 (+10.5%)	26,924
(3)	Model (A)	3.106 (+6.2%)	19,991
(4)	Model (B)	2.924 (+0.0%)	638

As Table 6.5 shows, timetable (4) performs best and average waiting time from timetable (3) is 6.2% higher. The average waiting time of the timetable (2) is about 3.23 min (10.5% higher than (4)). The current peak/off-peak timetable (from *Google Maps*) offers the longest waiting time (46.3% higher than (4)). We also measured the number of passengers that are left-behind by the first coming train. In this case, the peak/off-peak timetable is the worst because of the large number of passengers who cannot board due to limited service capacity (about 231 times larger than Timetable (4)). Timetable (2) and (3) are comparable with number of left behind 26,924 (42 times) and 19,991 (31 times), respectively.

To test the robustness of our results, we conducted a training/testing experiment by using demand from Monday to Wednesday as input to determine optimal timetables (4), and testing such timetable on passenger demand on Thursday and Friday, respectively. The timetable determined by demand from Thursday is identical to the one from Monday to Wednesday. Applying the same timetable on demand of Friday results in average waiting time 2.93 min, while the waiting time of the best timetable (estimated using Fri demand) is 2.91 min. Given the result, we would argue that variation from daily operation is marginal in determining the timetable compared to weekly, monthly or seasonal variation of demand. Nevertheless, given that smart card data is available from daily operation, we suggest using demand from previous week to design timetables for the current week.

To further quantify the benefit of dynamical timetables under demand variation, we assess their performance by adjusting the current demand (from 85% to 115%). Figure 6.7 shows the sensitivity analysis of average waiting time and number of delayed passengers given the demand variation. As can be seen, the demand sensitive timetables (2), (3) and (4) show higher

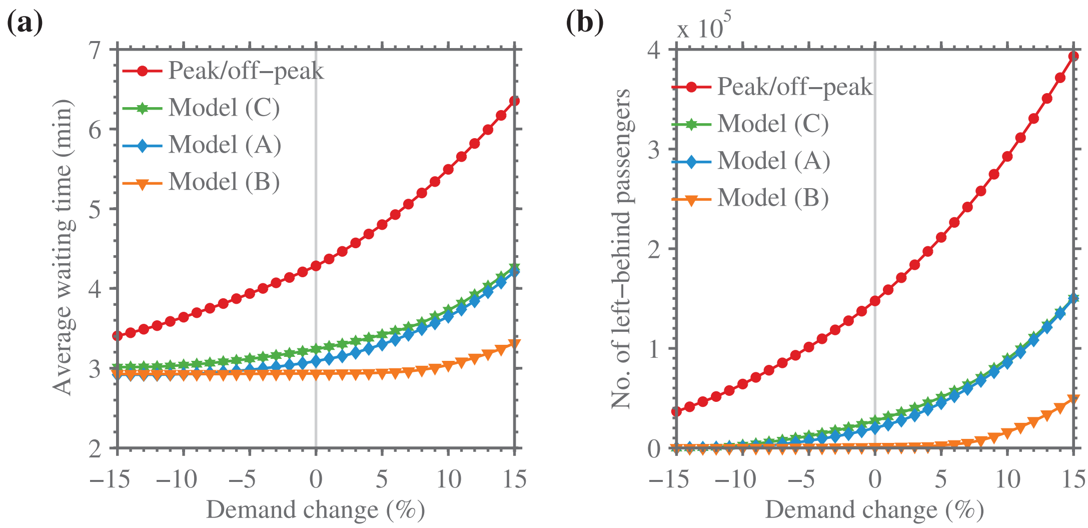

Figure 6.7: Performance of timetables under demand variation

resilience to the increase in demand than the current peak/off-peak timetable. However, Timetable (4) still performs good when demand increases 10%, while Timetable (2) and (3) becomes more sensitive. Taken together, all the three models can provide better timetables than the current peak/off-peak timetable.

Although capacity constraints are imposed on Model (C), timetable (2) performs not as well as (3) and (4) with current demand, being limited by the strict choices of N_{Peak} and N_{Off}. On the contrary, Model (A) and (B) can still benefit from the dynamical headway. Still, the optimal peak/off-peak schedule shows some advantages such as being easier to operate and more understandable to passengers. Model (A) is as good as (B) when passengers are seldom delayed by the capacity constraints (or train capacity is large enough). However, obviously, if passenger demand is further increased, Model (B) will have significant advantages over Model (A) and (C). In fact, the solution of Model (A) gives a lower bound of average waiting time since it offers equal weight to each passengers no matter if he/she can board or not. Any factors causing the violation of capacity constraints will prevent Model (A) from performing optimally. Despite increasing passenger demand, some other factors can also result in more passengers being delayed by capacity constraints, such as:

- Reduced number of services
- Reduced service capacity

Therefore, there are trade-offs among number of services, service capacity and timetable. Next, we use Case 2 to assess these balances for Model (A) and (B).

In fact, as stated before, Model (A) provides biased results under congested condition. In this case, we cannot tell which model is good taking only the computation time into account. To further evaluate their performance, we need to analyze the results and perform sensitivity analysis.

Considering that the computation time for Model (B) is very long for the full case (Case 1), we use the minor case (Case 2) to test sensitivity on number of services K_n and service capacity CAP.

6.5.2 Balancing number of services and timetable

We use morning peak hours from 6:00 – 9:00 to test the impact of number of services - K_n. For the peak/off-peak timetable, $K_n = 36$. To analyze the impact of K_n, sensitivity analysis is performed against $K_n = 34, 36, \cdots, 48, 50$. The results are shown in Figure 6.8.

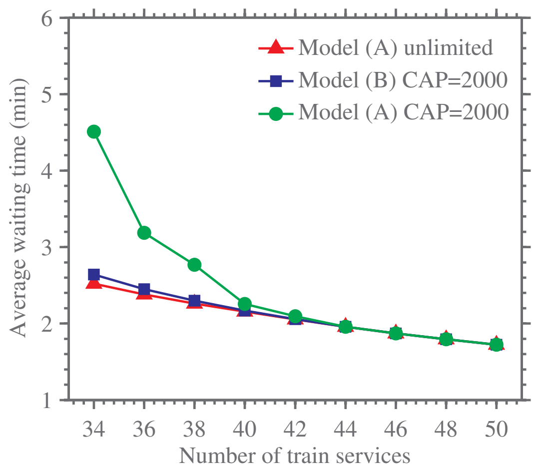

Figure 6.8: Balancing number of services and timetable

As seen, Model (A) and Model (B) provide similar average waiting time results. However, the real performance of timetables using results from Model (A) — with capacity constraints — has to be tested using simulation. In this case, Model (B) is always superior to the simulation using timetables obtained from Model (A), especially when the number of services is limited (less than 45). When $K_n = 34$, the real average waiting time is $\frac{4.51}{2.64} - 1 = 70.8\%$ higher than optimal result from Model (B).

These results indicate that the capacity constraints effect is substantial when number of services is limited. When number of services increases to 44, Model (B) does not produce different results from model (A) since capacity constrains are not a factor any more.

6.5.3 Balancing capacity and timetable

As with many services, there is also a balance of service capacity. Sensitivity analysis is conducted with $K_n = 36$ (same as the peak/off-peak timetable) against $CAP = 1900, 2000, \cdots, 2500$. The results are shown in Figure 6.9.

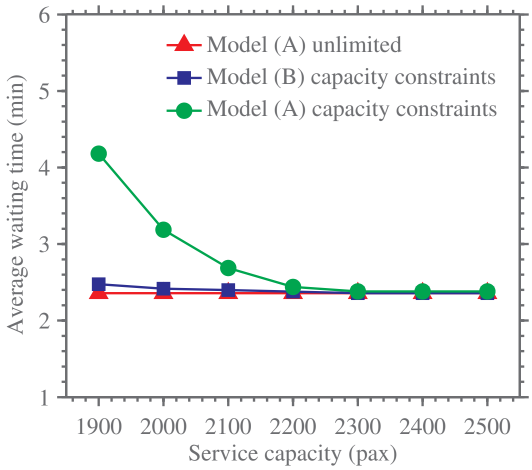

Figure 6.9: Balancing service capacity and timetable

Without considering capacity constraints, the ideal Model (A) always gives the best results with an average waiting time of 2.36 min. Model (B) produces slightly more waiting time than the ideal results. However, the simulated Model (A) provides quite different results than the ideal model. Owing to limited capacity, simulation on the obtained timetable from Model (A) performs poorly with less service capacity. In this case, average waiting time of timetable (A) with $CAP = 1900$ is $\frac{4.18}{2.47} - 1 = 69.2\%$ higher than timetable (B).

Taken together, in real operation, Model (B) always performs better than (A), particularly when resources, such as number of services and services capacity, are limited. Rather than providing the optimal timetable, Model (A) actually provides the benchmark for timetable design. On the other hand, as can be seen in Figure 6.6(b), although the services occupancy may exceed CAP, Model (A) shows what the crucial time is for operators to ramp up train capacity (by removing seats or setting up foldable seats).

6.6 Summary

The emergence of smart card-based automated fare collection system, as implemented in Singapore, enables us to better understand transit demand variation in a more detailed way. We propose three models for demand sensitive timetable design: the first model leaves train capacity out of account while the second allows for limited train capacity.

Both models are built on the concept of equivalent time (interval), which discretizes continuous time into discrete values. Although the models seem to provide better results if the equivalent interval is shorter, the computation time and accuracy of demand estimation will be important factors for application. In order to provide applicable strategy for our case, the length of equivalent interval is chosen as $\Delta\tau = 1$ min. In addition, it also determines the validity of assumption A2, since demand will change drastically if $\Delta\tau$ is sufficiently small. The problem is also crucial for transfer stations where passengers arrive in batch. In this case, the synchronization between different services may become more crucial. We use average waiting time as a measure of passenger cost without penalizing left-behind passengers; however, left-behind passengers might be more unsatisfied than passengers boarding the first coming train, given the same waiting time. Therefore, an additional penalty can be applied in future analysis to consider the cost of dissatisfaction.

Most developed metro systems are represented by well-connected networks, rather than a single track (on which this study has focused). For a simple network containing two intersecting tracks, we can still apply the concept of equivalent time by calculating offset times against the point of intersection (e.g., the transfer station) on each track and account for a corresponding transfer cost. In a more complex network with multiple transfer stations, though one may give priority to the main track, the strategy of applying equivalent time need to be adjusted accordingly. Our future study will consider the network case.

Considering that new timetables are designed using historical demand data, we cannot ascertain how much new demand (in coming weeks, for example) will differ from historical and how passengers will adjust their traveling behavior given a new timetable. Taking advantage of a continuous stream of smart card data, we can try to maintain demand homogeneity by frequent updates, such as using demand from previous week to design a timetable for the current week. We will also try to explore passenger response to a new timetable as a future research topic.

The proposed models are evaluated by simulating an MRT case service in Singapore; sensitivity analysis is conducted based on a minor case. Examining our analyses together, Model (B) provides exact optimal dynamic timetables under capacity constraints, whereas Model (A) shows significant potential for offering a dynamic timetable with dynamic capacity. Although the timetable (2) performs not as well as (3) and (4) with current demand, it shows some advantages such as being easier to operate and more understandable to passengers. All these optimal solutions can be used as benchmarks to measure current service levels. A major limitation of this study is the absence of crew team scheduling, which is critical for calculating transit operators' cost. On the other hand, given the principle of dynamic timetables, optimal train schedules will no longer involve regular intervals, but will vary over time. The irregular headway/arrival times would probably have an impact on expectations of some punctual passengers, resulting in a potential barrier to implementation. Nevertheless, given the more uniform arrival times across a larger population, the dynamic timetable has substantial potential to reduce total waiting time.

Chapter 7

An Integrated Bayesian Model for Passenger Flow Assignment in Metro Networks

Chapter information

An article based on this chapter was published in *Transportation Research Part C: Emerging Technologies*: Sun, L., Lu, Y., Jin, J.G., Lee, D.-H., Axhausen, K.W., 2015. An integrated Bayesian approach for passenger flow assignment in metro networks. *Transportation Research Part C: Emerging Technologies* 52, 116-131.

This chapter proposes an integrated Bayesian statistical inference framework to characterize passenger flow assignment model in a complex metro network. In doing so, we combine network cost attribute estimation and passenger route choice modeling using Bayesian inference. We build the posterior density by taking the likelihood of observing passenger travel times provided by smart card data and our prior knowledge about the studied metro network. Given the high-dimensional nature of parameters in this framework, we apply the variable-at-a-time Metropolis sampling algorithm to estimate the mean and Bayesian confidence interval for each parameter in turn. As a numerical example, this integrated approach is applied on the metro network in Singapore. Our result shows that link travel time exhibits a considerable coefficient of variation about 0.17, suggesting that travel time reliability is of high importance to metro operation. The estimation of route choice parameters conforms with previous survey-based study, showing that the disutility of transfer time is about twice of that of in-vehicle travel time in Singapore metro system.

7.1 Introduction

With the increasing demand and range of urban mobility, metro systems are playing more and more important roles in urban transportation, particularly in high-density mega-cities. Taking Singapore's Mass Rapid Transit (MRT) system as an example, around two million metro trips were made daily in the year 2012. Compared with other transport modes, metro systems have dedicated and exclusive rail-based infrastructures, making it possible to provide superior service with higher speeds and larger capacity. Due to their superiority, metro systems not only attract but also suffer from high passenger demand — especially during rush hours when passenger demand exceeds its designed capacity for not only trains, but also platforms — experiencing over-crowdedness, disturbances and disruptions time and again. These adverse impacts can jeopardize passenger's traveling experience and therefore should be minimized. From operators' point of view, understanding passenger demand and flow assignment patterns in a complex metro network becomes crucial to maintaining service reliability and developing efficient failure response strategies.

To characterize a passenger flow assignment model for metro network, two factors are of the most importance: O-D demand matrix and route choice behavior. Because of the widely adopted tap-in-tap-out fare collection system, the station-to-station OD matrix in a metro network is known; however the route choice decisions are usually not directly observable, therefore a widely used approach is to first develop a route choice model — characterized by some critical cost attributes influencing passenger perception, such as in-vehicle time, number of transfers and fare paid — and then employ observed preference data to calibrate model parameters. Despite the mathematical modeling, in principle there are two crucial issues to be solved in this approach before applying it on metro networks. The first is to accurately measure each attribute in the model, such as different stages of travel time and transit fares mentioned above. These values are used as input and assumed to be known in advance. In practice, experimenters need to determine such network properties by using train operation data and field surveys. However, accurate evaluation of route attributes, such as in-vehicle time, waiting time and transfer time, could be challenging considering possible congestion or interruption scenarios. The second issue is to obtain enough field observations, which register individual route choice preferences to support parameter estimation. However, in practice one may encounter many difficulties. On one hand, in the absence of detailed train operation logs recording train departure/arrival time and trajectories, it is difficult to measure exact network attributes, such as in-vehicle time, waiting time and transfer time. On the other hand, as most metro networks are designed as closed systems where passengers only leave traces at boarding/alighting stations for the purpose of fare collection, operators have limited knowledge on passenger route choice and trajectory within the system. In other words, we know little about which train or which transfer station an individual passenger has taken during his/her trip in the case where multiple alternative routes exist. In order to obtain passenger route choice preference data, a conventional approach is to conduct field surveys in train stations, asking people the exact route they will take to reach their destinations. However, some shortcomings of these methods have been identified, such as being subject to bias and errors and being both time-consuming and labor-intensive in conducting surveys and processing the data. In addition, since most surveys are conducted with focus on particular location and time, the results are often limited in scale and diversity. As a result, developing alternative methods to reveal individual route choice preference in large-scale networks remains challenging.

The emergence and wide deployment of automated fare collection (AFC) systems open a new data-driven approach for metro network analysis. Taking advantage of smart card-based fare collection systems, in which individual passenger's tapping-in/out transactions are recorded, researchers are now able to better understand metro operation with large quantities of real-world observations (Pelletier et al., 2011). Such data set also provides us with a good opportunity to study passenger behavior in a data-driven approach. In doing so, researchers have tried to combine passenger travel time information with train operation logs (Kusakabe et al., 2010; Sun and Xu, 2012; Zhou and Xu, 2012). However, without further investigating travel time variability, these approaches essentially assume that train services are always punctual to timetables and hence network cost attributes are assumed to be deterministic, even though there is clear evidence showing that train services can be delayed/disrupted by excessive passenger demand. On the other hand, owing to the uncertainty in travel time, the difficulties in revealing individual trajectory from tap-in/tap-out information still remain, preventing us from collecting accurate preference data. In view of these unsolved issues, this chapter presents the development and empirical verification of a new integrated metro assignment framework using Bayesian inference approach. Taking advantage of large quantities of real-world observations provided by smart card data, the suggested model simultaneously estimate network attributes and passenger route choice preference. Consequently, the proposed framework utilizes only travel time observations along with static network data to construct the passenger flow assignment model in a closed metro network. With low social-economic cost and implementation convenience, such approach is appealing for metro operations and maintenance.

Bayesian inference method is a well established statistical model which has been applied to various transportation applications, including O-D estimation, route choice modeling and flow assignment inference (Hazelton, 2008, 2010; Wei and Asakura, 2013). It enables us to find a posterior distribution which integrates all our prior knowledge with the available observations. Although in this sense it is a powerful tool for our inference problem, in practice it is difficult to implement such models owing to the difficulty in computing the Bayesian posterior analytically. However, thanks to the rapid increase of computational power, nowadays we can characterize properties of the Bayesian posterior using computational approaches, of which the most notable one is Markov Chain Monte Carlo (MCMC) methods (Robert and Casella, 2004; Robert, 2014). The proposed framework in this chapter is also based on solution algorithms provided by MCMC methods.

The contribution of this chapter is threefold. First, we construct an integrated network characterization and flow assignment framework through a data-driven approach, allowing us to better understand passenger route choice behavior from large quantities of smart card observations. Second, by taking travel time variability caused by possible interruption during metro operation into consideration, our model can better characterize network travel time and its uncertainty given any origin-destination (O-D) pairs, providing better travel information to metro users. Finally, as will be shown in the following, the Bayesian formulation has the capacity to estimate network cost attributes and characterize passenger route choice model in a simultaneous manner, showing great potential in practice, in particular in cities with large/complex metro networks such as Beijing, London, New York, Seoul and Tokyo.

This remainder of this chapter is organized as follows: in Section 7.2, we review previous studies on several related topics, including travel time reliability, passenger route choice behavior, the use of smart card data in understanding metro operation and flow assignment, and in particular the application of Bayesian inference in transport network modeling; in Section 7.3, we propose the modeling framework, which contains several components including reconstructing network, identifying choice set and building the Bayesian inference model. In Section 7.4, we present the variable-at-a-time solution algorithm to characterize Bayesian posterior distribution. As an illustration, we apply the proposed framework on the simplified Singapore MRT network as a case study in Section 7.5. Finally, we conclude our study, summarize our main findings and discuss future research directions in Section 7.6.

7.2 Background

Travel time reliability on urban road networks has been documented extensively in the literature, for both buses and private vehicles (Li et al., 2012; Strathman and Hopper, 1993; van Nes and van Oort, 2009). However, as mentioned, metro systems have long been considered as punctual to timetables (except during service interruptions/disruptions) and metro travel time reliability has attracted little attention in the literature. This is likely due to the lack of empirical observations regarding metro travel time reliability, which has now become available with the emergence of smart card data.

The large quantities of smart card transactions offer us a great opportunity to investigate passenger transit behavior and demand patterns (Bagchi and White, 2005). For example, Barry et al. (2002) first used smart card data to estimate metro O-D demand. By analyzing transit smart card data in Seoul, Park et al. (2008) suggested that smart card holders exhibit no difference from other users in terms of travel behavior, and travel patterns can be analyses in an aggregated manner. Using the same data set, Jang (2010) presented an empirical study on identifying transfer patterns of inter-modal transportation. Apart from understanding travel behavior, smart card data have been used to improve public transport services at strategic, tactical and operational levels as well. A comprehensive review of using smart card data at different levels of management can be found in (Pelletier et al., 2011). Using passenger demand extracted from smart card data in Singapore, Jin et al. (2014) studied a practical problem about integrating localized bus service with metro network in order to enhance the resilience to service disruptions of metro systems, offering new design principles of multi-modal transit networks. Using the same data set, Sun et al. (2014c) proposed three optimization models to design demand-driven timetables for a single-track metro service. The results show that demand-sensitive timetables have great potential in reducing passenger waiting time and crowdedness on trains.

Bus smart card systems record not only boarding/alighting stop/time, but also the ID of the vehicle. Thus, it may play the same role as data collected from automated vehicle location (AVL) and automated passenger counting (APC) systems (Lee et al., 2012). However, for metro systems, in which smart card readers are not deployed on trains but at stations, we cannot identify the particular train that an individual passenger takes from the transactions directly. Thus, it remains a challenge to understand metro trips at a microscopic level, in particular when travel time variability is taken into account. Besides, without an in-depth understanding of passenger route choice behavior, the flow assignment problem still need to be studied carefully.

In terms of calibrating flow assignment models, the field has long been relying on collecting preference data (e.g., stated preference and revealed preference) from field surveys and analyses. Thanks to the emergence of smart card data, the challenge now may shift to reveal passenger route choice using historical transactions rather than collecting route choice data with physical surveys. In doing so, Kusakabe et al. (2010) developed a methodology to estimate the exact train which an individual passenger occupies during his/her journey. This method could be used to accurately estimate train occupancy, which is an important factor influencing passenger's perception on service quality. Zhou and Xu (2012) proposed a maximum likelihood estimation method of individual passenger route choice given his/her entry and exit times. Based on the individual estimation, a flow assignment model was proposed to map the macroscopic passenger flow in reality for comparison. Given that the model relies on service timetable, it cannot characterize special events such as passengers being left-behind by a full train. Using the same data set in Beijing, Sun and Xu (2012) introduced the stochastic cost nature of different segments of a metro trip — walking-in, waiting, transfer and walking-out. The method first characterizes the distribution of travel time on each alternative and then uses the mean and variance (moments) to estimate the weight parameter of each component. This approach also requires accurate train operation timetables/logs as input, which may not available for other cases. However, these studies essentially ignore the stochastic nature of train travel time between successive stations, assuming that trains are always punctual to the scheduled timetable and requiring scheduled timetable data as input. By analyzing real-world passenger travel in Singapore, we found clearly that there is an increasing trend of standard deviation of travel time against mean travel time, suggesting that variability increases with travel time. In order to infer the exact train that one passenger took in the absence of operation logs, Sun et al. (2012) proposed a linear regression model to estimate train operation properties on a single-track and used the results to compute individual trajectory during a metro trip. By aggregating trajectories for all passengers by time, this method can help to identify train/service trajectory and estimate spatial-temporal occupancy of trains. However, the approach is only applied on a single-track, while at a network level the transfers and synchronization between different services need to be further investigated. In a recent paper, Zhu et al. (2014) presented an framework to calibrate passenger flow assignment model in metro networks based on genetic algorithm. The core of this framework is to first generate candidate set by using statistically-based criteria and then use genetic algorithm to find optimal solution.

All previous studies focus on one particular part of the overall problem. To our knowledge, in the literature little attention was paid to deal with the case where both network characteristics and passenger choice behavior are unavailable/unknown, and few researchers characterized route choice behavior in metro networks in large scale. It remains a challenge to develop a comprehensive framework which can solve both mentioned issues simultaneously using only travel time observations. In this sense, the Bayesian computational tools become attractive as it builds a posterior distribution by simply combining likelihood of the observable and our prior knowledge about the model (see Robert (2014) for a review). In a previous study, Hazelton (2010) developed an unified framework which integrates a statistical linear inverse structure with network-based transport model. The author illustrated the performance of this framework by estimating perception parameters in logit route choice models in Leicester, UK. The successful application of this model also inspired us to apply Bayesian inference on metro networks in this chapter. Despite calibrating choice models, Bayesian inference also exhibits excellent performance in stochastic traffic assignment modeling (Wei and Asakura, 2013) and vehicle travel time estimation using only global positioning system (GPS) data (Westgate et al., 2013). With the help of Bayesian inference and large quantities of travel time observations provided by smart card data , this chapter introduces an integrated modeling framework to quantify both network attributes and passenger route choice behavior.

7.3 Modeling Framework

To associate the observed passenger travel time with link costs and route choices, in this section we first propose a network reconstruction process, which distinguishes transfer stations by services and adds transfer links among different platforms correspondingly. Afterwards, we present a brief description of the integrated inference problem and introduce all model parameters in this framework. Then, we determine route choice set R_w for each O-D pair w. Given actual network configuration and property, in doing so one may apply a brute-force-search (BFS) method or k-shortest path method. After obtaining choice set, a Multinomial Logit (MNL) model is applied to measure the probability of choosing each choice r among the available set R_w given route attributes, where travelers' sensitivity to each attribute is parameter to be estimated. Finally, as a key component of the proposed framework, a Bayesian inference model is built to estimate the unknown parameter vectors, by taking all registered travel time from smart card transactions as observations.

7.3.1 Network reconstruction

In order to better model passenger travel time and route choice behavior, we reconstruct a metro network following the examples illustrated in Figure 7.1. In general, we can model each station as a single node in a sense similar to a map. However, by doing so we essentially miss the transfer cost for interchanging from one service to another (including walking and waiting), which is a crucial component of total travel time. In order to take transfer cost into consideration, we reconstruct a metro network by separating each transfer station as different nodes by services. For example in Figure 7.1, nodes marked as "T" represent an identical transfer station in the metro system; however, we distinguish them on each metro service and add transfer links to characterize transfer cost (including waiting) from platforms of one service to another. Essentially, in the case that n $(n \geq 2)$ services pass through a single transfer station, C_n^2 transfer links will be created between every pair.

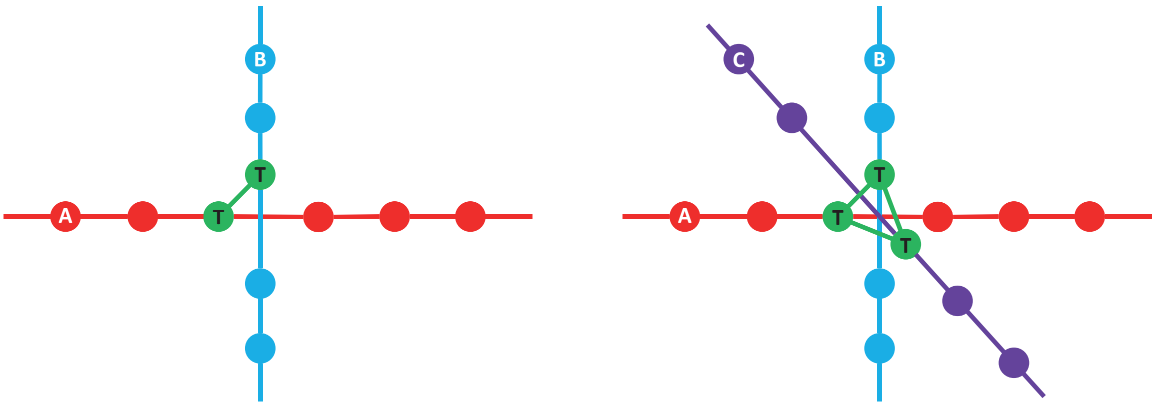

Figure 7.1: Reconstructing network by distinguishing transfer stations and adding transfer links

Despite that links could be directed as trains are operated in two-way, we model a metro network as undirected in this study for simplification, assuming that bi-directional travel costs between two adjacent stations are characterized by an identical distribution. In other words, we assume that two reciprocal links have the same properties.

7.3.2 Problem description

We consider a general metro network $G(N, A)$, consisting of a set of nodes N $(|N| = n_a)$ and a set of links A $(|A| = m_a)$. As we use travel time as cost measure in this study, 'cost' and 'time' as treated the same (interchangeable) throughout the chapter. We assume that link travel time $\boldsymbol{x} = (x_1, \cdots, x_a, \cdots x_{m_a})^\top$ are random variables, in the sense that services are not punctual to exact timetables due to various disturbances; as a result, stochastic travel time will be observed as in reality. This is also prerequisite to apply Bayesian statistical inference in our framework. Despite the fact that statistical properties of link travel time can be obtained from large quantities of service operation logs, the detailed train arrival/departure time and trajectory data along the service is seldom available. In this case, the Bayesian inference might be advantageous by taking unknown parameters as random variables and using travel time transactions as observations.

Let W be the set of O-D pairs; R_w denotes the set of possible routes connecting O-D pair w; $\boldsymbol{T}_w$ is the set of individual travel time obtained from those passengers traveling on O-D pair w, which is the final observable in this framework. We denote $\boldsymbol{T} = \bigcup_{w \in W} \boldsymbol{T}_w$ as the union of travel time observations from all O-D pairs. We start by introducing a combination of four parameter vectors, which capture different aspects of a metro system in our model:

- $\boldsymbol{c}$: describing network link costs;
- α : describing link cost variation (coefficient of variation);
- $\boldsymbol{\theta}$: describing passenger route choice behavior;
- m : describing extra cost on waiting/access/egress/failed boarding.

The details of these parameter vectors will be introduces in the following. In principle, our aim in this study is to use available observations (travel time $\boldsymbol{T}$) to infer all the unknown parameters above.

To allow for travel time reliability in our model, we assume that link cost x_a are random variables characterized by normal distribution $\mathcal{N}(c_a, (\alpha c_a)^2)$, of which the standard deviation is in proportion to its mean ($\sigma = \alpha\mu$). We assume that all link costs are independent. Thus, the overall distribution for all links can be written as:

$$\boldsymbol{x} \sim \mathcal{N}\left(\boldsymbol{c}, \mathrm{diag}\{\alpha \boldsymbol{c}\}^2\right), \tag{7.1}$$

where $\boldsymbol{c} = (c_1, \cdots, c_a, \cdots c_{m_a})^\top$ represents the mean travel time for all links and $\alpha = \sigma/\mu$ is the coefficient of variance. The independent normality assumption of link cost is crucial in our modeling, as it provides us a simplified way to measure route travel time given the additive property of normal distributions.

In modeling passenger route choice behavior in the metro network, we assume that choice probability is characterized by a Multinomial Logit (MNL) model and the representative utility of each route is measured as a linear combination of different route attributes with parameters $\boldsymbol{\theta} = (\theta_1, \cdots, \theta_K)^\top$.

As stated, the smart card system only provides us with the inter-tapping interval for each individual traveler, which is treated as travel time observations. In spite of transfer costs, the inter-tapping interval still involves in the access/egress walking time at boarding/alighting stations respectively, and waiting time at boarding platforms. In order to capture these extra costs, we impose a universal cost y on all O-D pairs and assume it to be characterized by a normal distribution:

$$y \sim \mathcal{N}\left(m, \sigma_y^2\right), \tag{7.2}$$

where m is an unknown parameter representing the mean of extra time and σ_y is standard deviation of y.

Note that the normal distribution assumption of link travel time is not mandatory in the proposed framework, but it will simplify the following step on calculating route cost. One can replace the normal assumption with any other distributions to facilitate the modeling requirements.

7.3.3 Generating route choice set

Before modeling passenger route choice behavior, we need to generate a choice set R_w for each O-D pair w, comprising all possible alternatives. In doing so, one may apply different strategies, such as link elimination, labeling and k-shortest-paths. Nevertheless, given the limited size and its simple structure of a metro network, a brute-fore-search (BFS) algorithm could be more advantageous than other methods in generating choice sets in shorter time.

Note that the proposed network reconstruction processes may produce some redundant alternatives, which are in principle illogical in reality, such as

- route with first link being a transfer link;
- route with last link being a transfer link;
- route containing two consecutive transfer links (appears where more than two services go through the same transfer station).

To better model choice behavior, we identify those routes with previous attributes and discard them when generating the final route choice set R_w.

7.3.4 Bayesian formulation

In this subsection we derive the Bayesian posterior distribution of parameter vectors given travel time observations. Based on the previous description, the unknown parameters are mean of link travel time $\boldsymbol{c}$, coefficient of variation α of link cost, parameters $\boldsymbol{\theta}$ for the MNL route choice model and average extra cost m. The observables we have are the travel time transactions for each O-D pair obtained from smart card data.

Taken together, applying Bayes' theorem on the unknown parameters and observations will give us the posterior density

$$\pi\left(\boldsymbol{c}, \alpha, \boldsymbol{\theta}, m|\boldsymbol{T}\right) = \frac{p\left(\boldsymbol{T}|\boldsymbol{c}, \alpha, \boldsymbol{\theta}, m\right)\pi\left(\boldsymbol{c}, \alpha, \boldsymbol{\theta}, m\right)}{p\left(\boldsymbol{T}\right)}, \tag{7.3}$$

where the denominator $P\left(\boldsymbol{T}\right)$ is the marginal density for T over all unknown parameters

$$p\left(\boldsymbol{T}\right) = \int\int\int\int \pi\left(\boldsymbol{c}, \alpha, \boldsymbol{\theta}, m\right) p\left(\boldsymbol{T}|\boldsymbol{c}, \alpha, \boldsymbol{\theta}, m\right) \mathrm{d}\boldsymbol{c}\mathrm{d}\alpha\mathrm{d}\boldsymbol{\theta}\mathrm{d}m. \tag{7.4}$$

With this formulation, $P\left(\boldsymbol{T}\right)$ is in fact a normalizing constant expressed as high-dimensional integrals, being independent of any unknown parameters. Thus, by further assuming that all unknown parameter vectors (and all elements in each vector) are independent, we have

$$\pi\left(\boldsymbol{c}, \alpha, \boldsymbol{\theta}, m|\boldsymbol{T}\right) \propto p\left(\boldsymbol{T}|\boldsymbol{c}, \alpha, \boldsymbol{\theta}, m\right)\pi\left(\boldsymbol{c}\right)\pi\left(\alpha\right)\pi\left(\boldsymbol{\theta}\right)\pi\left(m\right), \tag{7.5}$$

where $\pi(\delta)$ is the prior distribution of unknown parameter δ. Note that the probability of observing travel time $\boldsymbol{T}$ conditional on all unknown parameters equals the likelihood of all parameters given travel time observations, which means $p(\boldsymbol{T}|\boldsymbol{c},\alpha,\boldsymbol{\theta},m) = \mathcal{L}(\boldsymbol{c},\alpha,\boldsymbol{\theta},m|\boldsymbol{T})$.

Next, we focus on the likelihood function $\mathcal{L}(\boldsymbol{c},\alpha,\boldsymbol{\theta},m|\boldsymbol{T})$. By distinguishing travel time observations by their O-D pairs, we can re-write the likelihood as

$$\mathcal{L}(\boldsymbol{c},\alpha,\boldsymbol{\theta},m|\boldsymbol{T}) = \prod_{w\in W} p(\boldsymbol{T}_w|\boldsymbol{c},\alpha,\boldsymbol{\theta},m). \tag{7.6}$$

As stated, there often exists more than one possible route for an O-D pair w, so that the probability of observation travel time t from an individual also depends on the the alternative routes he/she may take. Therefore, by applying the formula of total probability on each observation t against all possible routes R_w, the probability of observing travel time t on O-D pair w can be expressed as

$$p_w(t|\boldsymbol{c},\alpha,\boldsymbol{\theta},m) = \sum_{r\in R_w} h(t|r,\boldsymbol{c},\alpha,\boldsymbol{\theta},m)\, f_w(r|\boldsymbol{c},\alpha,\boldsymbol{\theta},m), \tag{7.7}$$

where $f_w(r|\boldsymbol{c},\alpha,\boldsymbol{\theta},m)$ is the conditional probability of choosing route r from choice set R_w given all model parameters, and $h(t|r,\boldsymbol{c},\alpha,\boldsymbol{\theta},m)$ represents the conditional probability of observing travel time t given that route r is taken on O-D pair w.

Based on our primary assumption that link costs all follow normal distribution independently, we know that $t|r,\boldsymbol{c},\alpha,\boldsymbol{\theta},m$ also follows a normal distribution given its additive property

$$t|r,\boldsymbol{c},\alpha,\boldsymbol{\theta},m \sim \mathcal{N}\left(\sum_{a\in r} c_a + m, \alpha^2 \sum_{a\in r} c_a^2 + \sigma_y^2\right), \tag{7.8}$$

and thus

$$h(t|r,\boldsymbol{c},\alpha,\boldsymbol{\theta},m) = \frac{1}{\sqrt{2\pi\left(\alpha^2 \sum\limits_{a\in r} c_a^2 + \sigma_y^2\right)}} \exp\left(\frac{\left(t-\left(\sum\limits_{a\in r} c_a + m\right)\right)^2}{2\left(\alpha^2 \sum\limits_{a\in r} c_a^2 + \sigma_y^2\right)}\right). \tag{7.9}$$

To model passenger route choice behavior, we apply a Multinomial Logit (MNL) choice model, which usually assumes that representative utility V_r on route r is a linear function of route attributes $\boldsymbol{X}_r = (X_{r1}, \cdots, X_{rK})^\top$ (which is a function of cost parameters)

$$V_r(\boldsymbol{\theta}; \boldsymbol{c}, \alpha, m) = \boldsymbol{\theta}^\top \boldsymbol{X}_r = \sum_k \theta_k X_{rk}, \tag{7.10}$$

where θ_k is sensitivity parameter for attribute X_{rk}. Researchers have tried to quantify the impact of various attributes in determining passenger route choices in metro systems, such as in-vehicle time, waiting time, walking time, number of transfers and occupancy (Raveau et al., 2014). However, we cannot apply previous estimations directly since such behavioral parameters vary enormously from system to system, from city to city. Thus, one of the main purposes of such modeling framework is to infer parameter vector $\boldsymbol{\theta}$ case by case (Hazelton, 2010). Note that here the utility function are defined in a manner $\boldsymbol{X}_r$ are fixed value instead of random variables. Therefore, the error term of the utility function does not capture the randomness in $\boldsymbol{X}_r$. Taken together, when traveling on O-D pair w, the conditional probability $f_w(r|\cdot)$ of choosing route r conditional on other parameters $(\cdot)$ is

$$f_w(r|\boldsymbol{c}, \alpha, \boldsymbol{\theta}, m) = \frac{\exp(V_r)}{\sum_{r' \in R_w} \exp(V_{r'})}. \tag{7.11}$$

Therefore, the likelihood of O-D pair w can be given as

$$p(\boldsymbol{T}_w|\boldsymbol{c}, \alpha, \boldsymbol{\theta}, m) = \prod_{t \in \boldsymbol{T}_w} \left(\sum_{r \in R_w} h(t|r, \boldsymbol{c}, \alpha, \boldsymbol{\theta}, m) f_w(r|\boldsymbol{c}, \alpha, \boldsymbol{\theta}, m) \right). \tag{7.12}$$

Substituting Eqs. (7.6) and (7.12) in to Eq. (7.5), we can write the posterior probability as

$$\begin{aligned} &\pi(\boldsymbol{c}, \alpha, \boldsymbol{\theta}, m|\boldsymbol{T}) \\ &\propto \prod_{w \in W} \left(\prod_{t \in \boldsymbol{T}_w} \left(\sum_{r \in R_w} h(t|r, \boldsymbol{c}, \alpha, \boldsymbol{\theta}, m) f_w(r|\boldsymbol{c}, \alpha, \boldsymbol{\theta}, m) \right) \right) \times \pi(\boldsymbol{c}) \times \pi(\alpha) \times \pi(\boldsymbol{\theta}) \times \pi(m) \end{aligned} \tag{7.13}$$

Before implementing the Bayesian inference framework, we need to specify exact prior distributions $\pi(\delta)$ for the unknown parameters $\boldsymbol{c}$, α, $\boldsymbol{\theta}$ and m. Prior distributions are important if the number of observations is limited. However, for a metro system, the smart card system actually provide us with large quantities of travel time observations, helping us to correct our prior knowledge to a great extent. In practice, it would be better to propose prior distributions based on our experience or existing knowledge about the systems. In the case that we almost have no information about the parameters, a broad distribution such as uniform should be used.

The posterior distribution can provide not only point estimations for the unknown parameters but also their Bayesian confidence interval and Bayesian p-values for the purpose of hypothesis tests. However, in practice, it is usually impossible to get analytic estimations given its complex formulation. In the next section, we show a computational way to obtain the posterior distribution.

7.4 Solution Algorithm

If the conditional distribution can be written in closed form, ideally one can compute the marginal posterior distribution for each individual parameter analytically by calculating integrals. However, in our case, this approach is essentially impossible due to the difficulties in deriving the posterior distribution in Eq. (7.13) given its complicated formulation, the high-dimensional nature of the parameter space and in particular the normalizing integrals appearing in the denominator of Eq. (7.3). For such problems, in practice one usually uses the Monte Carlo Markov Chain (MCMC) approach to construct an updating algorithm to generate $\delta^{(t+1)}$ once we know $\delta^{(t)}$ (Robert and Casella, 2004). The Metropolis-Hastings (M-H) algorithm is a widely applied MCMC method, which enables us to sample candidate from a posterior distribution without knowing the closed form (Metropolis et al., 1953; Hastings, 1970). In each iteration, the M-H algorithm will generate a candidate from a pre-defined proposal distribution and then determine whether to accept it by calculating acceptance probability, which is a function of the ratio between target distribution density of the new candidate and the current sample respectively. By this means, we clear out the normalizing constant during the sampling. On the other hand, the Markov chain also shows advantages in a way that its stationary distribution is the target (or posterior) distribution we want to sample. Therefore, after obtaining enough realizations $\delta^{(1)}, \cdots, \delta^{(M)}$, one can estimate property I of parameter δ using

$$\hat{I} = \frac{1}{M-B} \sum_{i=B+1}^{M} f\left(\delta^{(i)}\right), \tag{7.14}$$

where B is a fixed number representing the burn-in period and M is the total number of samples. The burn-in samples are discarded as they might be biased given the arbitrarily chosen initial value $\delta^{(0)}$. After the burn-in period, the marginal distribution of the Markov chain is converging to its stationary state. To better determine the length of burn-in period, researchers have proposed different techniques in the literature (Geweke, 1992). The real characteristics of parameter δ can be measured using samples drawn from the posterior distribution π after the burn-in stage.

Given the high-dimensional nature of the studied problem, we perform a Variable-at-a-Time Metropolis sampling scheme (Metropolis et al., 1953). In doing so, we combine all parameter vectors in the posterior distribution as a full vector

$$\delta = \left(\boldsymbol{c}^\top, \alpha, \boldsymbol{\theta}^\top, m\right)^\top = \left(c_1, \cdots, c_N, \alpha, \theta_1, \cdots \theta_K, m\right)^\top = \left(\delta_1, \cdots, \delta_{N+K+2}\right)^\top. \tag{7.15}$$

The variable-at-a-time Metropolis then performs Metropolis sampling scheme on each coordinate of the parameter space in sequence, in the meanwhile other coordinates (parameters) remain fixed. Essentially, we may take an arbitrary proposal distribution $q\left(\delta_i^* | \delta_i^{(t)}\right)$ to draw samples for the i^{th} coordinate, and accepting new candidate δ_i^* based on M-H algorithm. However, in practice choosing an appropriate proposal distribution is crucial to performing the sampling process effectively. For simplicity, we apply a Gaussian random walk Metropolis (RWM) proposal to generate new candidates in a sequential order, in which

$$\delta_i^* = \delta_i^{(t)} + \epsilon_i^{(t)}, \tag{7.16}$$

where $\epsilon_i^{(t)} \sim \mathcal{N}\left(0, \sigma_i^2\right)$ and σ_i is the proposal standard deviation for the i^{th} coordinate. In other words, conditioning on the current sample, the new candidate follows a normal distribution $\delta_i^* | \delta_i^{(t)} \sim \mathcal{N}\left(\delta_i^{(t)}, \sigma_i^2\right)$. Thus, for the symmetric Gaussian distribution proposal, we have $q\left(\delta_i^* | \delta_i^{(t)}\right) = q\left(\delta_i^{(t)} | \delta_i^*\right)$, which simplifies the acceptance probability in M-H algorithm to

$$\mathcal{A}\left(\delta_i^*, \delta_i^{(t)}\right) = \min\left\{1, \frac{\pi'\left(\delta_i^*\right) q\left(\delta_i^{(t)} | \delta_i^*\right)}{\pi'\left(\delta_i^{(t)}\right) q\left(\delta_i^* | \delta_i^{(t)}\right)}\right\} = \min\left\{1, \frac{\pi'\left(\delta_i^*\right)}{\pi'\left(\delta_i^{(t)}\right)}\right\}, \tag{7.17}$$

where $\pi'(\delta_i')$ is the target (posterior) probability by changing only the i^{th} parameter to δ_i' and keeping other parameters as their latest updated values. In other words, by updating parameters in sequential order, $\pi'(\delta_i')$ is calculated as the posterior density

$$\pi'(\delta_i') = \pi\left(\delta_1^{(t+1)}, \cdots, \delta_{i-1}^{(t+1)}, \delta_i', \delta_{i+1}^{(t)}, \cdots, \delta_{N+K+2}^{(t)} | \boldsymbol{T}\right). \tag{7.18}$$

Taken together, we summarize the variable-at-a-time Metropolis algorithm as the following processes:

Variable-at-a-Time Metropolis Sampling

(V1) Specify initial samples $\delta^{(0)} = \left(c_1^{(0)}, \cdots, c_N^{(0)}, \alpha^{(0)}, \theta_1^{(0)}, \cdots, \theta_K^{(0)}, m^{(0)}\right)^\top$; set $t \leftarrow 1$.

(V2) For $\delta^{(t)}$, sampling new value $\delta_i^{(t+1)}$ conditional on its current value $\delta_i^{(t)}$ in sequential order $(i = 1, \cdots, N+K+2)$ using M-H sampling scheme (see following).

(V3) If $t < M$, set $t \leftarrow t+1$ and return to Step (V1); Otherwise, stop sampling.

In order to avoid generating candidate from a high-dimensional distribution directly, the variable-at-a-time generate new sample for each coordinate in turn in Step (V2). In doing so, new candidate on each coordinate is sampled based on the following M-H scheme.

Metropolis-Hasting Sampling

(M1) Sample candidate value δ_i^* using the Gaussian random walk proposal (see Eq. (7.16)).

(M2) Compute acceptance probability using Eq. (7.17). The target (posterior) distributions are calculated as:

$$\begin{aligned}\pi'(\delta_i^*) &= p\left(\boldsymbol{T}|\delta_i^*, \delta_{-i}^{(t)}\right)\pi\left(\delta_i^*, \delta_{-i}^{(t)}\right)/p(\boldsymbol{T}) \\ &\propto p\left(\boldsymbol{T}|\delta_1^{(t+1)}, \cdots, \delta_{i-1}^{(t+1)}, \delta_i^*, \delta_{i+1}^{(t)}, \cdots, \delta_{N+4}^{(t)}\right)\pi(\delta_i^*),\end{aligned} \tag{7.19}$$

and

$$\begin{aligned}\pi'\left(\delta_i^{(t)}\right) &= p\left(\boldsymbol{T}|\delta_i^{(t)},\delta_{-i}^{(t)}\right)\pi\left(\delta_i^{(t)},\delta_{-i}^{(t)}\right)/p\left(\boldsymbol{T}\right)\\ &\propto p\left(\boldsymbol{T}|\delta_1^{(t+1)},\cdots,\delta_{i-1}^{(t+1)},\delta_i^*,\delta_{i+1}^{(t)},\cdots,\delta_{N+4}^{(t)}\right)\pi\left(\delta_i^{(t)}\right),\end{aligned} \tag{7.20}$$

where $\delta_{-i}^{(t)} = \left(\delta_1^{(t+1)},\cdots,\delta_{i-1}^{(t+1)},\delta_{i+1}^{(t)},\cdots,\delta_M^{(t)}\right)$ is parameter set from the latest updated coordinates except the i^{th} (i.e., $\delta_i^{(t)}$). The normalizing constant $p\left(\boldsymbol{T}\right)$, together with $\pi\left(\delta_{-i}^{(t)}\right)$ in both numerator and dominator, can be canceled out when calculating $\pi'\left(\delta_i^*\right)/\pi'\left(\delta_i^{(t)}\right)$.

(M3) Sample a value $\delta_i^{(t+1)}$ according to the following:

$$\delta_i^{(t+1)} = \begin{cases}\delta_i^* & \text{with probability } \mathcal{A}\left(\delta_i^*,\delta_i^{(t)}\right)\\ \delta_i^{(t)} & \text{otherwise.}\end{cases} \tag{7.21}$$

The variable-at-a-time Metropolis is a good choice for high-dimensional problems as our case, since it keeps only one dimension (i.e., the i^{th} coordinate) as variable each time; while the general Metropolis moving all coordinates at once, resulting in large rejection rate. For each unknown parameter, the algorithm outputs a collection of iteration-stamped samples, whose stationary distribution is its marginal posterior distribution.

7.5 Case Study

For the purpose of model illustration and verification, in this section we apply the proposed modeling framework on Singapore's Mass Rapid Transit (MRT) network. The Bayesian inference model is built on real-world travel time (between tapping-in and tapping-out) observations collected on one day (19th, March, 2012) in Singapore as an example.

7.5.1 Singapore MRT network

We only consider the arterial network of Singapore's metro systems by removing extensions and light rail transit services. Figure 7.2 shows the basic structure of the adapted network, which consists of four services (shown in different colors) and 88 stations. The reconstructed network contains 99 nodes and 107 links, of which 95 are in-vehicle links and 12 are transfer links. In this network, most transfer stations connect only two services. In the center of the figure we can see a special case that three services pass through the same transfer station — Dhoby Ghaut. For this special case, three transfer links will be created.

Figure 7.2: Adapted MRT network of Singapore used in this study

Table 7.1 lists all transfer links and the corresponding platforms they connect.

Table 7.1: Transfer links in Singapore MRT network

station	platform A	platform B
Bishan	NS17	CC15
Buona Vista	EW21	CC22
City Hall	EW13	NS25
Dhoby Ghaut	NS24	CC1
Dhoby Ghaut	NS24	NE6
Dhoby Ghaut	NE6	CC1
HarbourFront	NE1	CC29
Jurong East	EW24	NS1
Outram Park	EW16	NE3
Paya Lebar	EW8	CC9
Raffles Place	EW14	NS24
Serangoon	NE12	CC13

7.5.2 Route choice behavior

In order to generate route choice set R_w, we performed BFS method described in the modeling framework and removed all redundant alternatives. After obtaining choice set R_w, we used an Multinomial Logit model route choice model as defined in Eq. (7.11) to computed route choice probability. A variety of studies on passenger route choice behavior have been conducted based on field survey data in the literature (Guo and Wilson, 2007; Wardman and Whelan, 2011; Raveau et al., 2014). For instance, Raveau et al. (2014) studied route choice behavior in two metro networks — London Underground and Santiago Metro, by taking various attributes into consideration, including different time components, transfer experience, level of crowdedness, network topology and other social-demographic characteristics. In fact, our modeling framework provides us with enough flexibility to apply diverse types of utility function in the choice model. Nevertheless, in this study we only examined a simple example, in which the representative utility V_r of route r is completely characterized by two attributes ($K = 2$): (1) total in-vehicle travel time $X_{r1} = \sum_{a \in r \setminus r_t} c_a$, and (2) total transfer time $X_{r2} = \sum_{a \in r_t} c_a$, quantifying route utility as

$$V_r = \theta_1 \sum_{a \in r \setminus r_t} c_a + \theta_2 \sum_{a \in r_t} c_a, \tag{7.22}$$

where route r is considered as a set of links and r_t is the set of transfer links in route r. In this formulation we do not take transit fares and waiting time of the first stage into consideration, because fare is only computed by the shortest alternative in distance (i.e., transit fares are the same for different route alternatives) and waiting time of the first stage is assumed to be the same across all trips. Therefore, both terms can be canceled our in the utility function. Note that V_r is also a function of unknown parameters. Under the above assumptions, the probability of choosing route r conditional on other parameters is given by

$$f_w\left(r|\boldsymbol{c}, \alpha, \boldsymbol{\theta}, m\right) = \frac{\exp\left(\theta_1 \sum\limits_{a \in r \setminus r_t} c_a + \theta_2 \sum\limits_{a \in r_t} c_a\right)}{\sum\limits_{r' \in R_w} \exp\left(\theta_1 \sum\limits_{a \in r' \setminus r'_t} c_a + \theta_2 \sum\limits_{a \in r'_t} c_a\right)}. \tag{7.23}$$

7.5.3 Prior Distribution

In the Bayesian inference framework, prior distributions should be given in closed form as chosen by the experimenter. Prior knowledge is crucial to inferring parameters when we have limited number of observations. In our case, as all metro users have to use their smart cards to tap-in/-out for the purpose of fare payment, large quantities of travel time observation is produced, stamped with both spatial and temporal information. Although the large number of observations can help us to correct our prior knowledge on the unknown parameters to a great extent, we still may benefit from an appropriate prior distribution.

Previous travel experience in Singapore's metro network indicates that travel time between two successive stations is about 2min (Sun et al., 2012). We therefore assume a normal prior with $\mu = $ 2min and $\sigma = $ 1min on average link cost c_a (for all links), giving that $\pi\left(c_a\right) = \frac{1}{\sqrt{2\pi}} \exp\left(-\frac{1}{2}\left(c_a - 2\right)^2\right)$. Given the independent link cost assumption, the total prior for all links can be expressed as $\pi\left(\boldsymbol{c}\right) \propto \exp\left(-\frac{1}{2}\sum_{c_a \in \boldsymbol{c}}\left(c_a - 2\right)^2\right)$. Here we do not assign different priors to distinguish in-vehicle links and transfer links.

Extra cost y in a metro trip is also estimated based on previous study. We proposed that $m \sim \mathcal{N}\left(4, 1\right)$ — a normal distribution with mean 4min and variance 1min^2. For the variance of extra cost, we take an empirical value that $\sigma_y^2 = 1.5$min^2.

In terms of coefficient of variation α and route choice parameters $\boldsymbol{\theta} = \left(\theta_1, \theta_2\right)$, we almost have no available prior information to make a first guess. Therefore, we assigned uniform priors on these three parameters: $\alpha \sim \mathcal{U}\left(0, 1\right)$ and $\theta_i \sim \mathcal{U}\left(-4, 0\right)$ for $i = 1, 2$.

7.5.4 Results and Analysis

The final parameter vector δ contains $N + K + 2 = 111$ elements. In each iteration, the variable-at-a-time Metropolis updates these parameters in turn. We implemented the sampling algorithm described in previous section using MATLAB. To avoid biased travel time observations, we discarded observations from O-D pairs with less than 100 transactions and selected a subset (by choosing 100 observations randomly) from each O-D pair in the remaining data sets as final observable $\boldsymbol{T}_w$. The size of O-D pair set is $|W| = 1897$; hence, total number of travel time observations used in this study is 189,700. We employed Gaussian random walk Metropolis proposals on all the unknown parameters; however, in order to build a well-mixed chain of realizations for each parameter, we chose different proposal standard deviations to allow for their characteristics. For instance, the proposal standard deviations of in-vehicle links and transfer links are chosen as 0.2min and 0.5min, respectively. The initial values and the corresponding proposal standard deviations for all parameters are listed in Table 7.2. In fact, the initial value $\delta_i^{(0)}$ for each parameter is chosen as the mean of its prior distribution. We conducted computation experiments on a PC with an Intel Core i7 3.40GHz CPU and 16GB RAM. Considering the large size of O-D pairs, calculating posterior density (or log-posterior density) becomes computationally intensive. It takes about 30sec for each iteration of the variable-at-a-time sampling.

The sampling is run for $M = 10000$ iterations, of which $B = 5000$ are discarded as the burn-in period. We observed significant serial correlation in the sampled values of each coordinate δ_i. Figure 7.3 shows the autocorrelation plots for chains of α, θ_1, θ_2 and m. Despite a good acceptance rate for all chains, we still found that the realizations are strongly dependent. To avoid such correlation, one may use thinning approach to get spaced samples. For example, one may retain every 50th value generated to obtain a subset with correlation less than 0.1. However, given the considerable cost in obtaining each sample, in this study we did not thin the results (Geyer, 1992).

As stated, we started the MCMC algorithm using the initial value and proposal standard deviation for each parameter as given in Table 7.2. In total, 5000 effective samples for each parameter were drawn. The Bayesian analysis provides us with not only a point estimator but also a distribution to construct Bayesian confidence interval. The last two columns of Table 7.2 show the final results of our inference based on those effective samples, including the mean and 95% Bayesian conference interval (CI). As can be seen, the large number of travel time observations have vastly corrected our biased prior knowledge of the system.

We display the estimation results of link cost on the EW service (shown in green in Figure 7.2) in Figure 7.4. The dots depict the mean values of each link and the corresponding errorbar shows the 95% Bayesian confidence interval. As a guide, the two insets show the distribution of c_1 and c_{28}, which are the first and last links on the East-West service. Despite

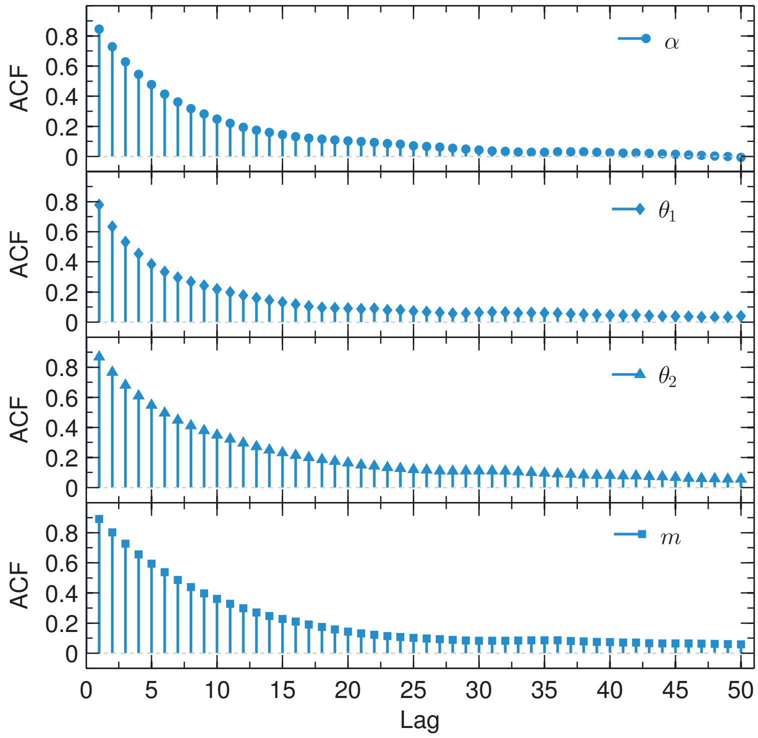

Figure 7.3: Autocorrelation plots for chains of α, θ_1, θ_2 and m.

Table 7.2: Parameter description and estimation

parameter	prior	σ_i proposal	$\delta_i^{(0)}$	mean	95% Bayesian CI
α	$\mathcal{U}(0,1)$	0.005	0.500	0.168	[0.167,0.169]
θ_1	$\mathcal{U}(-4,0)$	0.050	-2.000	-0.462	[-0.473,-0.451]
θ_2	$\mathcal{U}(-4,0)$	0.050	-2.000	-0.959	[-0.988,-0.931]
m	$\mathcal{N}(4,1)$	0.010	4.000	3.270	[3.255,3.283]
c_1	$\mathcal{N}(2,1)$	0.200	2.000	3.651	[2.584,3.718]
c_2	$\mathcal{N}(2,1)$	0.200	2.000	2.947	[2.880, 3.013]
c_3	$\mathcal{N}(2,1)$	0.200	2.000	3.660	[3.591, 3.728]
c_4	$\mathcal{N}(2,1)$	0.200	2.000	3.107	[3.038, 3.169]
...					
c_{107}	$\mathcal{N}(2,1)$	0.500	2.000	5.247	[5.151, 5.333]

the same initial values and proposal standard deviation were used in the inference process, the MCMC algorithm has successfully distinguished cost attributes for different links.

Figure 7.5 displays the results of Bayesian inference on α, m, θ_1 and θ_2. In all the panels, the solid lines depict the kernel density estimates of parameters. As comparison, the dashed lines depict their prior distributions. The coefficient of variation α is characterized by a centralized distribution, the mean of which is far from its initial value. The posterior mean and standard

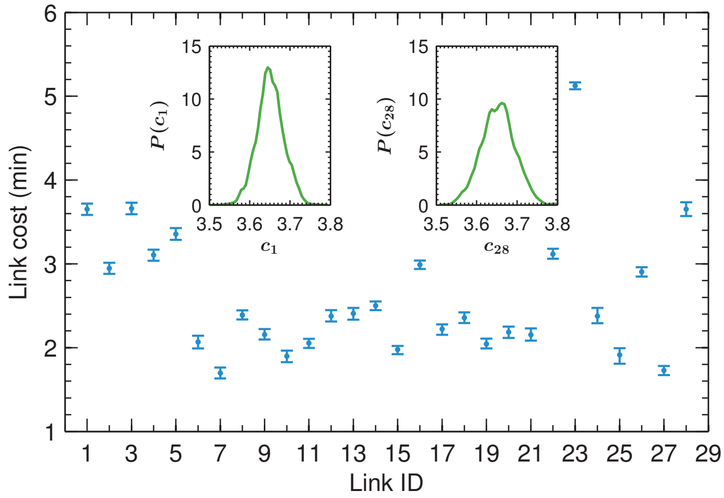

Figure 7.4: Link cost estimation (mean and 95% Bayesian confidence interval) for the EW line (shown in green in Figure 7.2). Link with ID n represents in-vehicle link between station EW n and EW $n+1$.

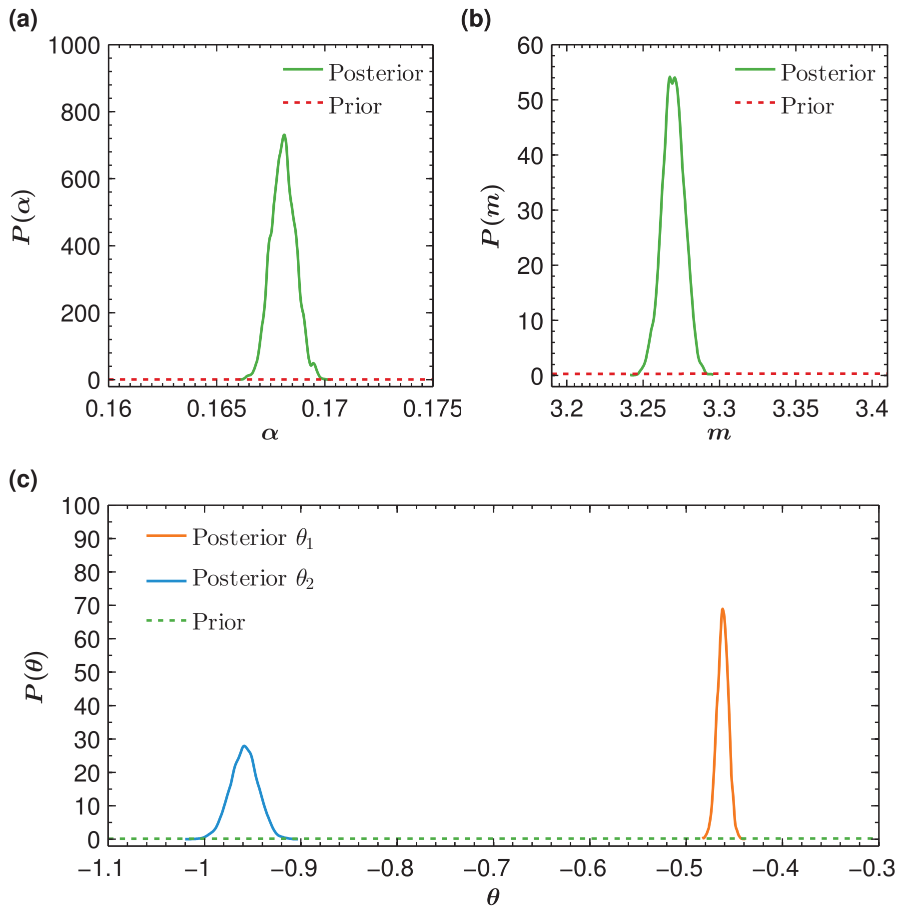

Figure 7.5: Prior and posterior density for (a) α, (b) m, and (c) θ_1 and θ_2.

deviation are 0.1681 and 0.0006, respectively. Although we expect that a flat normal prior $\mathcal{N}(4,1)$ could characterize m, in contrast the estimation process gives us a more centralized distribution shown in panel (b), with a very small standard deviation of about 0.007min, suggesting that in average passengers may spend about 3min in total as extra cost. In fact, the reason we did not get a distribution with higher variance is that m only capture the mean of extra cost y, while the variance of extra cost is assumed to be known as $\sigma_y^2 = 1.5\text{min}^2$. Thus, the result is consistent with our expectation, suggesting that we may use a more appropriate prior distribution to characterize m.

Essentially, by combining the estimation results on link cost $\boldsymbol{c}$, coefficient of variation α and extra cost m, operators and agencies can better estimate travel time and its variability for all O-D pairs in the network, helping metro users to better plan their trips. Both users and agencies can benefit from such information.

Passenger route choice behavior is reflected in parameter $\boldsymbol{\theta}$. Panel (c) in Figure 7.5 shows the distribution of θ_1 and θ_2, respectively. The same uniform prior is also plotted as a guide. As can be seen, the Bayesian inference has significantly distinguished the effect of transfer time from in-vehicle time. The posterior mean of θ_1 is -0.462 and its standard deviation is 0.006. For θ_2, the posterior mean is -0.959 and the posterior standard deviation is 0.015. The significant difference between θ_1 and θ_2 suggests that metro users value transfer time more than in-vehicle time. The result conforms to previous survey-based studied in London Underground and Santiago Metro (Raveau et al., 2014). In addition, the inference framework also provides Bayesian confidence interval for both θ_1 and θ_2.

Finally, we plot the joint posterior density for (θ_1, θ_2) in Figure 7.6. To estimate the joint density, we fixed all other parameters as the mean values of their effective samples (as provided in Table 7.2) and took only θ_1 and θ_2 as parameters. Clearly, the maximum value can be found around $(-0.462, -0.959)$; however, the density decreases at different speed given different parameter direction. The figure provides us with two implications. On one hand, the peaked shape of joint posterior distribution shows that the density is sensitive to the oscillation of both θ_1 and θ_2, suggesting that changing route choice parameters arbitrarily may strongly influence the assignment results. This also indicates that the proposed choice model exhibits great potential in capturing passenger route choice behavior. On the other hand,

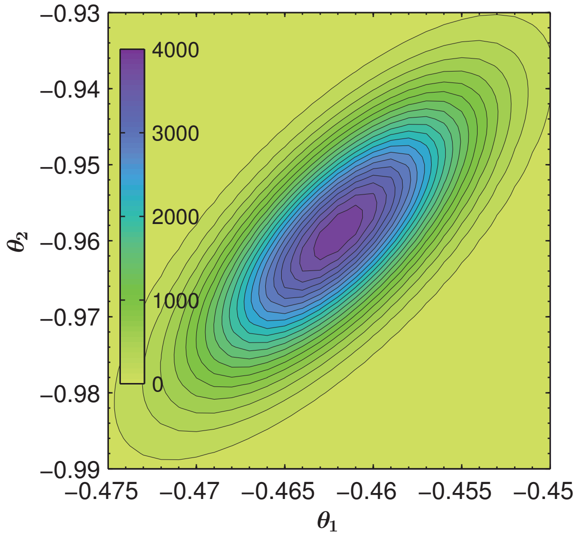

Figure 7.6: Contour plot of the joint posterior density for θ_1 and θ_2 when other parameters are set to be mean values of their effective samples.

one may see that the slowest decrease could be achieved by increasing/decreasing (θ_1, θ_2) simultaneously. This suggests that, instead of sampling each parameter separately, we may modify the Metropolis algorithm to obtain the samples of θ_1 and θ_2 collectively by considering their correlation. By doing so, we may get a faster convergence of the MCMC chains with less computation time.

In fact, in this numerical example we employed a simple model containing only two parameters to characterize passenger route choice behavior. For this special case, only in-vehicle time and transfer time are considered as important attributes influencing passenger perception. However, essentially one may take more attributes into consideration in route choice modeling, such as level of crowdedness, number of transfers (Raveau et al., 2014) and path correlation correction terms (Cascetta et al., 1996; Ben-Akiva and Bierlaire, 1999). The proposed framework has the capacity to handle a more sophisticated route choice model.

By using the route choice parameter $\boldsymbol{\theta}$, we computed the probability $f_w(r|\boldsymbol{c}, \alpha, \boldsymbol{\theta}, m)$ of choosing route r for each O-D pair w. After integrating f_w into O-D passenger demand, we obtained the flow assignment results in the studied network. We depict the assignment profile in Figure 7.7. In this figure, panel (a) and (b) show the estimated link flow profiles based on passenger demand before 12 p.m in both directions, while panel (c) and (d) illustrate the flow

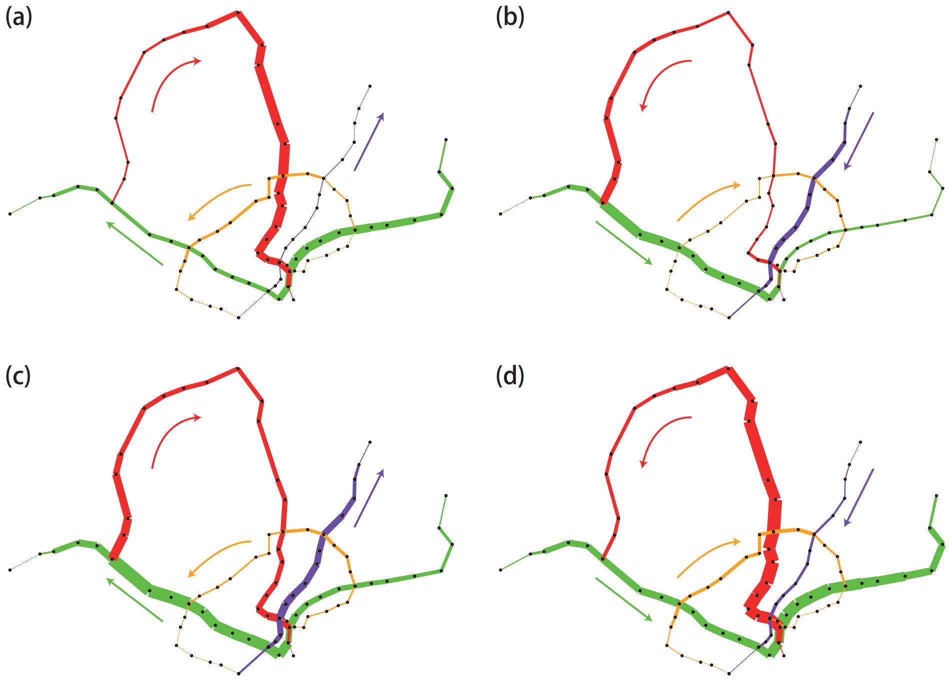

Figure 7.7: Passenger flow assignment in MRT network (a-b) before and (c-d) after 12p.m.

assignment of passenger demand after 12 p.m. As can be seen, flow assignment shows strong heterogeneity given the specific passenger demand pattern.

7.6 Summary

In this chapter, we have made use of large quantities passenger travel time observations in a metro network to develop an integrated Bayesian approach to infer both network attributes and passenger route choice behavior. The advantage of this framework lies in the Bayesian statistical paradigm, which requires limited/partial information as input, but provides comprehensive posterior knowledge of the system.

Travel time reliability has been documented extensively in terms of urban road transport; however, as another major component of public transport, metro system attracts little attention in previous literature. One possible explanation is that metro systems have dedicated infrastructure. On the other hand, this may also due to the lack real-world travel time and route choice observations, making researchers underestimate its reliability issues: metro services have long been assumed punctual to timetables. The emergence of smart card ticketing systems, as implemented in Singapore, provide us great opportunities to understand travel time reliability than ever before. The inference results for link travel time and coefficient of variation offered by the proposed Bayesian framework could be applied in real-world scenarios to better predict travel time and its variability, providing metro users with better travel information.

As service reliability is highly determined by passenger demand (such as disruption caused by huge demand in peak hours), passenger flow assignment problem in a complex metro network is particularly important with respect to providing good services and sharing profit among operators. On the other hand, knowing the number of passengers traveling on each link at given time is also a central question in disruption/emergency scenarios, where operators have to make quick response such as introducing shuttle bus services (Jin et al., 2013, 2014). Previous studies use discrete choice analysis extensively to predict passenger choice behavior. However, such a model requires preference data and still displays great variability in real-world estimation. In this context, revealing route choice from observed passenger travel time, can be more advantageous (Kusakabe et al., 2010; Sun and Xu, 2012; Zhou and Xu, 2012; Zhu et al., 2014). Applying the inference results on real passenger demand, link flow profile can be estimated in temporal scale, helping us to infer temporal train loading and measure level of crowdedness. The results could also be used to reveal transfer demand to help us identify critical transfer stations/platforms/facilities, providing valuable information to operators and agencies to better design and operate the whole metro system.

Our results also have a number of potential implications for both practice and research. First, link travel time and its variability is characterized using real-world travel time observations from smart card transactions. This data-driven approach can be widely applied in other analyses. Second, the proposed cost estimation framework may help operators identify the bottleneck of a metro network; the route inference solution may contribute to better understand transit demand patterns, more accurate profit sharing and more effective disruption/emergency response. Third, by applying this framework, we can further reveal other service satisfactory indicators, such as the availability of seats, the standing and walking times; hence, the results of this chapter can applied on various choice modeling problems, serving future decision making processes.

Chapter 8

Conclusions

8.1 Concluding Remarks

The smart card fare collection systems, as implemented in Singapore, have inundated us with remarkable amount of information and provided us with more opportunities to understand the reliability of public transport systems than ever before. The continuous flow of data on passenger behavior and service operation characteristics have the potential to fundamentally transform our understanding in a variety of fields in transportation research, from engineering optimization to behavioral study. Through conducting extensive analyses and constructing realistic models in a data-driven approach, the research presented in this thesis has shed new light on those unexplored operational characteristics and attributes of both bus and metro systems, with a particular focus on real-world problems faced by transit agencies and operators. In the era of big data, the successful use of smart card data also implies that the data-driven approach may emerge as a new direction in general transportation research, allowing us to refine and improve our current knowledge and understanding to a greater extent. The research questions, as outlined in this thesis, place extra emphasis on different aspects and modes of public transport systems. In terms of modes, **Chapter 3** and **Chapter 4** study bus systems, while **Chapter 5**, **Chapter 6** and **Chapter 7** focus on metro operation. However, taken together, these research questions can be also identified into three parts/levels as shown in Figure 8.1.

- Part 1: Understanding transit service reliability (Chapter 3 and Chapter 7)

- Part 2: Modeling transit service reliability (Chapter 4, Chapter 5 and Chapter 7)
- Part 3: Developing methodologies to improve transit service reliability (Chapter 3 and Chapter 6)

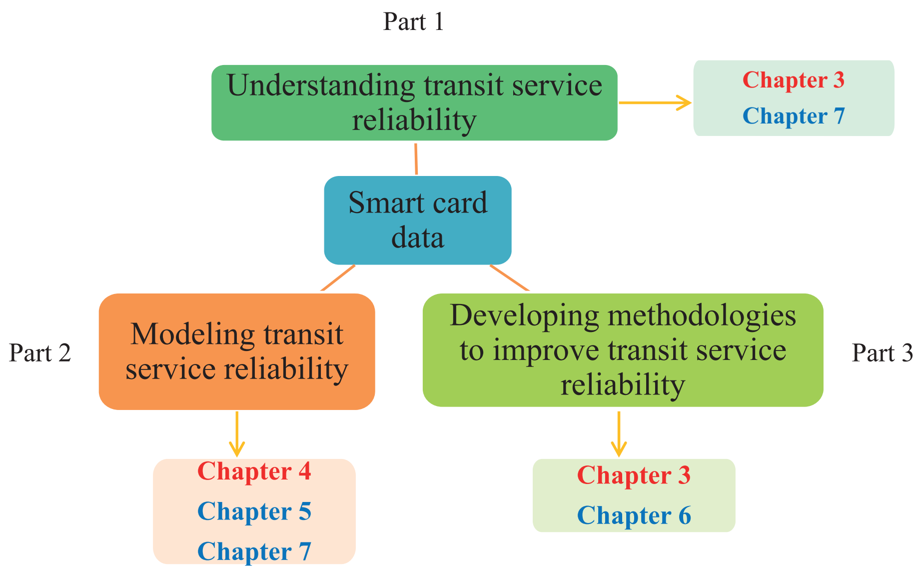

Figure 8.1: Thesis organization

Chapter 3 is an exploratory and descriptive study on the operation of bus systems, illustrating the data processing methods to reconstruct vehicle trajectories and occupancy profiles from historical smart card data. The characteristics of a particular bus route are analyzed in terms of headway distribution and average travel speed, from which it is found that the variance of headway increases almost linearly with increasing travel distance without any control strategies. Based on the analysis of the average velocity, it is also feasible to find how traffic condition varies with time of day. For instance, we find that evening peak demonstrates stronger impact on reducing operation speed than the morning peak on the selected route. Such long services are highly sensitive to service reliability. In practice operators often use holding strategy, adding slack time to avoid bus bunching. In order to identify the optimal control stop, we propose two simple optimization models which take passenger waiting time and demand profile into account. We discuss the results of the two models based on real passenger demand data extracted from smart card data and then test their performance using the proposed simulation framework. Although the two models have different objectives, a consistent optimal solution is obtained.

In **Chapter 4**, we investigate the statistical properties of bus dwell time, with a particular focus on the impact of bus types. Having reconstructed the operations for each combination of (service, stop), we are able to describe and model the three processes of interest here: boarding, alighting and total dwell time. Based on extensive observations, we find that boarding is consistently slower than alighting by about 0.3 s. It becomes apparent that low floor buses and buses with a higher internal capacity are faster in terms of both boarding and alighting processes. An upper deck does not slow down boarding, but it does do so for alighting, as the steep stairs discourage passengers to walk down until the bus has come to a complete stop. The joint model of dwell times shows clearly that the number of passengers who are on-board determines the regime of the two processes and the overall dwell time. Beyond a critical occupancy level, which is about 60% of the total bus capacity, has been reached, the internal friction slows both boarding and alighting. The aggregate analyses of the boarding and alighting process by bus type, and the disaggregate analysis of the dwell times show that the variability and therefore the risk of bus bunching increases with structurally slower buses and heavily loaded buses. Still, on average the boarding and alighting are faster when the demand is greater in total. Our results provide potential implications for practice and policy, such as identifying optimal vehicle type for a particular route and modelling transit service reliability.

Chapter 5 focuses on a crucial problem in metro operation — to understand the demand and occupancy profile over time of day. Since most metro systems are closed environments, which only register transactions when passengers enter and leave the system, matching individual passenger to particular train service becomes a challenging problem. However, such information is critical to operators for various purposes, such as preventing disruptions from happening and providing better travel information to users. In order to characterize train trajectory and occupancy profile, we model train operation with a linear regression model. We estimate the speed and dwell time using travel time observations of passenger with least travel time for each origin-destination pair. With this model, the location of a certain train and the number of on-board passengers can be estimated, helping transit agencies to improve their response to service disruptions. Since the final destinations of passengers can also be derived from the data set, one can develop more efficient failure response strategies such as the planning of bridging bus services. The result of this study also shows the potential of using smart card data to design a better operational timetable.

In **Chapter 6**, we propose three models for demand sensitive timetable design, which are examined on the East-West service in Singapore with real passenger demand extracted from one week's smart card data. The first model aims at making timetable more dynamic to demand profiles; the second model is a natural extension with train capacity constraints taken into consideration. The third model tries to design a capacitated demand-sensitive peak/off-peak timetable. All the three models are built on the concept of equivalent time (interval), which discretizes the continuous time into discrete intervals. Regardless of the fact that the models seem to provide better result if the equivalent interval is shorter, the computation time and the accuracy of demand estimation will be a hindrance for application. The absence of crew scheduling and the irregular interval are major limitations of this study, resulting in potential barriers to implementation. Nevertheless, given the principle of introducing more interaction between demand and supply, the demand-sensitive timetables show great potential in reducing total waiting time and increasing the total social welfare.

Chapter 7 studies travel time reliability and passenger flow assignment problems in closed metro systems. Despite the fact that full information on origin-destination and travel time is available from smart card data, we still have limited knowledge about passenger route choice and the composition of total travel time in closed metro systems. As a consequence, few studies have looked at the flow assignment problem in a complex metro network. In this chapter, we construct an integrated Bayesian statistical inference framework to characterize link travel time and passenger flow assignment model in a complex metro network. The posterior distribution is built by taking together the likelihood of observing passenger travel time provided by smart card data and our prior knowledge about metro operation. A variable-at-a-time Metropolis sampling algorithm is implemented to obtain the stationary distribution of each parameter. The numerical example in this chapter is the MRT network in Singapore, in which we find considerable variation of link travel time. The framework is flexible to route choice modeling and parameter selection, showing great potential in being applied on other larger metro networks. The data-driven approach can be also developed on numerous choice modeling problems, serving better decision making processes.

8.2 Remarks for Future Research

Public transport mobility is increasingly paid by passengers with smart cards, particularly in large cities such as Beijing, London and Singapore. Although the system is designed for fare collection, it generates millions of transactions corresponding to passenger boarding, alighting and transfer activities. The continuous flow of smart card data provides researchers and planners with more information than ever before.

Despite the studies presented in this thesis, transportation researchers can continue utilizing this data for strategic, tactical and operational purposes in both science and engineering levels, helping to provide better public transport services and more sustainable future transportation (Pelletier et al., 2011). In doing so, researcher and planners should design advanced practical operational guidelines and strategies, for example, proposing and implementing control strategies to avoid bus bunching. The large quantities of historical observations also show potential in building a better prediction system. The use of smart card data in designing travel time and service indicator prediction system remains to be explored. Apart from practical applications, I want to emphasize one particular research question, which the behavioral study of transit users. As reviewed in Chapter 2, there has been and increasing need of studying behavior patterns of transit users, to support people-centric transportation/urban planning, build advanced agent-based models and provide innovated ideas for future mobility. Apart from transportation, studying individual mobility pattern and regularity is a promising future research direction, which has attracted substantial attention in other fields including social science, computer science and epidemiology (González et al., 2008; Song et al., 2010).

With the rapid progress in urbanization and civilization, understanding the impact of the urban evolution/revolution and the nature and sciences behind the phenomenon is emerging as a promising research direction (Zheng et al., 2014). During the last years of my research, I realized that the importance of urban big data — such as the smart card data in the presented thesis — which gives us a chance to solve thousands of minor potential problems, should not confine itself to a particular research field like transportation, but serve as functional sensors of the whole society. Despite privacy concerns, the various urban data we generate every day, from individual human being to large urban functional systems, open new doors to understanding urban complexity with creative ideas and revolutionary techniques. For example, the smart card data presented in this thesis have also been successfully used in understanding social phenomenon (Sun et al., 2013), analyzing urban structures (Roth et al., 2011; Sun et al., 2014b) and providing early warning for city-scale contagious outbreaks (Sun et al., 2014a).

At the very beginning of this century, the emergence of complex urban data has become both a great challenge and an excellent opportunity for researchers in science and engineering. Nevertheless, with more and more research outcomes and industrial applications from such data-driven research, I believe that we will design more effective strategies and more intelligent systems to improve our quality of living, making our cities better and smarter (Batty et al., 2012).

Bibliography

Aashtiani, H. Z., Iravani, H., 2002. Application of dwell time functions in transit assignment model. Transportation Research Record: Journal of the Transportation Research Board 1817, 88–92.

Abkowitz, M., Eiger, A., Engelstein, I., 1986. Optimal control of headway variation on transit routes. Journal of Advanced Transportation 20 (1), 73–88.

Abkowitz, M., Engelstein, I., 1983. Factors affecting running time on transit routes. Transportation Research Part A: General 17 (2), 107–113.

Abkowitz, M., Lepofsky, M., 1990. Implementing headway-based reliability control on transit routes. Journal of Transportation Engineering 166 (1), 49–63.

Abkowitz, M., Tozzi, J., 1986. Transit route characteristics and headway-based reliability control. Transportation Research Record: Journal of the Transportation Research Board 1078, 11–16.

Adamski, A., Turnau, A., 1998. Simulation support tool for real-time dispatching control in public transport. Transportation Research Part A: Policy and Practice 32 (2), 73–87.

Adebisi, O., 1986. A mathematical model for headway variance of fixed-route buses. Transportation Research Part B: Methodological 20 (1), 59–70.

Agard, B., Morency, C., Trépanier, M., 2006. Mining public transport user behaviour from smart card data. In: 12th IFAC Symposium on Information Control Problems in Manufacturing - INCOM. Saint-Etienne, France, pp. 17–19.

Asakura, Y., Iryo, T., Nakajima, Y., Kusakabe, T., 2012. Estimation of behavioural change of railway passengers using smart card data. Public Transport 4, 1–16.

Bagchi, M., White, P., 2004. What role for smart-card data from bus systems? Municipal Engineer 157, 39–46.

Bagchi, M., White, P. R., 2005. The potential of public transport smart card data. Transport Policy 12 (5), 464–474.

Barnett, A., 1974. On controlling randomness in transit operations. Transportation Science 8 (2), 102–116.

Barry, J. J., Freimer, R., Slavin, H., 2009. Use of entry-only automatic fare collection data to estimate linked transit trips in new york city. Transportation Research Record: Journal of the Transportation Research Board 2112, 53–61.

Barry, J. J., Newhouser, R., Rahbee, A., Sayeda, S., 2002. Origin and destination estimation in New York City with automated fare system data. Transportation Research Record: Journal of the Transportation Research Board 1817, 183–187.

Bates, J., Polak, J., Jones, P., Cook, A., 2001. The valuation of reliability for personal travel. Transportation Research Part E: Logistics and Transportation Review 37 (2), 191–229.

Batley, R., Ibáñez, N., 2012. Randomness in preference orderings, outcomes and attribute tastes: An application to journey time risk. Journal of choice modelling 5 (3), 157–175.

Batty, M., Axhausen, K., Giannotti, F., Pozdnoukhov, A., Bazzani, A., Wachowicz, M., Ouzounis, G., Portugali, Y., 2012. Smart cities of the future. The European Physical Journal Special Topics 214 (1), 481–518.

Ben-Akiva, M., Bierlaire, M., 1999. Discrete choice methods and their applications to short term travel decisions. In: Handbook of transportation science. Springer, pp. 5–33.

Brimberg, J., Korach, E., Eben-Chaim, M., Mehrez, A., 2001. The capacitated p-facility location problem on the real line. International Transactions in Operational Research 8, 727–738.

Caprara, A., Fischetti, M., Toth, P., 2002. Modeling and solving the train timetabling problem. Operations Research 50 (5), 851–861.

Cascetta, E., Nuzzolo, A., Russo, F., Vitetta, A., 1996. A modified logit route choice model overcoming path overlapping problems: specification and some calibration results for interurban networks. In: Proceedings of the 13th International Symposium on Transportation and Traffic Theory. Pergamon Lyon, France, pp. 697–711.

Ceder, A., 1984. Bus frequency determination using passenger count data. Transportation Research Part A: General 18 (5), 439–453.

Ceder, A., 1986. Methods for creating bus timetables. Transportation Research Part A: General 21 (1), 59–83.

Ceder, A., 2007. Public transit planning and operation: theory, modeling and practice. Elsevier, Butterworth-Heinemann.

Ceder, A., Golany, B., Tal, O., 2001. Creating bus timetables with maximal synchronization. Transportation Research Part A: Policy and Practice 35 (10), 913–928.

Ceder, A., Wilson, N., 1986. Bus network design. Transportation Research Part B: Methodological 20 (4), 331–344.

Chan, J., 2007. Rail transit OD matrix estimation and journey time reliability metrics using automated fare data. Master's thesis, Massachusetts Institute of Technology.

Chang, S., Chung, Y., 2005. From timetabling to train regulation—a new train operation model. Information and Software Technology 47 (9), 575–585.

Chapleau, R., Chu, K. K. A., Allard, B., 2011. Synthesizing AFC, APC, GPS and GIS data to generate performance and travel demand indicators for public transit. In: Transportation Research Board (TRB) 90th Annual Meeting. Washington DC.

Chu, K. K. A., Chapleau, R., 2008. Enriching archived smart card transaction data for transit demand modeling. Transportation Research Record: Journal of the Transportation Research Board 2063, 63–72.

Chu, K. K. A., Chapleau, R., 2010. Augmenting transit trip characterization and travel behavior comprehension. Transportation Research Record: Journal of the Transportation Research Board 2183, 29–40.

Clarke, R., 2001. Person location and person tracking-technologies, risks and policy implications. Information Technology & People 14 (2), 206–231.

Cui, A., 2006. Bus passenger origin-destination matrix estimation using automated data collection systems. Master's thesis, Massachusetts Institute of Technology.

Daamen, W., Hoogendoorn, S. P., 2003. Experimental research of pedestrian walking behavior. Transportation Research Record: Journal of the Transportation Research Board 1828, 20–30.

Daamen, W., Lee, Y., Wiggenraad, P., 2008. Boarding and alighting experiments: Overview of setup and performance and some preliminary results. Transportation Research Record: Journal of the Transportation Research Board 2042, 71–81.

Daganzo, C. F., 2009a. A cheap and resilient way to eliminate bus bunching. In: The 4th International Conference on Future Urban Transport. Gothenburg, Sweden.

Daganzo, C. F., 2009b. A headway-based approach to eliminate bus bunching: Systematic analysis and comparisons. Transportation Research Part B: Methodological 43 (10), 913–921.

Daganzo, C. F., Pilachowski, J., 2011. Reducing bunching with bus-to-bus cooperation. Transportation Research Part B: Methodological 45 (1), 267–277.

de Palma, A., Lindsey, R., 2001. Optimal timetables for public transportation. Transportation Research Part B: Methodological 35 (8), 789–813.

Delgado, F., Muñoz, J., Giesen, R., Cipriano, A., 2009. Real-time control of buses in a transit corridor based on vehicle holding and boarding limits. Transportation Research Record: Journal of the Transportation Research Board 2090, 59–67.

Ding, Y., Chien, S. I., 2001. Improving transit service quality and headway regularity with real-time control. Transportation Research Record: Journal of the Transportation Research Board 1760, 161–170.

Dorbritz, R., Lüthi, M., Weidmann, U., Nash, A., 2009. Effects of onboard ticket sales on public transport reliability. Transportation Research Record: Journal of the Transportation Research Board 2110, 112–119.

Dueker, K. J., Kimpel, T. J., Strathman, J. G., Callas, S., 2004. Determinants of bus dwell time. Journal of Public Transportation 7 (1), 21–40.

Eberlein, X. J., Wilson, N. H. M., Bernstein, D., 2001. The holding problem with real-time information available. Transportation Science 35 (1), 1–18.

El-Geneidy, A., Vijayakumar, N., 2011. The effects of articulated buses on dwell and running times. Journal of Public Transportation 14 (3), 63–86.

El-Geneidy, A. M., Horning, J., Krizek, K. J., 2011. Analyzing transit service reliability using detailed data from automatic vehicular locator systems. Journal of Advanced Transportation 45, 66–79.

Eom, J. K., Sung, M. J., 2011. Analysis of travel patterns of the elderly using transit smart card data. In: Transportation Research Board (TRB) 90th Annual Meeting. Washington DC.

Farzin, J. M., 2008. Constructing an automated bus origin-destination matrix using farecard and global positioning system data in Sao Paulo, Brazil. Transportation Research Record: Journal of the Transportation Research Board 2072, 30–37.

Fernández, R., De Los Angeles Del Campo, M., Swett, C., 2008. Data collection and calibration of passenger service time models for the transantiago system. In: European Transport Conference. The Netherlands.

Fernández, R., Zegers, P., Weber, G., Tyler, N., 2010. Influence of platform height, door width, and fare collection on bus dwell time. Transportation Research Record: Journal of the Transportation Research Board 2143, 59–66.

Fletcher, G., El-Geneidy, A., 2013. The effects of fare payment types and crowding on dwell time: a fine-grained analysis. Transportation Research Record: Journal of the Transportation Research Board 2351, 124–132.

Fu, L., Liu, Q., Calamai, P., 2003. Real-time optimization model for dynamic scheduling of transit operations. Transportation Research Record: Journal of the Transportation Research Board 1857, 48–55.

Fu, L., Yang, X., 2002. Design and implementation of bus-holding control strategies with real-time information. Transportation Research Record: Journal of the Transportation Research Board 1791, 6–12.

Furth, P. G., 2000. Data analysis for bus planning and monitoring, TCRP Synthesis 34. Transportation Research Board, Washington DC.

Furth, P. G., Muller, T. H. J., 2006. Service reliability and hidden waiting time: Insights from automatic vehicle location data. Transportation Research Record: Journal of the Transportation Research Board 1955, 79–87.

Furth, P. G., Muller, T. H. J., 2007. Service reliability and optimal running time schedules. Transportation Research Record: Journal of the Transportation Research Board 2034, 55–61.

Furth, P. G., Wilson, N. H. M., 1981. Setting frequencies on bus routes: Theory and practice. Transportation Research Record: Journal of the Transportation Research Board 818, 1–7.

Geweke, J., 1992. Evaluating the accuracy of sampling-based approaches to calculating posterior moments. In: Bernardo, J. M., Berger, J., Dawid, A. P., Smith, J. F. M. (Eds.), Bayesian Statistics. Vol. 4. Oxford University Press, pp. 169–193.

Geyer, C. J., 1992. Practical Markov Chain Monte Carlo. Statistical Science 7 (4), 473–483.

González, M. C., Hidalgo, C. A., Barabási, A.-L., 2008. Understanding individual human mobility patterns. Nature 453 (7196), 779–782.

Gordon, J. B., Koutsopoulos, H. N., Wilson, N. H. M., Attanucci, J. P., 2013. Automated inference of linked transit journeys in london using fare-transaction and vehicle location data. Transportation Research Record: Journal of the Transportation Research Board 2343, 17–24.

Guenthner, R. P., Hamat, K., 1988. Transit dwell time under complex fare structure. Journal of Transportation Engineering 114 (3), 367–279.

Guenthner, R. P., Sinha, K. C., 1983. Modeling bus delays due to passenger boardings and alightings. Transportation Research Record: Journal of the Transportation Research Board 915, 7–13.

Guo, Z., Wilson, N., 2007. Modeling effects of transit system transfers on travel behavior: Case of commuter rail and subway in downtown boston, massachusetts. Transportation Research Record 2006 (1), 11–20.

Hastings, W. K., 1970. Monte Carlo sampling methods using markov chains and their applications. Biometrika 57, 97–109.

Hazelton, M. L., 2008. Statistical inference for time varying origin-destination matrices. Transportation Research Part B: Methodological 42 (6), 542–552.

Hazelton, M. L., 2010. Bayesian inference for network-based models with a linear inverse structure. Transportation Research Part B: Methodological 44 (5), 674–685.

Helbing, D., Buzna, L., Johansson, A., Werner, T., 2005. Self-organized pedestrian crowd dynamics: experiments, simulations, and design solutions. Transportation Science 39 (1), 1–24.

Hickman, M. D., 2001. An analytic stochastic model for the transit vehicle holding problem. Transportation Science 35 (3), 215.

Hofmann, M., Wilson, S. P., White, P., 2009. Automated identification of linked trips at trip level using electronic fare collection data. In: Transportation Research Board (TRB) 88th Annual Meeting. Washington DC.

Hollander, Y., 2006. Direct versus indirect models for the effects of unreliability. Transportation Research Part A: Policy and Practice 40 (9), 699–711.

Horbury, A. X., 1999. Using non-real-time automatic vehicle location data to improve bus services. Transportation Research Part B: Methodological 33 (8), 559–579.

Ibarra-Rojas, O. J., Rios-Solis, Y. A., 2012. Synchronization of bus timetabling. Transportation Research Part B: Methodological 46 (5), 599–614.

Jang, W., 2010. Travel time and transfer analysis using transit smart card data. Transportation Research Record: Journal of the Transportation Research Board 2144, 142–149.

Jara-Díaz, S., Tirachini, A., 2013. Urban bus transport: open all doors for boarding. Journal of Transport Economics and Policy 47 (1), 91–106.

Jin, J. G., Tang, L. C., Sun, L., Lee, D.-H., 2014. Enhancing metro network resilience via localized integration with bus services. Transportation Research Part E: Logistics and Transportation Review 63, 17–30.

Jin, J. G., Teo, K. M., Sun, L., 2013. Disruption response planning for an urban mass rapid transit network. In: Transportation Research Board (TRB) 92nd Annual Meeting. Transportation Research Board, Washington DC.

Kaspi, M., Raviv, T., 2012. Service-oriented line planning and timetabling for passenger trains. Transportation Science 47 (3), 295–311.

Koffman, D., 1978. A simulation study of alternative real-time bus headway control strategies. Transportation Research Record: Journal of the Transportation Research Board 663, 41–46.

Koutsopoulos, H. N., Odoni, A., Wilson, N. H. M., 1985. Determination of headways as function of time varying characteristics on a transit network. In: Rousseau, J. M. (Ed.), Computer scheduling of public transport. Vol. 2. North-Holland Publishing Co., pp. 391–413.

Kraft, W. H., Bergen, T. F., 1974. Evaluation of passenger service times for street transit systems. Transportation Research Record: Journal of the Transportation Research Board 505, 13–20.

Kusakabe, T., Asakura, Y., 2014. Behavioural data mining of transit smart card data: A data fusion approach. Transportation Research Part C: Emerging Technologies 46, 179–191.

Kusakabe, T., Iryo, T., Asakura, Y., 2010. Estimation method for railway passengers' train choice behavior with smart card transaction data. Transportation 37 (5), 731–749.

Land Transport Authority, 2008. LT-MASTERPLAN — a people-centred land transport system. Land Transport Authority, Singapore.

Larrain, H., Muñoz, J. C., 2008. Public transit corridor assignment assuming congestion due to passenger boarding and alighting. Networks and Spatial Economics 8 (2), 241–256.

Lee, D.-H., Sun, L., Erath, A., 2012. Study of bus service reliability in singapore using fare card data. In: 12th Asia Pacific ITS Forum & Exhibition. Kuala Lumpur.

Lehnhoff, N., Janssen, S., 2003. Untersuchung und optimierung der fahrgastwechselzeit. Der Nahverkehr 21 (7/8), 14–20.

Levine, J. C., Torng, G. W., 1994. Dwell-time effects of low-floor bus design. Journal of Transportation Engineering 120 (6), 914–929.

Levinson, H. S., 1983. Analyzing transit travel time performance. Transportation Research Record: Journal of the Transportation Research Board 915, 1–6.

Li, M. T., Zhao, F., Chow, L. F., Zhang, H., Li, S. C., 2006. Simulation model for estimating bus dwell time by simultaneously considering numbers of disembarking and boarding passengers. Transportation Research Record: Journal of the Transportation Research Board 1971, 59–65.

Li, Z., Tirachini, A., Hensher, D. A., 2012. Embedding risk attitudes in a scheduling model: Application to the study of commuting departure time. Transportation Science 46 (2), 170–188.

Liebchen, C., 2008. The first optimized railway timetable in practice. Transportation Science 42 (4), 420–435.

Lin, T., Wilson, N. H. M., 1992. Dwell time relationships for light rail systems. Transportation Research Record: Journal of the Transportation Research Board 1361, 287–295.

Love, R. F., 1976. One-dimensional facility location-allocation using dynamic programming. Management Science 22, 614–617.

MATSim, 2013. Multi-agent transport simulation toolkit. Online; accessed April, 2013. URL http://www.matsim.org/

Meignan, D., Simonin, O., Koukam, A., 2007. Simulation and evaluation of urban bus-networks using a multiagent approach. Simulation Modelling Practice and Theory 15 (6), 659–671.

Metropolis, N., Rosenbluth, A. W., Rosenbluth, M. N., Teller, A. H., Teller, E., 1953. Equation of state calculations by fast computing machines. Journal of Chemical Physics 21 (6), 1087–1092.

Milkovits, M. N., 2008. Modeling the factors affecting bus stop dwell time: use of automatic passenger counting, automatic fare counting, and automatic vehicle location data. Transportation Research Record: Journal of the Transportation Research Board 2072, 125–130.

Mojica, C. H., 2008. Examining changes in transit passenger travel behavior through a smart card activity analysis. Master's thesis, Massachusetts Institute of Technology.

Morency, C., Trépanier, M., Agard, B., 2007. Measuring transit use variability with smart-card data. Transport Policy 14 (3), 193–203.

Moreno González, E. G., Romana, M. G., Álvaro, O. M., 2012. Bus dwell-time model of main urban route stops: case study in Madrid, Spain. Transportation Research Record: Journal of the Transportation Research Board 2274, 126–134.

Munizaga, M. A., Palma, C., 2012. Estimation of a disaggregate multimodal public transport origin-destination matrix from passive smartcard data from Santiago, Chile. Transportation Research Part C: Emerging Technologies 24, 9–18.

National Research Council, Transportation Research Board, 2010. Highway Capacity Manual. Transportation Research Board, Washington DC.

Newell, G. F., 1971. Dispatching policies for a transportation route. Transportation Science 5 (1), 91–105.

Newell, G. F., 1993. A simplified theory of kinematic waves in highway traffic, part ii: Queueing at freeway bottlenecks. Transportation Research Part B: Methodological 27 (4), 289–303.

Newell, G. F., Potts, R. B., 1964. Maintaining a bus schedule. In: 2nd Australian Road Research Board (ARRB) Conference. Australian Road Research Board, Melbourne.

Niu, H., Zhou, X., 2013. Optimizing urban rail timetable under time-dependent demand and oversaturated conditions. Transportation Research Part C: Emerging Technologies 36, 212–230.

Osuna, E. E., Newell, G. F., 1972. Control strategies for an idealized public transportation system. Transportation Science 6 (1), 52–72.

Park, J. Y., Kim, D. J., Lim, Y., 2008. Use of smart card data to define public transit use in Seoul, South Korea. Transportation Research Record: Journal of the Transportation Research Board 2063, 3–9.

Peeters, L., Kroon, L., 2001. A cycle based optimization model for the cyclic railway timetabling problem. In: Stefan, V., Daduna, J. R. (Eds.), Computer-aided scheduling of public transport. Lecture Notes in Economics and Mathematical Systems. Springer Berlin Heidelberg, pp. 275–296.

Pelletier, M. P., Trépanier, M., Morency, C., 2011. Smart card data use in public transit: a literature review. Transportation Research Part C: Emerging Technologies 19, 557–568.

Pilachowski, J. M., 2009. An approach to reducing bus bunching. Ph.D. thesis, University of California, Berkeley.

Prakasam, S., 2008. The evolution of e-payments in public transport: Singapore's experience. Japan Railway & Transport Review 50, 36–39.

Rajbhandari, R., Chien, S. I., Daniel, J. R., 2003. Estimation of bus dwell times with automatic passenger counter information. Transportation Research Record: Journal of the Transportation Research Board 1841, 120–127.

Rapp, M. H., Gehner, C. D., 1976. Transfer optimization in an interactive graphic system for transit planning. Transportation Research Record: Journal of the Transportation Research Board 619, 27–33.

Raveau, S., Guo, Z., Muoñz, J. C., Wilson, N. H. M., 2014. A behavioural comparison of route choice on metro networks: Time, transfers, crowding, topology and socio-demographics. Transportation Research Part A: Policy and Practice 66, 185–195.

Robert, C. P., 2014. Bayesian computational tools. Annual Review of Statistics and Its Application 1 (1), 153–177.

Robert, C. P., Casella, G., 2004. Monte Carlo Statistical Methods, 2nd Edition. Springer-Verlag, New York, USA.

Roth, C., Kang, S. M., Batty, M., Barthélemy, M., 2011. Structure of urban movements: polycentric activity and entangled hierarchical flows. PloS one 6 (1), e15923.

Rudloff, C., Bauer, D., Matyus, T., Seer, S., 2011. Mind the gap: Boarding and alighting processes using the social force paradigm calibrated on experimental data. In: 14th International IEEE Conference on Intelligent Transportation Systems. IEEE, Washington DC, pp. 353–358.

Seaborn, C., Attanucci, J., Wilson, N. H. M., 2009. Analyzing multimodal public transport journeys in london with smart card fare payment data. Transportation Research Record: Journal of the Transportation Research Board 2121, 55–62.

Seber, G. A. F., Wild, C. J., 2003. Nonlinear regression. Vol. 503. Wiley, Newark, New Jersey.

Serafini, P., Ukovich, W., 1989. A mathematical model for periodic scheduling problems. SIAM Journal on Discrete Mathematics 2 (4), 550–581.

Simon, J., Furth, P. G., 1985. Generating a bus route OD matrix from on-off data. Journal of Transportation Engineering 111 (6), 583–593.

Song, C., Qu, Z., Blumm, N., Barábasi, A. L., 2010. Limits of predictability in human mobility. Science 327 (5968), 1018–21.

Strathman, J. G., Hopper, J. R., 1993. Empirical analysis of bus transit on-time performance. Transportation Research Part A: Policy and Practice 27 (2), 93–100.

Strathman, J. G., Kimpel, T. J., Dueker, K. J., Gerhart, R. L., Callas, S., 2002. Evaluation of transit operations: Data applications of Tri-Met's automated bus dispatching system. Transportation 29 (3), 321–345.

Suh, W., Chon, K. S., Rhee, S. M., 2002. Effect of skip-stop policy on a korean subway system. Transportation Research Record: Journal of the Transportation Research Board 1793, 33–39.

Sun, A., Hickman, M., 2005. The real-time stop-skipping problem. Journal of Intelligent Transportation Systems 9 (2), 91–109.

Sun, A., Hickman, M., 2008. The holding problem at multiple holding stations. Computer-aided Systems in Public Transport 600, 339–359.

Sun, L., Axhausen, K. W., Lee, D. H., Cebrian, M., 2014a. Efficient detection of contagious outbreaks in massive metropolitan encounter networks. Scientific Reports 4, 5099.

Sun, L., Axhausen, K. W., Lee, D. H., Huang, X., 2013. Understanding metropolitan patterns of daily encounters. Proceedings of the National Academy of Sciences of the United States of America 110 (34), 13774–13779.

Sun, L., Jin, J. G., Axhausen, K. W., Lee, D.-H., Cebrian, M., 2014b. Quantifying long-term evolution of intra-urban spatial interactions. arXiv preprint arXiv:1407.0145.

Sun, L., Jin, J. G., Lee, D.-H., Axhausen, K. W., Erath, A., 2014c. Demand-driven timetable design for metro services. Transportation Research Part C: Emerging Technologies 46, 284–299.

Sun, L., Lee, D.-H., Erath, A., Huang, X., 2012. Using smart card data to extract passenger's spatio-temporal density and train's trajectory of MRT system. In: ACM SIGKDD International Workshop on Urban Computing. ACM, Beijing, China, pp. 142–148.

Sun, Y., Xu, R., 2012. Rail transit travel time reliability and estimation of passenger route choice behavior. Transportation Research Record: Journal of the Transportation Research Board 2275, 58–67.

Ting, C.-J., Schonfeld, P., 2005. Schedule coordination in a multiple hub transit network. Journal of Urban Planning and Development 131 (2), 112–124.

Tirachini, A., 2013a. Bus dwell time: the effect of different fare collection systems, bus floor level and age of passengers. Transportmetrica A: Transport Science 9 (1), 28–49.

Tirachini, A., 2013b. Estimation of travel time and the benefits of upgrading the fare payment technology in urban bus services. Transportation Research Part C: Emerging Technologies 30, 239–256.

Trépanier, M., Morency, C., Agard, B., 2009a. Calculation of transit performance measures using smartcard data. Journal of Public Transportation 12 (1), 76–96.

Trépanier, M., Morency, C., Blanchette, C., 2009b. Enhancing household travel surveys using smart card data. In: Transportation Research Board (TRB) 88th Annual Meeting. Washington DC.

Trépanier, M., Tranchant, N., Chapleau, R., 2007. Individual trip destination estimation in a transit smart card automated fare collection system. Journal of Intelligent Transportation Systems 11 (1), 1–14.

Turnquist, M. A., 1978. A model for investigating the effects of service frequency and reliability on bus passenger waiting times. Transportation Research Record: Journal of the Transportation Research Board 663, 70–73.

Turnquist, M. A., Blume, S. W., 1980. Evaluating potential effectiveness of headway control strategies for transit systems. Transportation Research Record: Journal of the Transportation Research Board 746, 25–29.

Uniman, D. L., Attanucci, J., Mishalani, R. G., Wilson, N. H. M., 2010. Service reliability measurement using automated fare card data. Transportation Research Record: Journal of the Transportation Research Board 2143, 92–99.

Utsunomiya, M., Attanucci, J., Wilson, N. H. M., 2006. Potential uses of transit smart card registration and transaction data to improve transit planning. Transportation Research Record: Journal of the Transportation Research Board 1971, 119–126.

van Nes, R., van Oort, N., 2009. Line length versus operational reliability. Transportation Research Record: Journal of the Transportation Research Board 2112, 104–110.

van Oort, N., 2011. Service reliability and urban public transport design. Ph.D. thesis, TRAIL Research School, Delft University of Technology.

van Oort, N., Wilson, N. H. M., van Nes, R., 2010. Reliability improvement in short headway transit services: schedule-based and headway-based holding strategies. Transportation Research Record: Journal of the Transportation Research Board 2143, 67–76.

Vuchic, V. R., 2005. Urban transit: operations, planning and economics. Wiley, Hoboken.

Vuchic, V. R., 2007. Urban public transportation: systems and technology. Wiley, Hoboken.

Wardman, M., Whelan, G., 2011. Twenty years of rail crowding valuation studies: Evidence and lessons from british experience. Transport Reviews 31 (3), 379–398.

Wei, C., Asakura, Y., 2013. A Bayesian approach to traffic estimation in stochastic user equilibrium networks. Transportation Research Part C: Emerging Technologies 36, 446–459.

Weidmann, U., 1992. Transporttechnik der Fussgänger. IVT, Institut für Verkehrsplanung, Transporttechnik, Strassen- und Eisenbahnbau, ETH Zürich, Zürich.

Weidmann, U., 1994. Der fahrgastwechsel im öffentlichen personenverkehr. Ph.D. thesis, IVT, Institut für Verkehrsplanung, Transporttechnik, Strassen- und Eisenbahnbau, ETH Zürich.

Westgate, B. S., Woodard, D. B., Matteson, D. S., Henderson, S. G., 2013. Travel time estimation for ambulances using Bayesian data augmentation. The Annals of Applied Statistics 7 (2), 1139–1161.

Wong, R. C. W., Yuen, T. W. Y., Fung, K. W., Leung, J. M. Y., 2008. Optimizing timetable synchronization for rail mass transit. Transportation Science 42 (1), 57–69.

Wright, L., Hook, W. B., 2007. Bus rapid transit planning guide, 3rd Edition. Institute for Transportation & Development Policy, New York.

Xuan, Y., Argote, J., Daganzo, C. F., 2011. Dynamic bus holding strategies for schedule reliability: Optimal linear control and performance analysis. Transportation Research Part B: Methodological 45 (10), 1831–1845.

York, I. O., 1993. Factors affecting bus-stop times, Project report 2. Transport Research Laboratory, Crowthorne.

Zhao, J., 2008. The planning and analysis implications of automated data collection systems : Rail transit OD matrix inference and path choice modeling examples. Master's thesis, Massachusetts Institute of Technology.

Zhao, J., Bukkapatnam, S., Dessouky, M. M., 2003. Distributed architecture for real-time coordination of bus holding in transit networks. IEEE Transactions on Intelligent Transportation Systems 4 (1), 43–51.

Zhao, J., Dessouky, M., Bukkapatnam, S., 2006. Optimal slack time for schedule-based transit operations. Transportation Science 40 (4), 529–539.

Zhao, J., Rahbee, A., Wilson, N. H. M., 2007. Estimating a rail passenger trip origin-destination matrix using automatic data collection systems. Computer-Aided Civil and Infrastructure Engineering 22 (5), 376–387.

Zheng, Y., Capra, L., Wolfson, O., Yang, H., 2014. Urban computing: concepts, methodologies, and applications. ACM Transaction on Intelligent Systems and Technology (ACM TIST).

Zhou, F., Xu, R., 2012. Passenger flow assignment model for urban rail transit based on entry and exit time constraints. Transportation Research Record: Journal of the Transportation Research Board 2284, 57–61.

Zhu, W., Hu, H., Huang, Z., 2014. Calibrating rail transit assignment models with genetic algorithm and automated fare collection data. Computer-Aided Civil and Infrastructure Engineering 29 (7), 518–530.

Appendix A

Recent Research Accomplishments

Journal Articles

[1] Wu, X., Lee, D.-H., and Sun, L. (2013) Limited Information-Sharing Strategy for Taxi-Customer Searching Problem in Nonbooking Taxi Service. *Transportation Research Record: Journal of the Transportation Research Board*, 2333, 46-54.

[2] Sun, L., Axhausen, K. W., Lee, D.-H., Huang, X. (2013) Understanding metropolitan patterns of daily encounters. *Proceedings of the National Academy of Sciences of the United States of America (PNAS)* 110(34), 13774-13779.

[3] Sun, L., Jin, J. G., Lee, D.-H., Axhausen, K. W., Erath, A. (2014) Demand-driven timetable designing for metro services. *Transportation Research Part C: Emerging Technologies* 46, 284-299.

[4] Jin, J. G., Tang, L. C., Sun, L., Lee, D.-H. (2014) Improving metro network resilience by incremental bus service adjustment. *Transportation Research Part E: Logistics and Transportation Review* 63, 17-30.

[5] Sun, L., Axhausen, K. W., Lee, D.-H., Cebrian, M. (2014) Efficient detection of contagious outbreaks in massive metropolitan encounter networks. *Scientific Reports* 4:5099.

[6] Sun, L., Tirachini, A., Axhausen, K. W., Lee, D.-H. (2014) Models of bus boarding/alighting dynamics and dwell time variability. *Transportation Research Part A: Policy and Practice* 69, 447-460.

[7] Sun, L., Jin, J. G., Axhausen, K. W., Lee, D.-H., Cebrian, M. (2015) Quantifying long-term evolution of intra-urban spatial interactions. *Journal of the Royal Society Interface* 12:20141089.

[8] Sun, L., Lu, Y., Jin, J. G., Axhausen, K. W., Lee, D.-H. (2015) An integrated Bayesian approach for passenger flow assignment in metro networks. *Transportation Research Part C: Emerging Technologies* (in press).

[9] Tirachini, A., Sun, L., Erath, A. (2015) Valuation of sitting and standing in public transport using revealed preferences. *Transport Policy* (under review).

[10] Sun, L., Jin, J. G., Lee, D.-H., Axhausen, K. W. (2015) Characterizing multimodal transfer time using smart card data: the effect of time, passenger age, crowdedness and collective pressure. *Transportation Research Record: Journal of the Transportation Research Board* (under review).

Conference Proceedings/Presentations

[1] Lee, D.-H., Sun, L., Erath, A. (2012) Study of bus service reliability in singapore using fare card data. In Proceeding of *12th Asia Pacific ITS Forum & Exhibition*, Kuala Lumpur, Malaysia.

[2] Sun, L., Lee, D.-H., Erath, A., Huang, X. (2012) Using smart card data to extract passenger's spatio-temporal density and train's trajectory of MRT system. In Proceeding of *ACM SIGKDD International Workshop on Urban Computing*, Beijing, China.

[3] Lee, D.-H., Sun, L., Erath, A. (2012) Determining optimal control stop to improve bus service reliability. In Proceeding of *1st Symposium of the European Association for Research in Transportation*, Lausanne, Switzerland.

[4] Jin, J. G., Teo, K. M., Sun, L. (2013) Disruption response planning for an urban Mass Rapid Transit network. In Proceeding of *Transportation Research Board (TRB) 92nd Annual Meeting*, Washington DC, USA.

[5] Sun, L., Axhausen, K. W., Lee, D.-H., Huang, X. (2013) Familiar strangers: understanding metropolitan patterns of daily encounters. *NetSci2013, International School and Conference on Network Science*, Copenhagen, Denmark.

[6] Sun, L., Jin, J. G., Axhausen, K. W., Lee, D.-H., Cebrian, M. (2014) Quantifying long-term evolution of intra-urban spatial interactions. *NetSci2014, Urban Systems and Networks Satellite*, Berkeley, CA, USA.

[7] Sun, L., Axhausen, K. W., Lee, D.-H., Cebrian, M. (2014) Efficient detection of contagious outbreaks in massive metropolitan encounter networks. *NetSci2014, International School and Conference on Network Science*, Berkeley, CA, USA.

[8] Sun, L., Jin, J. G., Axhausen, K. W., Lee, D.-H. (2014) Characterizing travel time reliability and passenger path choice in a metro network. In Proceeding of *3rd Symposium of the European Association for Research in Transportation*, Leeds, UK.

Appendix B

Curriculum Vitae

SUN LIJUN

updated: August 25, 2015

CONTACT INFORMATION

1 Create Way, #06-01 CREATE Tower
Future Cities Laboratory, Singapore-ETH Centre
Singapore, 138602

Phone: (+65) 8298 · 2976
Email: sunlijun@u.nus.edu
Personal Website
ResearchGate

RESEARCH INTERESTS

- Data-driven transport modeling: I focus on understanding various unexplored properties of transport systems by utilizing new data sources.
- Human mobility and travel behavior: I am very interested in understanding ourselves—the mobility and behavior patterns of human beings with the help of big data.
- Urban dynamics & urban complexity: I want to explore the impact of the urban evolution/revolution and the nature behind various critical urban phenomena.
- Agent-based modeling: I am interested in implementing large-scale agent-based transport simulations.
- Public transport: I try to use data to provide better public transport services (bus, MRT & taxi).

EDUCATION

National University of Singapore, Singapore

PhD Candidate in Civil Engineering **Aug 2011–present**

- Expected graduation date: July 2015
- Advisors: Prof. Der-Horng Lee (NUS) & Prof. Kay W. Axhausen (ETH Zürich)
- Committee: Prof. Qiang Meng & Prof. Mi Diao

Tsinghua University, Beijing, China

BEng in Civil Engineering **Aug 2007–July 2011**

- Graduate thesis: Research on micro-simulation models of urban mixed traffic flow
- Advisors: Prof. Huapu Lu

HONOURS AND AWARDS

Graduate

- IEEE ITSC2015 Student Travel Grant. 2015
- The Best Scientific Visualizations of 2013 - WIRED. 2013
- Singapore-ETH Centre Research Scholarship. 2011

Undergraduate

- First Prize of China Undergraduate Mathematical Contest in Modeling. 2010
- Gammon Scholarship Award of Tsinghua University. 2010
- Second Prize of Competition of Transport Science and Technology of Tsinghua University. 2010
- Third Prize of Mathematical Contest in Modeling. 2010

- Second Prize of China Undergraduate Mathematical Contest in Modeling. 2009

PROFESSIONAL EXPERIENCE

Future Cities Laboratory, Singapore-ETH Centre, Singapore
Senior Research Fellow **Dec 2014–present**
Senior research fellow for MATSim Capstone Project.

National ICT Australia, Australia
Visiting Research **Feb 2015–Mar 2015**
Visiting researcher at NICTA **Optimisation group**.

Media Lab, Massachusetts Institute of Technology, US
Visiting Researcher **Feb 2014–June 2014**
Visiting student at Human Dynamics group under Prof. **Alex (Sandy) Pentland**.

Future Cities Laboratory, Singapore-ETH Centre, Singapore
PhD Researcher **Aug 2011–Nov 2014**
Graduate researcher in Module VIII - Mobility and Transportation Planning.

National University of Singapore, Singapore
Teaching Assistant **Aug 2014–Jan 2015**
Teaching assistant for graduate course CE5205 Transportation Planning.
Teaching Assistant **Aug 2013–Jan 2014**
Teaching assistant for graduate course TP5025 Intelligent Transport Systems.
Teaching Assistant **Aug 2012–Jan 2013**
Teaching assistant for graduate course CE5205 Transportation Planning.

PROJECT GRANTS

1. "Network Resilience Analyses and Control Strategies for Urban Transit Rail Systems under Heavy Demands". Funded by State Key Lab of Rail Traffic Control & Safety. Investigator. 50,000 RMB 2015-2016
2. "Matsim capstone project–preparing MATSim Singapore for planning practice". Urban Redevelopment Authority (URA) and Land Transport Authority (LTA) of Singapore. Investigator. 315,900 SGD 2014-2015

REFEREED JOURNAL PUBLICATIONS

1. Jin JG, Lu L, Sun L, Yin J (2015) Optimal allocation of protective resources in urban rail transit networks against intentional attacks. *Transportation Research Part E: Logistics and Transportation Review* (under review).
2. Sun L, Erath A (2015) A Bayesian network approach for population synthesis. *Transportation Research Part C: Emerging Technologies* (under review).
3. Sun H-J, Li T-F, Wu J-J, Sun L (2015) Optimized planning strategy of land use for doubly uncertain transportation networks. *Transportation* (under review).
4. Tirachini A, Sun L, Erath A, Chakirov A (2015) Valuation of sitting and standing in metro trains using revealed preferences. *Transport Policy* (under review).

5. Sun L, Jin JG, Lee D-H, Axhausen KW (2015) Characterizing multimodal transfer time using smart card data: the effect of time, passenger age, crowdedness and collective pressure. *Transportation* (under review).

6. Long Y, Sun L, Tao S (2015) A review of urban studies based on transit smart card data. (in Chinese) *Urban Planning Forum* (doi:10.16361/j.upf.201503009).

7. Sun L, Lu Y, Jin JG, Lee D-H, Axhausen KW (2015) An integrated Bayesian approach for passenger flow assignment in metro networks. *Transportation Research Part C: Emerging Technologies* 52:116-131. (doi:10.1016/j.trc.2015.01.001).

8. Sun L, Jin JG, Axhausen KW, Lee D-H, Cebrian M (2015) Quantifying long-term evolution of intra-urban spatial interactions. *Journal of the Royal Society Interface* 12:20141089 (doi:10.1098/rsif.2014.1089).

9. Sun L, Tirachini A, Axhausen KW, Erath A, Lee D-H (2014) Models of bus boarding and alighting dynamics. *Transportation Research Part A: Policy and Practice* 69:447-460. (doi: 10.1016/j.tra.2014.09.007)

10. Sun L, Axhausen KW, Lee D-H, Cebrian M (2014) Efficient detection of contagious outbreaks in massive metropolitan encounter networks. *Scientific Reports* 4:5099. (doi: 10.1038/srep05099)

11. Sun L, Jin JG, Lee D-H, Axhausen KW, Erath A (2014) Demand-driven timetable design for metro services. *Transportation Research Part C: Emerging Technologies* 46:284-299. (doi: 10.1016/j.trc.2014.06.003)

12. Jin JG, Tang LC, Sun L, Lee D-H (2014) Enhancing metro network resilience via localized integration with bus services. *Transportation Research Part E: Logistics and Transportation Review* 63:17-30. (doi: 10.1016/j.tre.2014.01.002)

13. Sun L, Axhausen KW, Lee D-H, Huang X (2013) Understanding metropolitan patterns of daily encounters. *Proceedings of the National Academy of Sciences of the United States of America (PNAS)* 110(34):13774-13779. (doi: 10.1073/pnas.1306440110)

14. Lee D-H, Wu X, Sun L (2013) Limited information-sharing strategy for the taxi-customer searching problem in the non-booking taxi services. *Transportation Research Record: Journal of the Transportation Research Board*. 2284:57-61. (doi: 10.3141/2333-06)

REFEREED CONFERENCE PROCEEDINGS

1. Sun L, Lu Y, Lee D-H (2015) Understanding the structure of urban bus networks: the C-space representation approach. *15th COTA International Conference of Transportation Professionals* (Beijing, China).

2. Zhao K, Sun L, Jin JG, Lee D-H (2015) Analysis of crowding effect on passengers' movement time based on smart card data. *15th COTA International Conference of Transportation Professionals* (Beijing, China).

3. Sun L, Jin JG, Lee D-H, Axhausen KW (2015) Characterizing multimodal transfer time using smart card data: the effect of time, passenger age,

crowdedness and collective pressure. *Transportation Research Board (TRB) 94th Annual Meeting* (Washington, DC, USA).

4. Jin JG, Teo KM, Sun L (2013) Disruption response planning for an urban Mass Rapid Transit network. *Transportation Research Board (TRB) 92nd Annual Meeting* (Washington DC, USA).
5. Lee D-H, Wu X, Sun L (2013) Limited information sharing strategy for the taxi-customer searching problem in the non-booking taxi service. *Transportation Research Board (TRB) 92nd Annual Meeting* (Washington DC, USA).
6. Sun L, Lee D-H, Erath A, Huang X (2012) Using smart card data to extract passenger's spatio-temporal density and train's trajectory of MRT system. *ACM SIGKDD International Workshop on Urban Computing* (Beijing, China). (doi: 10.1145/2346496.2346519)
7. Lee D-H, Sun L, Erath A (2012) Study of bus service reliability in Singapore using fare card data. *12th Asia Pacific ITS Forum & Exhibition* (Kuala Lumpur, Malaysia).
8. Sun L, Chen X, Xie W, Yang X (2010) Calibration of acceleration-based and multi-anticipative car-following models by NGSIM trajectory data. *10th ASCE International Conference of Chinese Transportation Professionals, ICCTP 2010* (Beijing, China)

CONFERENCE PRESENTATIONS

1. "Characterizing multimodal transfer time using smart card data: the effect of time, passenger age, crowdedness and collective pressure," *Transportation Research Board (TRB) 94th Annual Meeting*. Washington, DC, USA. January 12, 2015.
2. "Characterizing travel time reliability and passenger route choice in a metro network," *3rd Symposium of the European Association for Research in Transportation*. Leeds, UK. September 12, 2014.
3. "Efficient detection of contagious outbreaks in massive metropolitan encounter networks," *NetSci2014, International School and Conference on Network Science*. Berkeley, CA, USA. June 5, 2014.
4. "Quantifying long-term evolution of intra-urban spatial interactions," *NetSci2014, Urban Systems and Networks Satellite*. Berkeley, CA, USA. June 2, 2014.
5. "Demand-driven timetable design for metro services," *20th ITS World Congress*. Tokyo, Japan. October 15, 2013.
6. "Familiar strangers: understanding metropolitan patterns of daily encounter patterns," *NetSci2013, International School and Conference on Network Science (Young Research Session)*. Copenhagen, Denmark. June 3, 2013.
7. "Disruption response planning for an urban Mass Rapid Transit network." *Transportation Research Board (TRB) 92nd Annual Meeting*. Washington, DC, USA. January 13, 2013.

8. "Limited information sharing strategy for the taxi-customer searching problem in the non-booking taxi service," *Transportation Research Board (TRB) 92nd Annual Meeting*. Washington, DC, USA. January 13, 2013.
9. "Designing a demand-sensitive timetable for metro services," *2nd International Future Cities Conference – Territorial Encounters*. Zurich, Switzerland. September 10, 2012.
10. "Determining optimal control stop to improve bus service reliability," *1st European Symposium on Quantitative Methods in Transportation Systems*. Lausanne, Switzerland. September 4, 2012.
11. "Using smart card data to extract passenger's spatial-temporal density and train trajectory of MRT systems," *ACM SIGKDD International Workshop on Urban Computing (UrbComp)*. Beijing, China. August 12, 2012.
12. "Study of bus service reliability in Singapore using smart card data," *12th Intelligent Transport Systems Asia Pacific Forum & Exhibition*. Kuala Lumper. April 16, 2012.

INVITED TALKS

1. August 2014, "Familiar strangers"—understanding metropolitan patterns of daily encounters, Tsinghua University, China.
2. October 2014, The role of "familiar stranger" network in shaping our society, Singapore Management University, Singapore.

IN THE PRESS

- Double deckers not right fit for Singapore roads? My Paper. (July 18, 2014)
- Are you a super-spreader of disease? Communications of the ACM. (January 27, 2014)
- Are you a super-spreader of disease? MIT Technology Review. (January 23, 2014)
- When social networks meet public transport. Urban Demographics. (December 30, 2013)
- The best scientific visualizations of 2013. WIRED. (December 25, 2013)
- NUS looking for solution to shuttle bus squeeze. Straits Times. (September 20, 2013)
- Commuters generate close-knit social network. Swissinfo. (August 8, 2013)
- Familiar Strangers. ETH Life. (August 6, 2013)
- Secret network of 'familiar strangers' uncovered. Science World Report. (August 6, 2013)
- Travel smart card data may help fight spread of infectious disease. PNAS News. (August 5, 2013)
- Using subway cards to track infections. SciLogs. (August 5, 2013)
- Singapore bus study reveals hidden social networks. GuangMing Online. (August 2, 2013)
- Now we can actually count and track the 'familiar strangers' in our lives. CITYLAB. (July 26, 2013)
- Singapore bus study reveals hidden social networks. Scientific American. (July 23, 2013)

- Social networks between 'familiar strangers' could predict how diseases spread in urban areas. Medical Daily. (July 23, 2013)
- The 'familiar stranger' is your friend. The Wire. (July 23, 2013)
- Nothing random about 'familiar strangers'. Straits Times. (July 22, 2013)
- Study examines the role of 'familiar strangers' on public transport. WIRED UK. (July 11, 2013)
- The science of familiar strangers: society's hidden social network. MIT Technology Review. (July 9, 2013)

COMPUTER SKILLS

Programming: C, C++, Matlab, Python, R, SQL, Java, C#, IBM ILOG CPLEX

Software packages: igraph, networkx, MATSim

STUDENTS SUPERVISED

Bachelor thesis supervision, National University of Singapore

- Pang Ying, Li Guo: Demand estimation for KTM rail. 2012
- Chua Er Jian, Song Xiang Long: Regularity of intra-urban movements. 2013
- Lim Tian Yan Brandon, Wong Wenshun: Route choice inference in metro networks. 2014
- Lee Ren Huan, Mathieu Liong: Variability of bus dwell time. 2014

MEMBERSHIP AND SERVICE

Professional Membership

- hEART: European Association for research in transportation — Scientific Committee
- Chinese Overseas Transportation Association (COTA) — Student Member
- TRB Standing Committee on Public Transport Planning and Development (AP025) — Friend Member
- TRB Standing Committee on Traveler Behavior and Values (ADB10) — Friend Member
- TRB Standing Committee on Urban Transportation Data and Information Systems (ABJ30) — Friend Member

Journal Referees

- EPJ Data Science
- IEEE Transactions on Intelligent Transportation Systems
- International Journal of Intelligent Transportation Systems Research
- Journal of Transportation Engineering
- Journal of Transport Geography
- Physics Letter A
- Social Science Research
- Transportation
- Transportation Research Part C: Emerging Technologies
- Transportation Research Part E: Logistics and Transport Review

Conference Referees

- COTA International Conference of Transportation Professionals

- IEEE Conference on Intelligent Transportation Systems
- hEART, European Association for Research in Transportation

REFEREES

Dr. Der-Horng Lee
Professor
National University of Singapore
Email: dhl@nus.edu.sg
Dr. Lee is my graduate advisor.

Dr. Kay W. Axhausen
Professor
ETH Zürich
Email: axhausen@ivt.baug.ethz.ch
Dr. Axhausen is my graduate advisor.

Dr. Alexander Erath
Module Coordinator
Future Cities Laboratory
Email: erath@ivt.baug.ethz.ch
Dr. Erath is coordinator of Module VIII.

Dr. Qiang Meng
Associate Professor
National University of Singapore
Email: ceemq@nus.edu.sg
Dr. Meng is my PhD committee member.